ABSTRACT

The Effect of Hypoxia on the Cytotoxicity of Diesel Exhaust Particles and a Novel Oxygenating Therapeutic in Four Cell Lines

Amjad Dabi, M.S.

Advisor: Erica D. Bruce, Ph.D.

Hypoxia is characterized by oxygen levels in tissue below 2% and is implicated in many diseases and adverse health outcomes including chronic lung disease, neurodegenerative diseases, and delayed wound-healing. Many solutions for tackling hypoxia to alleviate such conditions have been proposed but all carry significant limitations. This study attempts to characterize a novel oxygenating therapeutic known as Ox66™. Another major human health concern is diesel exhaust particles (DEP), a prominent component of air pollution. This study evaluates the toxicity of DEP, Ox66™, and a mixture of both during both hypoxia and normoxia and in 24- and 48-hour exposures using four cell lines. The effect of hypoxia on cytotoxicity carries implications for the health risk assessment of air pollution in patients suffering from hypoxia-related diseases. Additionally, the effect of Ox66™ on the hypoxia induced changes in DEP exposures as observed in their mixture may provide clues about its efficacy.

The Effect of Hypoxia on the Cytotoxicity of Diesel Exhaust Particles and a Novel Oxygenating Therapeutic in Four Cell Lines

by

Amjad Dabi, B.M.

A Thesis

Approved by the Department of Environmental Science

_____

George P. Cobb, Ph.D., Chairperson

Submitted to the Graduate Faculty of
Baylor University in Partial Fulfillment of the
Requirements for the Degree
of
Master of Science

Approved by the Thesis Committee

_____

Erica D. Bruce, Ph.D., Chairperson

_____

Joseph Taube, Ph.D.

_____

Ramon Lavado, Ph.D.

_____

Dana Dean, Ph.D.

Accepted by the Graduate School
August 2020

_____

J. Larry Lyon, Ph.D., Dean

Page bearing signatures is kept on file in the Graduate School.

TABLE OF CONTENTS

LIST OF FIGURES

LIST OF TABLES

DEDICATION

To my parents,
whose love is the warm, gentle light that illuminates even the darkest of times.

To Dr. Bradley C. Bolen,
without whose kindness and support this work would never exist.

CHAPTER ONE

Introduction

Hypoxia and its effects on cells are a topic of interest in both biomedical and environmental disciplines of study. From a biomedical perspective, hypoxia plays a role in the initiation and exacerbation of a number of adverse health outcomes such as organ transplant failure (Andrade et al., 2006; De Perrot et al., 2002), insulin-resistance in cases of obesity (Ye, 2008), impedance of wound-healing and the continuation of chronic wound onset (Campillo et al., 2017; Chandan & Sashwati, 2010; Schreml et al., 2010), and the onset and prognosis of traumatic brain injury (R.-Q. Huang et al., 2010; Jeremitsky, Omert, Dunham, Protetch, & Rodriguez, 2003). Furthermore, hypoxic conditions are a major feature of solid cancerous tumor microenvironments, contributing to radiation therapy resistance via lack of available free-oxygen radicals required to induce cell-death via DNA damage (Vaupel, 2004). While cancer microenvironment represent a physiological niche that is not directly relevant to the purpose of this study, cancers remain are the primary targets of studies involving the effects of hypoxia on cytotoxicity, with findings indicating that hypoxia increases the resistance of tumors to cytotoxic chemical therapeutics and is associated with a worse prognosis (J. M. Brown & Giaccia, 1998; Graeber et al., 1996; Yao et al., 2005).

At the cellular level, hypoxia induces a number of changes in cellular function and phenotype and alters the expression of genes involved in homeostatic disturbances (Tuder, Yun, Bhunia, & Fijalkowska, 2007). This results in the reduction of cell growth

and proliferation (Schmelzle & Hall, 2000) and mitochondrial respiration (Schumacker, Chandel, & Agusti, 1993; D. E. Taylor, Kantrow, & Piantadosi, 1998) and a reduction in the rate of ATP consumption to 7% of that consumed in normoxic conditions (Hochachka, Buck, Doll, & Land, 1996). Some of these disturbances are entirely reversible upon return to normal oxygen conditions. However, longer periods of hypoxia may produce irreversible changes in cellular function and phenotype (Heerlein, Schulze, Hotz, Bartsch, & Mairbaurl, 2005). Given these changes, hypoxia may exacerbate cellular disturbances observed in cytotoxic responses to foreign compounds and environmental pollutants.

The importance hypoxia plays in a wide array of medical outcomes contrasts with the available options for treatment and mitigation for affected individuals. Currently, the only option available to most patients struggling with hypoxia-induced injury is hyperbaric oxygen therapy (HBO), whose popularity as a treatment method has steadily increased since the 1960s (Gill & Bell, 2004). While generally safe, HBO's biggest disadvantages are a lack of mobility and the associated costs for maintaining and operating the compressed chamber. Research on other modes of treatment have emerged to address these limitations and attempt to offer higher efficacy while limiting costs. This includes hemoglobin-based oxygen carriers which rely on the engineering of animal hemoglobin to deliver oxygen directly in the bloodstream (Winslow, 2000), and perfluorocarbon compounds which attempt to leverage their enhanced solubility of oxygen for use as molecular carriers of oxygenation to hypoxic tissues (K. C. Lowe, 1999). One novel oxygenating therapeutic is Ox66™, an aluminum oxide-based novel oxygen-containing compound developed by Hemotek, LLC with the aim of addressing

the challenge of providing an effective, portable, and affordable oxygenating agent for use in both trauma and long-term biomedical situations. It has shown promise in providing potential oxygenation following ingestion while also exhibiting a favorable safety profile (Zhang et al., 2019). However, challenges remain in understanding its mechanism of action and the ideal conditions and administration routes for maximizing efficacy.

Another area of great interest for human health is air pollutants and their effects on disease and morbidity. Produced by a variety of natural and anthropogenic sources, air pollutants have become global in nature, often spreading to remote areas where they are not originally produced, thereby affecting a vast portion of human populations on the planet (Borrell, Burrows, Platt, Richter, & Wagner, 2003; Gille et al., 2010; Lamarque et al., 2003). The adverse effects of exposure to air pollutants affect a wide array of organ systems, leading to increased mortality rates and decreased life-expectancy (Brunekreef & Holgate, 2002). These effects include an increase in lung-cancer and non-malignant pulmonary disease (Abbey et al., 1999; Pope III et al., 2002), cardiovascular disease and adverse implications for blood coagulation (Riediker et al., 2004). Components such as heavy metals and dioxins in polluted air have been linked to neurological and renal adverse health outcomes (Damek-Poprawa & Sawicka-Kapusta, 2003; Ewan & Pamphlett, 1996; Ratnaike, 2003; Walkowiak et al., 2001).

One important component of the particulate matter portion of air pollution are diesel exhaust particles (DEP), which constitute a significant portion of elemental carbon present in urban areas, pointing to widespread exposure among human populations (Donaldson et al., 2005). The composition of these particles varies depending on the type

of vehicles from which emission occurs, but are generally composed of a complex mixture of both organic and non-organic materials such as PAHs, nitrates, sulfurs, and trace metals, with sizes ranging from less than 0.1 μm to larger than 2.5 μm (Wichmann, 2007). Exposure to such particulate matter has been linked to a number of diseases of the cardiovascular and pulmonary systems (Hazenkamp-von Arx et al., 2011; Raaschou-Nielsen et al., 2012), nervous system (S. Wang et al., 2009), reproductive system (Wilhelm & Ritz, 2003), and cancer (Yorifuji et al., 2013). *In vitro* studies have demonstrated a clear detrimental effect of DEP on lung epithelial cells (Amara et al., 2007; Watterson, Sorensen, Martin, & Coulombe Jr, 2007) and cardiovascular cells (Suzuki, Taneda, Fujitani, & Li, 2008). Furthermore, more recent studies have shown that certain size portions of DEP may translocate into circulation following inhalation and exhibit neurological toxicity (A. Peters et al., 2006).

Therefore, the general goal of this thesis is to examine and understand the interactions between low oxygen conditions, the toxicity of DEP, and the toxicity of a potential oxygenating therapeutic. Additionally, the toxicity of mixtures of DEP and the oxygenating compound will be assessed. The efficacy of the oxygenating compound will be assessed by investigating whether the effect of the mixture is additive or antagonistic.

CHAPTER TWO

Background

Molecular and Cellular Adaptations to Hypoxia

Preserving optimal oxygen levels is of vital importance for normal cell functioning in all metazoan organisms. Oxygen is a necessary component of cellular respiration and energy production due to its role in aerobic adenosine triphosphate (ATP) synthesis (Rich, 2003). In most eukaryotic cells, this synthesis process takes place in the mitochondria, and involves a series of electron transfer reactions, generating energy that is used to create a proton gradient across the mitochondrial membrane. This gradient is subsequently used to drive the phosphorylation of adenosine diphosphate (ADP) to ATP, which can then serve as a source of energy for cellular functions. This electron transport chain utilizes oxygen as a final receptor of electrons, without which aerobic respiration in non-photosynthetic cells would cease.

The major component of oxygen regulation in the body is hypoxia inducible factor 1 (HIF-1) (Gregg L. Semenza, 2007). HIF-1 is a transcription factor belonging to the helix–loop–helix-PER-ARNT-SIM family of transcription factors (Guang L Wang, Jiang, Rue, & Semenza, 1995). It is therefore a heterodimer composed of two subunits: HIF-1α and HIF-1β and is detected in cells under low oxygen conditions while its concentration rapidly declines at normal oxygen conditions. The production of both subunits is constitutive and oxygen-independent. However, only HIF-1α's degradation is regulated through oxygen-dependent mechanisms (Ivan et al., 2001). This degradation

occurs through the hydroxylation of two domains within HIF-1α by both proline and asparagine hydroxylase enzymes, in turn facilitating the subunit's interaction with the von Hippel–Lindau tumor suppressor protein through increasing the binding affinity by up to 1000 fold, the results of which is the destruction of HIF-1α through a ubiquitin-proteasome pathway (P. H. Maxwell et al., 1999; C. T. Taylor, 2008). The hydroxylation of the degradation domains on the alpha subunit requires the presence of oxygen, and is therefore inhibited in hypoxic conditions, allowing for the accumulation of HIF-1 (Kaelin & Ratcliffe, 2008). The accumulation of HIF-1 activates a response that relies on a number of genes related to angiogenesis, glycolysis, and other functions aimed at mitigating the effects of oxygen deprivation (Hu et al., 2006).

HIF-1 was first identified as a protein that binds to the 3′-flanking region of the human erythropoietin (EPO) gene during hypoxia in Hep3B liver cancer cells (Gregg L Semenza & Wang, 1992). Further experiments demonstrated that the induction of HIF-1 itself under hypoxia was not exclusive to EPO-producing cells such as Hep3B, but was present in other mammalian non-EPO-producing cell lines including CHO, Rat1 fibroblast cells, and C2C12 mouse myoblast cells, and that the transfection of the EPO enhancer into non-EPO-producing cells amplified the transcription of reporter genes under hypoxia (P. Maxwell, Pugh, & Ratcliffe, 1993; G. L. Wang & Semenza, 1993). This suggested a prime role for HIF-1 in oxygen sensing and response in a wide array of cells and a transcriptional activity that extended beyond EPO gene activation.

The next identified target of HIF-1 regulation as a set of genes encoding the production of several glycolytic enzymes. RNA levels of phosphoglycerate kinase 1, pyruvate kinase, and aldolase A genes were all observed to accumulate in mammalian

cells following hypoxia, a response which was inhibited by cycloheximide, indicating a HIF-1 mediated pathway (Gregg L Semenza, Roth, Fang, & Wang, 1994). Additional HIF-1α gene targets were identified by comparing gene expression patterns between VHL-null and wildtype cells (Wykoff, Pugh, Maxwell, Harris, & Ratcliffe, 2000). Since then, more than 60 different genes have been identified as possible HIF-1 targets, although the strength of evidence varies depending on the method of identification (Gregg L Semenza, 2003).

Other hypoxia regulatory molecules include HIF-2α, a paralogue of HIF-1α which was initially cloned and characterized in the endothelium of mouse embryos as a Per-Arnt-Sim protein domain transcription factor and was termed EPAS1 (Tian, McKnight, & Russell, 1997). HIF-2α is subject to similar protein regulation mechanisms, whereby post-translational modifications by proline and asparagine hydroxylase result in VHL-dependent proteolysis and a blocking of transcriptional activity (Schofield & Ratcliffe, 2004). Another oxygen regulatory factor, HIF-3α, was identified later. This factor dimerizes with HIF-1β and binds to the hypoxia response element on target genes, and is upregulated during low oxygen conditions as a result of HIF-1 binding to the regulatory *cis*-element of its gene (Gu, Moran, Hogenesch, Wartman, & Bradfield, 1998; Makino et al., 2007). However, unlike other HIFs, HIF-3α plays an inhibitory role in hypoxia-induced adaptations. The suppression of HIF-3α *in vivo* elevates physiological adaptions to hypoxia and increases physical endurance (Drevytska et al., 2012). The inhibitory mechanism occurs through a HIF-3α splicing variant acting as an inhibitor of HIFs by interfering with their binding to the hypoxia response element of target genes (Makino and others 2002). The result of the upregulation in HIF-3α production during hypoxia and

its inhibitory effects on other HIFs is a negative feedback loop whereby the onset of hypoxia permits HIF-1 accumulation, which in turn upregulates the expression of HIF-3α which undergoes hypoxia-mediated splicing into a protein inhibiting the binding of HIF-1to target genes.

While HIFs are the primary elements of cellular hypoxia regulation, some HIF-independent mechanisms of regulation have also been identified. For instance, the activity of mammalian target of rapamycin (mTOR) is inhibited by hypoxia, a response that is dominant over its activation from other growth factors and nutrients (Arsham, Howell, & Simon, 2003). mTOR regulates cellular functions related to cell proliferation, growth, and metabolism via its influence on ribosomal mRNA translation (Inoki, Li, Zhu, Wu, & Guan, 2002; Schmelzle & Hall, 2000). The exact pathway involved in the HIF-independent hypoxic regulation of mTOR may vary depending on the exact experimental conditions. In some cases, the hypoxic regulation of mTOR is dependent on the protein tuberous sclerosis complex 2 (TSC2) and the enzyme AMP-activated protein kinase (AMPK), both of which are known to be upstream regulators of mTOR signaling (Inoki et al., 2002; Liu et al., 2006). On the other hand, isolated AMPK from human embryonic kidney 293 cells did not exhibit significant activation (Arsham et al., 2003). To complicate matters further, mTOR also appears to be regulated by another pathway which is HIF-dependent (Brugarolas et al., 2004). While this pathway also relies on TSC2, it requires the regulated in development and DNA damage response 1 (REDD1) gene, which has been identified as a target of HIF-1 and is upregulated during hypoxia (Shoshani et al., 2002).

Given that numerous genes are targets of HIF-1, the result of these molecular adaptations is a set of wide-ranging shifts in cellular functions related to metabolism, angiogenesis, proliferation, apoptosis, and membrane permeability during hypoxia. Cellular metabolic shifts under low oxygen are characterized by an upregulation of the activity of glycolytic enzymes, resulting in an AMPK-mediated increase in the rate of glycolysis (Marsin, Bouzin, Bertrand, & Hue, 2002; Robin, Murphy, & Theodore, 1984). This is an important adaptation for maintaining cellular energy supplies as cells shift from aerobic oxidative phosphorylation to the far less efficient anaerobic respiration, a phenomenon known as the Pasteur effect (Seagroves et al., 2001). Furthermore, protein synthesis is largely inhibited in hypoxic conditions (Kwast & Hand, 1996; Tinton, Tran-Nguyen, & Buc-Calderon, 1997). This occurs primarily at the translational level and includes inhibition of both initiation and elongation via phosphorylation of proteins necessary for ribosomal function such as eIF2α and eEF2 (Koumenis et al., 2002; Liu et al., 2006). Given that protein synthesis drives the majority of ATP demand in cells (Rolfe & Brown, 1997), the reduction in protein synthesis is an effective adaptational shift for conserving ATP, reducing ATP demand in severe hypoxia down to around 7% of normoxic levels (Hochachka et al., 1996). Upregulation of anaerobic glycolysis and suppression of the protein synthesis allow cells to maintain homeostatic levels of ATP during hypoxia, as observed *in vivo* (Donohoe & Boutilier, 1998).

To further conserve energy, DNA replication is inhibited in hypoxic cells, thereby arresting the G1/S-phase transition as observed by accumulation of G1 cells in cultures subjected to hypoxia (G. Probst, Riedinger, Martin, Engelcke, & Probst, 1999; H. Probst, Hamprecht, & Gekeler, 1983). This cell cycle arrest occurs via regulation mechanisms

that are independent of the p53 tumor suppressor protein, and therefore distinct from those brought on by other types of cellular stress such as ionizing radiation (Graeber et al., 1994; Green & Giaccia, 1998). It is likely mediated by regulation of p21 and p27 expression indirectly via inhibition of the oncogene c-Myc, a known suppressor of their transcription (Gardner et al., 2001; Koshiji et al., 2004). The result of this cell cycle arrest is a decrease in proliferation in cells under hypoxic conditions in most cell types (Hubbi & Semenza, 2015). However, some cells may maintain their proliferate capacity under hypoxia, while other exhibit increased proliferation in certain hypoxic conditions. For instance, cancer cells are able to survive and proliferate despite the present of hypoxic regions within tumor masses, some of which are characterized by extreme hypoxia (Gwak et al., 2005; Muz, de la Puente, Azab, & Azab, 2015; Volm & Koomägi, 2000; Xue, Li, Li, & Chen, 2014).

Hypoxia and Disease

The wide range of effects induced at the cellular level by hypoxia translate to adaptations and disturbances at the physiological level, as evident by the role hypoxia plays in the onset, progression, and prognosis for several diseases. In the context of lung disease, prolonged alveolar and systemic tissue hypoxia may be the result of lung conditions such as chronic obstructive pulmonary disease (COPD), pneumonia, fibrosis, and some neurological conditions (Agustí et al., 2003; Wright, Levy, & Churg, 2005). Sustained hypoxia in lung tissue is linked to a remodeling of vascular structures, including an increase in the presence of small muscle-like cells of the alveolar wall (Stenmark Kurt, Fagan Karen, & Frid Maria, 2006). This is observed as the appearance of cells expressing alpha smooth muscle actin (α-SMA) in the alveolar wall. α-SMA is an

actin isoform typically associated with vascular smooth muscle cells (Hinz, Celetta, Tomasek, Gabbiani, & Chaponnier, 2001). Given that the alveolar wall is normally devoid of muscle cells, the appearance of small muscle-liked cells contributes to an increase in its thickness. Furthermore, phenotypic shifts of the endothelial cells comprising the pulmonary vasculature such an increases in the growth and size are observed (Belknap, Orton, Ensley, Tucker, & Stenmark, 1997; Meyrick & Reid, 1980; Stenmark & Mecham, 1997). Accompanying these shift are functional disruptions including increased permeability and vascular endothelial growth factor production (Carpenter, Schomberg, & Stenmark, 2005) and increases in the production of laminin, fibronectin, and elastin (Botto, Beretta, Daffara, Miserocchi, & Palestini, 2006). This vasculature remodeling links prolonged hypoxia to the onset of several pathologies such as high-altitude pulmonary edema and chronic pulmonary hypertension (Swenson, 2006; Voelkel & Tuder, 2000).

This link between hypoxia and lung disease may involve the induction of microRNAs, small stands of RNA which function as regulators of gene expression in animal cells via inhibiting the initiation of translation and promoting mRNA instability (Gebert & MacRae, 2019). It has been demonstrated that hypoxia induces the production of microRNAs involved in pathologies such as cancer (Kulshreshtha, Ferracin, Negrini, et al., 2007; Kulshreshtha, Ferracin, Wojcik, et al., 2007), and that some microRNAs may be involved in lung disease through the activation of immune cells linked to inflammatory lung pathways (Rodriguez et al., 2007). Another potential cellular mechanism is the effect of hypoxia on membrane voltage of pulmonary smooth muscle cells. Following acute hypoxia, voltage-gated potassium channels are closed resulting in

membrane depolarization and an influx of calcium ions into the cell (Reeve, Archer, & Weir, 1997). This disruption of ion channels could play a role in the pulmonary smooth muscle dysfunction observed during hypoxic pulmonary hypertension.

Aside from its induction of other pulmonary pathologies, COPD has also been linked to declines in cognition and the onset of neurodegenerative diseases like Alzheimer and its associated dementia (Antonelli-Incalzi et al., 2007; Hung, Wisnivesky, Siu, & Ross, 2009; R. A. Incalzi et al., 1993). This link does not necessarily establish the direct role of hypoxia in COPD-associated neurodegeneration and cognitive decline, especially since COPD exhibits comorbidity with a number of conditions associated with neurodegenerative disease including obesity (Gustafson, Rothenberg, Blennow, Steen, & Skoog, 2003) and metabolic cardiovascular syndrome (Kalmijn et al., 2000). However, several indicators point to hypoxia as a key element in the onset of neurodegeneration in COPD patients. For instance, cerebral hypoperfusion is a hallmark of hypoxemic COPD and its pathophysiology (De la Torre, 2000; Raffaele Antonelli Incalzi et al., 2003), and has been associated with an increase in cerebral hypoxia-induced mediators (Yang et al., 2013). Furthermore, the bioenergetics of patients with COPD have been observed to shift towards an elevated reliance on anaerobic metabolism, suggesting oxygen-starvation within cerebral tissue (Mathur et al., 1999).

The link between hypoxia and neurodegenerative disease is dependent upon inter-individual variation in the HIF-1-mediated cellular adaptations to low oxygen. In amyotrophic lateral sclerosis (ALS), disease onset and severity is linked to low levels of VEGF motor neuros within the central nervous system (Bogaert, Damme, Van Den Bosch, & Robberecht, 2006). Given that upregulation of VEGF expression is a HIF-1-

mediated cellular response to hypoxia (Namiki et al., 1995), the severity of hypoxia-induced neurodegeneration in ALS may be related to the robustness of the HIF-1 VEGF response. This is confirmed by studies which demonstrate lack of VEGF overexpression in response to hypoxia in ALS patients (Moreau et al., 2006), while mouse models lacking the VEGF hypoxia response element exhibit exaggerated motor neuron degeneration characteristic of ALS (Devos et al., 2004). The amelioration of neural degeneration by VEGF occurs through its induction of angiogenesis, resulting in a reinforcement of adequate blood and oxygen supplies to neurons undergoing hypoxia (Bogaert et al., 2006). VEGF also confers direct neuroprotective effects on neural cells undergoing duress as demonstrated by its ability to rescue hippocampal cells from death under serum deprivation (Jin, Mao, & Greenberg, 2000).

Some evidence also exists for a protective role of HIF-1 in Alzheimer's Disease (AD), another common neurodegenerative disorder. For instance, increased expression of HIF-1-α is associated with the protection of cultured neurons against amyloid β-peptide (25-35), a peptide fragment implicated in the pathology of AD (Avramovich-Tirosh, Bar-Am, Amit, Youdim, & Weinreb, 2010; Selkoe, 2001). The protective effect of HIF-1 in AD may be due to shifts in cellular functions that run counter to those observed in the course of disease onset (Soucek, Cumming, Dargusch, Maher, & Schubert, 2003).

Oxygenating Therapeutics

Given the implication of hypoxia in several disease pathologies, several existing and emerging solutions have been developed to deliver oxygen to hypoxic tissues and alleviate the immense cellular stress inflicted by oxygen deprivation. Currently, the only viable and available option (HBO), whose popularity as a treatment method has steadily

increased since the 1960s (Gill & Bell, 2004). In this type of treatment, patients are placed in a pressurized space containing oxygen pressures ranging between 2-3 atmospheric pressure for durations lasting up to 90 minutes (D'Agostino Dias, Fontes, Poggetti, & Birolini, 2008). The efficacy of HBO has been demonstrated in several applications such as the promotion of wound healing and the treatment of crush injury and traumatic brain injury (Bennett, Trytko, & Jonker, 2012; Daugherty, Levasseur, Sun, Rockswold, & Bullock, 2004; Mills, 2012; Myers, 2000). While generally safe, HBO's biggest disadvantages are a lack of mobility and the associated costs for maintaining and operating the compressed chamber. These limitations have necessitated the development of other alternatives for oxygenating therapeutics which can achieve the goal of delivering oxygen to hypoxic tissues while retaining mobility.

One such class of therapeutics are hemoglobin-based oxygen carriers, a blood substitute which relies on the isolation and engineering of hemoglobin from animal or human sources and their delivery into the bloodstream of target patients (Winslow, 2000). This engineering of isolated hemoglobin is typically aimed at the creation of hemoglobin tetramers which prolong its half-life in the blood and protects from the renal toxicity observed from the rapid excretion of hemoglobin dimers (Looker et al., 1992). The generation of such tetramers relies on two main approaches. The first involves the induction of cross-linking within the hemoglobin structure and between different hemoglobin molecules (Chang, 1998), and the second involves a process known as PEGylation, whereby polyethylene glycol is used to coat the surface of hemoglobin molecules, thereby increasing their weight and allowing for the formation of stable tetramers (Vandegriff, McCarthy, Rohlfs, & Winslow, 1997). These approaches have

yielded a variety of hemoglobin-based products, some as the result of refined chemical processing (Chatterjee et al., 1986; Y. Wang et al., 2017), and others a result of biological recombinant technology producing stable human hemoglobin from *E. coli* (Hoffman et al., 1990). Such different variants of hemoglobin-based blood substitutes have shown efficacy in delivering oxygen to various tissues and several have made it to phases II and III clinical trials, while a minority have been approved for veterinary use and the treatment of anemia in humans (Meng et al., 2018). Unfortunately, despite the promise of emerging hemoglobin-based solutions, many concerns about safety remain as several adverse effects are observed during trials, including pancreatic, cardiac, and elevated mortality issues (Alayash, 2004; Murray et al., 1995; Silverman & Weiskopf, 2009; Sloan et al., 1999).

Another class of oxygenating agents developed is perfluorocarbons. These large, inert substances have been studied as potent oxygen carriers due to their high capacity to dissolve oxygen, which can reach up to 25 times that of water or blood (K. C. Lowe, 1999). Unfortunately, due to their size and structure, perfluorocarbons are hydrophobic, and therefore are not soluble blood plasma or cell culture media, which limits their efficacy when used directly (Hendrik Bergert et al., 2005). A solution to this obstacle is the creation of perfluorocarbon emulsions using various phospholipids and other proprietary chemical techniques, producing emulsions with particle sizes as small as 0.2 µm (D. R. Spahn, 1999). These emulsions have demonstrated oxygenating efficacy both in cell culture systems and *in vivo* (Goh, Gross, Simpson, & Sambanis, 2010; Palumbo et al., 2014) and in clinical studies (Keipert et al., 1994; Mosca et al., 1996; Donat R. M. D. Spahn et al., 1999). However, like other blood substitute products, perfluorocarbons have

been implicated in problematic side effects involving changes in liver and spleen weights and the manifestation of flu-like symptoms (Kenneth C. Lowe, 1994; Kenneth C Lowe, 1997; Zuck, Riess, & Biro, 1994).

Ox66™ is an aluminum oxide-based novel oxygen-containing compound developed by Hemotek, LLC with the aim of addressing the challenge of providing an effective, portable, and affordable oxygenating agent for use in both trauma and long-term biomedical situations. Unlike hemoglobin-based and perfluorocarbon blood substitutes, Ox66™ is in powder form, and currently requires minimal post-production preparation, although solubility in aqueous solutions remains a concern. It has shown promise in providing oxygenation following ingestion while also exhibiting a favorable safety profile (Zhang et al., 2019). It is not yet clear what the mechanism of action by which Ox66™ may transport oxygen is. One possible hypothesis involves the trapping of oxygen inside the chemical structure in a manner similar to the storage of gases by metal-organic frameworks, although no visible gas desorption has been observed in aqueous solutions. These compounds are produced through a special synthesis process that links various molecular blocks containing metallic and organic elements together using strong bonds (Yaghi et al., 2003), and their unique molecular and structural properties allow them to store different gases such as hydrogen and methane (Rosi et al., 2003). Another hypothesis involves the chemical transfer and exchange of oxygen between Ox66™ and hemoglobin in the bloodstream, thereby rendering Ox66™ an active oxygenating agent only in specific physiological settings and conditions. Understanding the structure of Ox66™, the mechanism with which it transports and delivers oxygen, and the conditions

under which such a mechanism works optimally is of vital importance to the development of higher-efficacy versions and of new classes of oxygenating therapeutics.

Air Pollution and Particulate Matter Toxicity

The gradual increase in air contaminants has increasingly become a regional and global problem since the rapid industrialization that began to take place in the United States and Europe in the 18th century. Several analytical techniques have been leveraged to monitor the long-term trends of air quality components such as carbon dioxide and lead deposition measures since the industrial revolution (Bogan, Ohde, Arakaki, Mori, & McLeod, 2009; Weiss, Shotyk, Appleby, Kramers, & Cheburkin, 1999). Despite the breadth and reach of global air pollution, its health implications have only been the focus of intense scientific investigation in the last few decades. Up until the 1950s, health risk assessments involving inhalation routes of exposure were focused on agents of chemical warfare and certain hazardous work conditions (D. L. Costa, 2018).

Propelled by advances in the analytical characterization of air pollution and its components (Kay, 1957), and inspired by the increasingly noxious smog of large urban centers like Los Angeles and events such as the 1952 London Fog Incident, an understanding of the link between public health and air pollution began to emerge (Logan, 1953). In 2019, the mortality burden of air pollution was estimated by the World Health Organization to be around 4 million deaths annually (X. Li, Jin, & Kan, 2019). Furthermore, the risks posed by air pollution interfaces with socioeconomic inequalities and levels of urban development, posing an unequal burden where socioeconomic and developmental divides render certain populations more vulnerable and disproportionately affected (Ji, Zhu, Lv, & Shi, 2019; Samoli et al., 2019).

The mortality burden associated with air pollution stems from its role in the prevalence of several diseases and its detrimental effects on several organs and body systems both in the short and long term. The respiratory system, for instance, is highly vulnerable to contaminants present in the air given its role as the first line of defense against inhalation exposures, with irritation, bronchoconstriction, and shortness of breath observed followed short-term exposures (Balmes, Fine, & Sheppard, 1987; Kagawa, 1985). Chronic exposures, on the other hand, are associated with reduced lung function and the onset of chronic diseases such as asthma, emphysema, and lung cancer (Kuo, Wong, Lin, Lai, & Lee, 2006; Nawrot et al., 2006; Tager et al., 2005). The health consequences of air contamination is not confined to the respiratory tract, however, as components of air pollution have been observed to translocate across the lung epithelium and into circulation (Ghio & Huang, 2004). For the cardiovascular system, this translates into increased inflammation and impaired cardiac rhythm and blood coagulation in otherwise healthy adults (Riediker et al., 2004). Other serious cardiovascular health outcomes include an increased risk of myocardial infarctions (Vermylen, Nemmar, Nemery, & Hoylaerts, 2005) and ischemic heart disease (Dalton et al., 2001). In the central nervous system, increased air pollution is linked with the onset of neuropathies manifesting as decreased cognitive function, headaches, fatigues, and increased incidence of neurodegenerative and neurodevelopmental diseases (Xu, Ha, & Basnet, 2016). Other systems such as the urinary and digestive are also affected with increased prevalence of stone formation and liver damage (Damek-Poprawa & Sawicka-Kapusta, 2003; Mandal, 2005).

While air pollutants comprise a diverse set of compounds in various forms, one component of interest for its human health implications is particulate matter. This component is not a uniform compound but rather a complex mixtures of various organic and inorganic chemicals, metals, and dust particles all suspended within ambient air due to their small size, and is responsible for the majority of the reliably attributed contributions of air pollution to the global mortality burden (Anderson, Thundiyil, & Stolbach, 2012; Pope et al., 1995). Suspended particulate matter usually contains a wide distribution of size fractions, and the potential adverse effects on human health for specific particles is dependent of their size (Kim, Kabir, & Kabir, 2015). Given the irregular nature of particulate matter shape, standardized size categorizations are challenging. The Environmental Protection Agency (EPA) in the United States has categorized particulate matter based on its aerodynamic diameter, defined as the diameter of a sphere with a density of 1 g/cm^3 which settles in the air at a similar velocity (Esworthy, 2013). The EPA's two main designations within this system are particles with an aerodynamic diameter less than 10 μm, designated as PM_{10}, and those with an aerodynamic diameter less than 2.5 μm, designated as $PM_{2.5}$. A third category of fine particulate matter with an aerodynamic diameter of less than 0.1μm ($PM_{0.1}$), and referred to as ultra-fine particles (UFP) has emerged in recent toxicological research due to unique physiochemical and biological properties (Hasheminassab, Daher, Schauer, & Sioutas, 2013). The differential toxicity profiles of the various size distributions may be attributed to several factors relating to differences both in chemical composition and physical attributes. For instance, the size of particulate matter is linked to its penetration depth and retention time in human lungs, with smaller particle sizes able to escape various

respiratory filtering mechanisms and deposit deeper into the lung but exhibiting lower overall retention times (J. Brown, Cook, Ney, & Hatch, 1950). Furthermore, smaller particles sizes contain a larger fraction of redox active compounds and exhibit higher availability and ability to translocate across the lung epithelium and into circulation (Araujo & Nel, 2009). These properties allow particulate matter from air pollution to exhibit their extrapulmonary effects on the cardiovascular, hepatic, and central nervous systems (Furuyama, Kanno, Kobayashi, & Hirano, 2009; Kreyling, Semmler-Behnke, & Möller, 2006).

In urban areas, a major fraction of particulate matter contamination are diesel exhaust particles (DEP), formed as the result of exhaust emissions from incomplete combustion in diesel engines (Cassee, Héroux, Gerlofs-Nijland, & Kelly, 2013). These particles usually consist of complex mixtures of a carbon cores surrounded by inorganic and biologically active organic components such as polynuclear aromatic hydrocarbons and some of their quinone derivatives (Cho et al., 2004; Schuetzle, Lee, Prater, & Tejada, 1981). The large presence of DEPs in particulate matter air pollution has resulted in their use as a model for the health effects and mechanism of particulate matter exposure *in vivo* and *in vitro* (Lawal, Davids, & Marnewick, 2016; Møller et al., 2016).

In vitro studies of DEP exposure have demonstrated a dose-dependent cellular damage and inhibition of cellular growth in several human lung cell lines including endothelial and epithelial cells and macrophages (Bhavaraju et al., 2014; Lawal et al., 2016; Su et al., 2008). Similar cytotoxic effects have been observed in animal cell models such as mouse fibroblast and endothelial cells and rat endothelial cells and macrophages (Bünger, Krahl, Franke, Munack, & Hallier, 1998; Hirano, Furuyama, Koike, &

Kobayashi, 2003; Jacobsen et al., 2008; N. Li, Wang, Oberley, Sempf, & Nel, 2002). Furthermore, the ability of certain fractions of particulate matter to translocate across the lung epithelium and reach systemic circulation has prompted research into its effects on cells outside of the pulmonary tract. For instance, the cytotoxic effects of DEP are observed in human and cells including dopaminergic neuros and microvascular endothelial cells (Tobwala et al., 2013). Aside from their cytotoxic effects, DEP are linked to activation of inflammatory pathways in cell cultures as demonstrated by the elevation of pro-inflammatory cytokines following exposure, including interleukin 6, interleukin 8, tumor necrosis factor alpha, interleukin 1 beta (Hashimoto et al., 2000; Mitsushima et al., 2008; Tseng, Wang, & Chao, 2017). DEP also exert genotoxic effects and DNA damage in various cell lines (Don Porto Carero, Hoet, Verschaeve, Schoeters, & Nemery, 2001; Dybdahl et al., 2004; Jacobsen et al., 2008).

The adverse effects of air contaminants in general, and especially particulate matter is due to their exertion of oxidative stress via generation of reactive oxygen species (ROS) in excess of the cellular ability to neutralize (Crobeddu, Aragao-Santiago, Bui, Boland, & Squiban, 2017; MohanKumar, Campbell, Block, & Veronesi, 2008). These species are responsible for the damage of several cellular components including proteins, lipids and DNA, resulting in loss of cellular viability and integrity and an increased incidence of harmful mutations (Floyd, 1990; Halliwell, 1999; Stadtman & Berlett, 1991). While ROS also play a role in the elevation of pro-inflammatory markers observed during DEP exposure (Donaldson et al., 2003; Møller et al., 2014), other inflammatory mechanisms may be involved. Chemicals within DEP admixture may disrupt cellular membrane fluidity and structure and alter the function of transmembrane

proteins responsible for the control of calcium ion flux, thereby initiating cellular pathways that involve the production of pro-inflammatory cytokines (Fariss, Gilmour, Reilly, Liedtke, & Ghio, 2013; Johan Øvrevik, Refsnes, Låg, Holme, & Schwarze, 2015; Tekpli, A Holme, Sergent, & Lagadic-Gossmann, 2011; Tekpli, Holme, Sergent, & Lagadic-Gossmann, 2013). Another mechanism involves the activation by DEP of the cytosolic aryl hydrocarbon receptor protein, which is involved in the regulation of pro-inflammatory gene expression (Fardel, 2013; Totlandsdal, Cassee, Schwarze, Refsnes, & Låg, 2010). DEP exposure is also implicated in the activation of epidermal growth factor receptor signaling pathways leading to an upregulation of cytokine production (Pourazar et al., 2008). While the production of pro-inflammatory cytokines at the site of exposure is not necessarily a driver of systemic inflammation, such local inflammation is implicated in diseases such as COPD, AD, and coronary heart disease (He, Chen, Chen, Wu, & Cai, 2010; G. D. Lowe, 2006; McGeer & McGeer, 2002).

Aims and Objectives

Characterization of Ox66™

The exact chemical formula and structure of Ox66™ remains unknown. Furthermore, no conclusive hypothesis yet exists for the mechanism of action for any possible oxygenating efficacy. The first objective of this study is to gain more insight of the chemical structure and activity of Ox66™ using several chemical analytical techniques. Energy-dispersive x-ray spectroscopy, powder infrared spectroscopy, electron ionization mass spectrometry, and powder x-ray diffraction were chosen to study different aspects of structure and activity, including elemental composition, possible

ligands, ligand exchange activity in solution, and the presence and characteristics of a crystalline structure. Insights into structure and activity may provide the basis for formulating possible hypothesis about the mechanism of action and behavior in solution and biological tissue.

Cytotoxicity and the Effect of Hypoxia

Another objective of the study is to investigate the effect of hypoxia on the cytotoxic response of four different cell lines following exposure to diesel exhaust particles, Ox66™, and a mixture of both. The chosen cell lines represent two organs across two organisms: Human and rat astroglia cells and type II pneumocytes. The choice of cells from different organs and organisms allows for the comparison of the effect of hypoxia on cytotoxicity in different organs while assessing the translatability of certain rat cell models for human cytotoxicity. The choice of two compounds reveals whether the effect of hypoxia on cytotoxicity is compound-specific, while mixture exposures allow insights into the possible efficacy of Ox66™ oxygenation *in vitro*.

The three cytotoxic end points chosen for this assessment are cell integrity, cell proliferation, and the levels of three pro-inflammatory cytokines: interleukin-6, interleukin-8 (KC/gro in rat cells), and tumor necrosis factor alpha. Cell integrity measure membrane integrity damage caused by compound exposure in the studied conditions. Cell proliferation is dependent on the ability of the compound to kill cells and to induce cell-cycle arrest, although the results cannot distinguish between these two specific effects. Pro-inflammatory cytokine production is an indicator of general cellular stress and the capacity of compounds to induce local inflammation. In general, cells experiencing increased stress would demonstrate higher cell membrane damage, lower proliferation,

and higher pro-inflammatory cytokine production. The main hypothesis is that hypoxia would exacerbate the cytotoxicity of all compounds across all cell lines. In mixture exposures, the hypothesis is that the toxicity would not be additive, with a toxic trend that is lower than that which is calculated by adding the individual toxicities at each concentration, thereby pointing to the possibility of amelioration of the exacerbated toxicity caused by hypoxia.

CHAPTER THREE

Materials and Methods

Chemical Analysis

Energy-dispersive X-ray Spectroscopy (EDS)

This analytical technique allows for the analysis of the chemical composition of a sample under a scanning electron microscope (SEM) by using a focused x-ray beam (Goldstein et al., 2017). The main principle involves the dislocation of electrons from the inner shells of atoms, creating an energy vacancy that can be occupied by an electron from a higher shell. Since electrons in higher shells contain more energy, the energy difference is emitted as x-ray radiation with a specific wavelength. The unique distribution of electrons in shells for different atoms grants each element a unique distribution of energy differences and stability of inner shell electrons. Therefore, measuring the number of emitted rays and their energies allows the estimation of the presence of certain elements and their relative abundance. The advantages of EDS are its relative ease of use and its ability to estimate elemental composition at different spots on the target material, making it ideal for a preliminary exploration of the material composition of Ox66™.

To prepare a sample of the compound for analysis, a small amount of the raw material was placed on a sample holder before insertion into the SEM by placing it on a double-sided carbon adhesive tape. It is important to use an adhesive tape to ensure sample adhesion to the sample holder so as not to contaminate the microscope chamber.

The adhesive tape must also be conductive since non-conductive materials may collect the emitted electrons generating large noise. Once inside the SEM, several points on the surface of different particles were chosen and the elemental composition reading was captured. The choice of several points ensures result accuracy and provides clues about the heterogeneity of elemental composition across the surface of the particle. The SEM used for this analysis is a Versa 3D Focused Ion Beam SEM, with an EDS system provided by EDAX.

Fourier Transform Infrared Spectroscopy (FTIR)

This technique allows for the measurement of the infrared absorbance of a sample simultaneously across a wide range of wavelengths (Smith, 2011). Bonds between atoms in any substance are not entirely rigid and exhibit a range of possible motions including bending, stretching, and rotation. Much like other elastic substances, each chemical bond possesses a natural frequency of vibration which depends on the rigidity of the bond, the mass of the involved atoms, and the spatial distribution of the involved and surrounding atoms. As the energy of an infrared beam approaches the vibrational frequency of a certain bond, increasing amounts of the radiation are absorbed. Thereby, a spectrogram of infrared absorption provides information about the types of bonds and atoms present in a substance. Fourier transform allows the simultaneous capture of IR absorption across a wide range of frequencies as it allows for the generation of an absorption value at individual frequencies from an infrared interferogram of a sweep signal containing many different frequencies. This technique is also advantageous due to its relative ease of operation, although result interpretation is more complex than that of EDS.

To carry out FTIR on a solid sample of Ox66™ without the need for aqueous dissolution a proper accessory is used. A small amount of the sample is placed inside the accessory which is in turn placed inside the instrument, and the spectrogram is then collected and recorded. The instrument used in this study is a Thermo/Nicolet iS-10 FT-IR with a Smart iTX™ accessory containing a germanium crystal.

Electrospray Ionisation Mass Spectrometry (ESI-MS)

This mass spectrometry technique provides molecular mass data about a compound by utilizing the behavior of charged ions in a magnetic field (Ho et al., 2003). Once a sample is in a solution, a high voltage is applied to the liquid which allows its aerosolization and subsequent charge. The charged aerosols are then transported via electrical potential towards an analysis chamber, during which ionized gas is produced. Inside the analysis chamber, a magnetic field is applied and the behavior of the ions in the field indicates their mass to charge (m/z) ratio. In this study, an orbitrap analyzer was used, trapping the ions in an oscillating magnetic field, and producing an orbital motion for each ion. The radius of the rotation, which is dependent on the m/z ratio of trapped ions, is measured. A Fourier transform allows for the acquisition of m/z ratio for individual ions even while many are present in the trap. The ions are then ejected in order of increasing m/z ratios and detected, thereby measuring their abundance. The resulting spectrogram therefore provides a tally of m/z ratios with peaks corresponding to their abundance. One advantage of the ionization process is that molecules frequently fragment, and the acquisition of m/z ratios for the charged fragments provides additional information about the structure of the analyte.

To carry out ESI-MS analysis on Ox66™, the sample must first be dissolved in an aqueous solution. Since Ox66™ exhibits poor dissolution in water, chemical modification of the solution is necessary. Prior experiments have demonstrated that shifts in pH away from the neutral state allows for increase dissolution of Ox66™. To achieve this, a small sample of Ox66™ was extracted through the tip of a Pasteur pipette and added to 10 µl of water. Five drops of a 90% ammonia solution were then added to the aqueous mix. To achieve maximum dissolution, the solution vial was occasionally inverted for fifteen minutes. Afterwards, a 1:10 dilution of the solution in methanol was prepared and mixed well. While these dissolution procedures are not feasible for *in vivo* procedures due to large alterations in pH, they allow an exploration of Ox66™ structures using ESI-MS. The final resulting solution was then injected into the instrument and both positive and negative spectrograms were acquired and recorded. An ammonia methanol blank consisting of a 1:10 dilution of water and 5 drops of 95% ammonia in methanol was also analyzed to rule out background solution ions. The instrument used for this analysis was an LTQ Orbitrap Discovery from Thermo Fisher Scientific.

X-ray Powder Diffraction (XRD)

Powder diffraction is a technique which uses electromagnetic radiation to provide information about the structure of a target powder analyte via analysis of the radiation diffraction patterns (Le Bail et al., 2008). When x-ray beams are used, this observed diffraction results from electrons in the atoms of the analyte. The diffraction pattern provides information about the relative positions of atoms in the compound due to unique position-dependent phase shifts. In the case of crystalline structures containing parallel lattice planes, additional details about the structure can be inferred due to the Bragg

equation, which states that constructive interference of x-ray beams resulting in a maximum detected signal is only possible when $2dsin\theta$ is an integer multiple of the beam wavelength. Here, d referes to spacing between the parallel lattice planes and θ is half the diffraction angle. XRD therefore reveals whether a compound is crystalline or amorphous and gives information about its structure if it is crystalline.

XRD analysis was performed on a raw Ox66™ sample at the Texas A&M x-ray diffraction laboratory with a Lynx-Eye, Bruker-AXS. The source of the x-ray is 1kW Cu X-ray tube, maintained at an operating current of 40 kV and 25 mA. The experimental parameters were as follows:

Table 3.1. Experimental parameters of powder XRD.

Parameter	Value
Wavelength	1.54060Å
Detector	PSD (Lynx-Eye Bruker AXS)
Anti-scatter Slit	12.530mm
Divergence Slit	1.00mm
Anti-air-scatter	Knife edge
Scan type	Coupled theta/2theta
Goniometer radius	217.5mm
Start	3
End	70
Step Size	0.015
Total Scan Time	30 mins

Cytotoxicity

Cell Culture

Four cell lines were used in this study, all acquired from the American Type Culture Collection (ATCC). All culture media was supplemented with 10% fetal bovine serum and 1% penicillin to protect against bacterial contamination in addition to any

other cell-specific supplements. A549:are type II human lung carcinoma cells. The medium used for their culture was F-12K media. SVG p12 are human astrocyte cells from human fetal glial cells transfected with an origin-defective mutant simian virus 40 (SV40). The medium used was Eagle's Minimum Essential Medium. DITNC1 are rat astrocytes from the species Rattus norvegicus transfected with the early oncogenic region of SV40 with the pGFA-SV-Tt promoter. The medium used was Dulbecco's Modified Eagle's Medium. RLE6TN are type II lung epithelial cells and exhibiting spontaneous immortalization. The medium used was Ham's F12 containing 2 mM L-glutamine and supplemented with 0.01 mg/ml bovine pituitary extract, 0.005 mg/ml insulin, 2.5 ng/ml insulin-like growth factor, 0.00125 mg/ml transferrin, and 2.5 ng/ml epidermal growth factor. The choices of media and supplementation are all based on ATCC recommendations and established lab practice.

Upon receipt of the frozen cells, vials were stored in a liquid nitrogen Dewar until needed for culture. To establish the first in-lab passage of the cell from a frozen vial, the vial was left to thaw at room temperature until fully liquid, and then added to a collagen-coated culture flask containing approximately 15 mL of appropriate cold media. The flasks were then transferred to NuAire cell incubator to grow in conditions of atmospheric oxygen, 5% CO_2, and 37 ^{0}C. The media was aspirated and replaced with fresh media after 24 hours. Cells were then monitored daily under a phase shift contrast microscope to check viability and confluence, and the media was replaced every 48 hours. When cells reached 70-80% confluency they were prepared for passaging. For the passaging procedure, all reagents including cell media, magnesium-free and calcium-free phosphate-buffer saline (PBS), and TrypLE Express cell-dissociation enzyme from Gibco

agent were placed in a 37 ^{0}C water bath for 30 minutes to reach temperature equilibrium. The culture flask was then removed from the incubator, and the culture media was aspirated. 15 mL of PBS was then added for 1 minute to prepare cells for dissociation. PBS was then aspirated and 4 mL of TrypLE (1x) was added. Cells were monitored under a phase shift contrast microscope until sufficient detachment from flask bottom was observed. 6 mL of media was then added to the flask, and the mixture was transferred to a centrifuge tube. 10 μL was extracted and set aside for counting. The centrifuge tube was placed in a centrifuge set for 300 RCF for 7 minutes. During centrifugation, 10 μL of trypan blue (0.4%) were added to the counting aliquot, mixed thoroughly, and allowed 30 seconds for dye infiltration. To count the cells using the Countess II FL cell counter from Thermo Fisher, the mixture was placed into the two chambers of the reusable slide and inserted into the counting machine to assess number of cells and percentage of viability. The acceptable viability threshold was 80%. Following centrifugation, the media was visually assessed to ensure complete centrifugation. The media was then aspirated, and fresh media was added to the pellet. The volume was chosen so that one million cells corresponded to one mL of media. The cells were then vortexed for 10 seconds to ensure complete resuspension. Cells were seeded in a flask and in dark 96-well flat bottom plates coated with extracellular matrix proteins for adhesion. The density was one million cells per plate and one million cells per flask. Each plate well was seeded with 100 μL of cell-containing media, with random well-order seeding to minimize the statistical impact of cell density variation resulting from technical error. Seeded flasks and plates were transferred back into incubator. Extra cells were transferred to two mL cryogenic vials for storage. Media and DMSO were added for a final total volume and a DMSO

concentration of 10%. The cryogenic vials were transferred to a Mr. Frosty freezing container from Nalgene containing an adequate amount of isopropanol to ensure a safe freezing rate. The freezing container was then transferred to a -80 ^{0}C freezer, and the vials were transferred to liquid nitrogen storage no later than a week.

Compound Preparation and Dosing

Ox66™ powder was acquired from Hemotek, LLC. DEP from industrial forklift (SRM2975) was acquired from the National Institute of Standards and Technology. Prior to dosing with DEP, a solution of 200 μg/mL of DEP in the appropriate solution was prepared and vortexed for one minute followed by sonication for 45 minutes. After sonication the DEP mixture was filtered through a series of GD/X Glass Micro Fiber syringe filters from Whatman in the following order: 5 μM then 1.2 μM and then 0.45 μM. This serial filtering minimizes excessive blockage of the smallest filter with higher size fraction, ensuring a consistent filtration process. This filtering of DEP ensures a physiologically relevant size fraction as larger sizes are usually not deposited in the pulmonary region (Manojkumar, Srimuruganandam, & Nagendra, 2018). Prior to dosing with Ox66™, a solution of 1000 μg/mL in the appropriate media was prepared.

Plates were dosed one day after seeding unless confluence was less than 60%. For the dosing procedure, fresh cell media and all prepared compound solutions were left in a 37 ^{0}C water bath for 30 minutes. Before media aspiration from plate wells, the appropriate dilution was prepared to achieve the desired concentration. Media from the selected rows was aspirated and then replaced with the media containing the compound(s). The dosing process proceeded from the lowest to highest concentrations to minimize contamination of the lowest concentrations, and the positive control was added

last. For normoxia conditions, the plates were incubated in ambient oxygen and 5% CO_2 at 37 ^{0}C. For hypoxia conditions, the incubation was in 2% oxygen and 5% CO_2 at 37 ^{0}C. Nitrogen flushing was used to maintain oxygen levels in hypoxia. The exposure doses for DEP were 20 μg/mL, 50 μg/mL, and 100 μg/mL. The exposure doses for Ox66™ were 50 μg/mL, 100 μg/mL, and 200 μg/mL. The DEP doses were chosen to correspond to the concentration ranges tested for in previous studies on particulate matter cytotoxicity, and the Ox66™ concentrations correspond to those previously used in lab for cytotoxicity studies. For the mixed exposure scenarios, the same concentrations for each compound from its single exposure experiment was used. The exposure scenarios included normoxia and hypoxia, each in a 24-hour exposure and a 48-hour exposure time. Fresh media was used as negative control and Triton X-100 (1%) was used as a positive control for cell death in all exposure scenarios.

Cytotoxicity Assays

Lactate Dehydrogenase Assay (LDH)

This assay measures levels of the lactate dehydrogenase enzyme in the cell culture media, which is a good indicator of cytotoxicity and cell membrane damage (Korzeniewski & Callewaert, 1983). The detection of this enzyme in the media relies on leveraging the role of LDH in cellular respiration where it exhibits catalytic activity in the conversion of lactate to pyruvate (Parhamifar, Andersen, & Moghimi, 2013). In this process, nicotinamide adenine dinucleotide is converted from its oxidized form NAD^+ to its reduced form NADH, which in turns transforms 2-(p-iodophenyl)-3-(p-nitrophenyl)-

5-phenyltetrazolium chloride (INT), a yellow tetrazolium salt, into red formazan. The increased presence of red formazan's color in the media is therefore an indicator of increased cellular damage.

To carry out this assay, an LDH buffer assay is first prepared with the following components and concentrations: 3.2 mM β-nicotinamide adenine dinucleotide sodium salt, 160 mM lithium lactate, 15 μM 1-methoxyphenazine methosulfate, 2 mM iodonitrotetrazolium chloride in 0.2 M Tris-HCl. 50 μl from each well of the dosed plate was transferred to the well of a clear 96-well assay plate. Afterwards, 150 μL of LDH assay buffer was transferred to each well of the assay plate. The reaction was incubated at room temperature for 10 minutes. The assay plate absorbance at 490 nm was then measured and recorded using a plate reader.

Tetrazolium Assay (MTT)

This is a cell proliferation and metabolism assay that relies on the transformation of 3-[4,5-dimethylthiazol-2-yl]-2,5 diphenyl tetrazolium bromide (MTT) by mitochondrial dehydrogenase into blue formazan, a dye lacking water solubility (Morgan, 1998). Formazan production correlates well with cellular numbers, permitting the use of blue color intensity as a measure of cell viability.

To perform the MTT assay, a solution of 0.5 mg/ml MTT in Dulbecco's Modified Eagle Medium lacking phenol red was prepared. All media from the well plate was aspirated and a 100 μL of assay solution was added to each well. The plate was incubated for 1.5 hours in corresponding hypoxic or normoxic conditions to allow formation of formazan crystals. After incubation, the assay solution was aspirated and 100 μL of 1:1 ethanol to dimethyl sulfoxide was added to each plate to solubilize the crystals. The

plates were placed on a plate shaker with an orbital motion at 400 rpm for 15 minutes to ensure complete solubilization. Plates were then read for absorbance at 570 nm with a plate reader to measure blue formazan levels.

Cytokine and Chemokine Multiplex

To measure the levels of three cytokines in the media of cells following 48-hour exposures in hypoxia and normoxia, the multiplex assay of MAGPIX® from Luminex was performed. This assay relies on fluorescence-labeled magnetic beads bound to antibodies for target proteins (Perraut et al., 2014). The antibody is then bound to phycoerythrin-conjugated streptavidin (PE). The MAGPIX® instrument uses two lasers to determine the presence of the target analytes. The first laser identifies the bead, thereby categorizing the analyte, and another laser measures the signal from PE.

To measure the cytokines and chemokines, panels for human IL-6, IL-8, and TNFα and IL-6, KC/GRO, TNFα were purchased from Millipore Sigma. The inflammatory markers were chosen as a subset of commonly tested inflammatory cytokines in particulate matter cytotoxicity, and their number was kept to three to minimize family-wise statistical error. To perform the analysis, the beads for each analyte were first sonicated for 30 seconds and then vortexed for one minute. 60 µL from each bead vial was then added to the bead mixing vial and the volume was brought to 3 mL using the bead diluent followed by vortexing for one minute. Two quality controls were used for each panel by adding 250 µL of deionized water to each of the quality control vials and then vortexing. The supplied standards were reconstituted with 250 µL each, and serial dilutions were then used to obtain the five lower dilutions.

For each plate, 200 µL of wash buffer was added into each well and then mixed on a plate shaker for 10 mins, followed by decanting of the buffer. 25 µL of each standard and quality control was added to their respective wells, with assay buffer being used for the blank standard. Afterwards 25 µL of assay buffer and 25 µL of control media was added to each well, followed by 25 µL of the sample media collected from the exposed cells. The mixed beads were vortexed again for one minute and 25 µL of the mixed bead solution was added to each well. The plate was then sealed with a plastic seal and placed on a plate shaker set at 600 rpm for two hours at room temperature. Following this incubation, the plate was washed twice with 200 µL of wash buffer in each well. Before decanting the wash buffer in each wash, the plate was attached to a magnetic holder that allows the beads to settle and protects them from the decanting process. 25 µL of the detection antibodies were then added to each well and the plate was sealed and covered in foil and then incubated for one hour on a plate shaker at 600 rpm in room temperature. After incubation, 25 µL of streptavidin-phycoerythrin was added to each well, and the plate was again sealed and placed in foil and incubated on a plate shaker in room temperature at 600 rpm. The plate was then washed with wash buffer two more times repeating the procedure for preserving the beads. 150 µL of assay buffer was added to each well and the beads were resuspended using a plate shaker at 600 rpm for five minutes. Finally, the plate was read using a MAGPIX®, and the output was recorded using the xPONENT® software.

Statistical Analysis

Each experiment represents 3 plates, yielding an N=3. For the LDH and MTT data, data from each plate was standardized to the negative control by using the formula:

$$x_i = \frac{x - \overline{x_c}}{std.\overline{x_c}} + 1$$

Where x_i is the standardized fluorescence of a well, $\bar{x}_c$ is the mean of the negative control values, and $std.\bar{x}_c$ is the standard deviation of the negative control values. This minimizes biases in statistical analyses resulting from variation in the baseline seeding density of the cells and background absorbance for each plate. The values for every concentration were then averaged across the plate so that each plate represents a single sample.

To analyze the plate data for each assay, linear regression with an interaction effect for hypoxia and normoxia was performed for each cell line and in each exposure period (24- and 48-hours) and for each compound. For exposure scenarios that showed a significant interaction effect ($p<0.05$), a z-test was carried out for the slopes of the regression line to detect statistically significant differences.

For the cytokine data, the Mann–Whitney U test was used to detect significantly statistical differences between hypoxia and normoxia levels of expression for each cytokine and across all cell lines and exposure scenarios.

CHAPTER FOUR

Results

Chemical Analysis of Ox66™

Figure 4.1 shows the results of the EDS analysis on a sample of Ox66™. The main two elements present in the analysis are oxygen at 64% relative atomic abundance and aluminum at 23% relative atomic abundance, with an Al:O abundance ratio of 2.78. Chorine is present in small quantities amounting to a 1% atomic abundance, pointing to a possible trace contamination rather than a structural involvement. The prominence of aluminum and oxygen suggests that Ox66™ possesses a structure similar to aluminum oxide compounds. However, the relative abundance of oxygen in Ox66™ is higher than aluminum(III) oxide with its molecular formula of Al_2O_3 and an Al:O abundance ratio of 1.5. These results are from a single spot on a grain of Ox66. However, they are consistent with the results from a different spot on the same grain (Figure A.1), the results of a spot from a different grain of the same batch (Figure A.2), and the results of a spot in a different batch from a previous analysis carried out in the lab (A.3). These results all indicate a range of 2.47 to 2.95 for the Al:O abundance ratio. The results of the FTIR are shown in figure 4.2. Here a wide peak of absorbance exists in the 3000-3500 cm^{-1} range. This suggests a large presence of -OH ligands binding to the aluminum atoms in the structure.

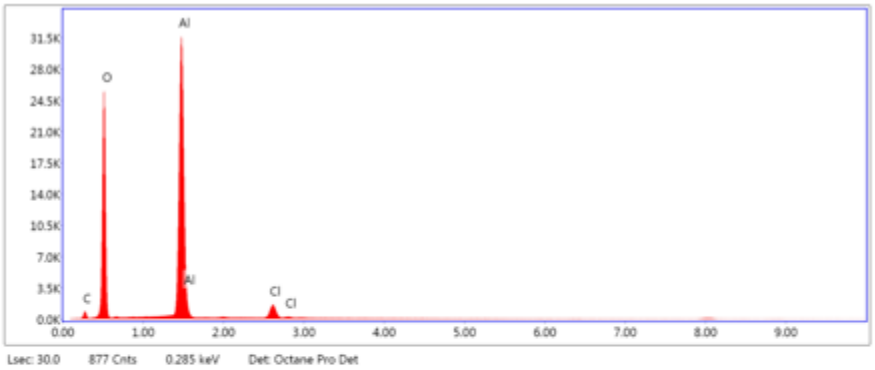

eZAF Smart Quant Results

Element	Weight %	Atomic %	Net Int.	Error %	Kratio	Z	R	A	F
C K	8.34	12.65	227.26	11.25	0.0146	0.0145	1.0823	0.9651	0.1601	1.0000
O K	55.78	63.51	7984.37	7.40	0.2159	0.2157	1.0360	0.9858	0.3732	1.0000
Al K	33.57	22.66	14836.62	4.02	0.2208	0.2204	0.9216	1.0246	0.7107	1.0025
Cl K	2.31	1.19	847.40	3.81	0.0170	0.0171	0.8772	1.0478	0.8381	1.0096

Figure 4. 1. The results of EDS analysis during SEM scan for a selected area on one grain of Ox66™. Aluminum and oxygen are the main two elements, with trace amounts of chlorine left. The oxygen:aluminum atomic abundance ratio is 2.78, higher than that of aluminum oxide.

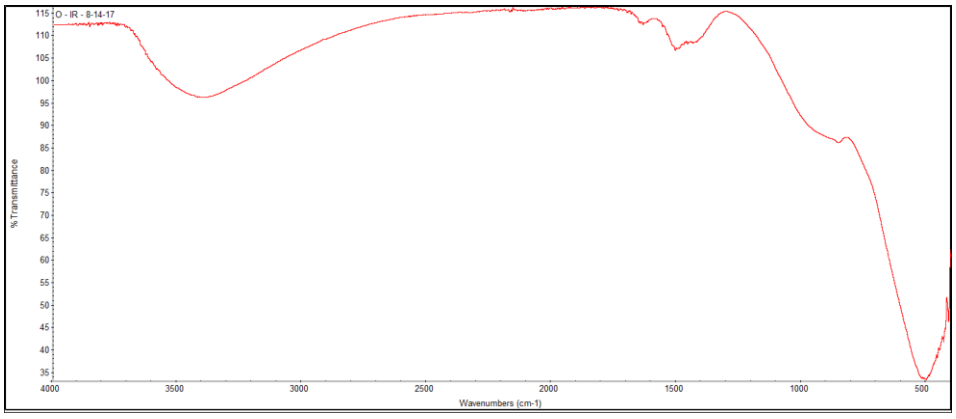

Figure 4. 2. FTIR results for Ox66™ powder. A wide absorbance peak is seen between the 3000 and 3500 cm^{-1} wavenumbers, suggesting a large presence of -OH ligands bound within the structure.

The spectrogram of the positive (figure 4.3) and negative (figure 4.4) ESI-MS analysis for methanol and ammonia shows a number of peaks, however, the low abundance of background peaks from the spectrogram with the presence of Ox66™ in both positive (Figure 4.5) and negative (4.6) spectra suggests no strong background confounding of the results by background noise.

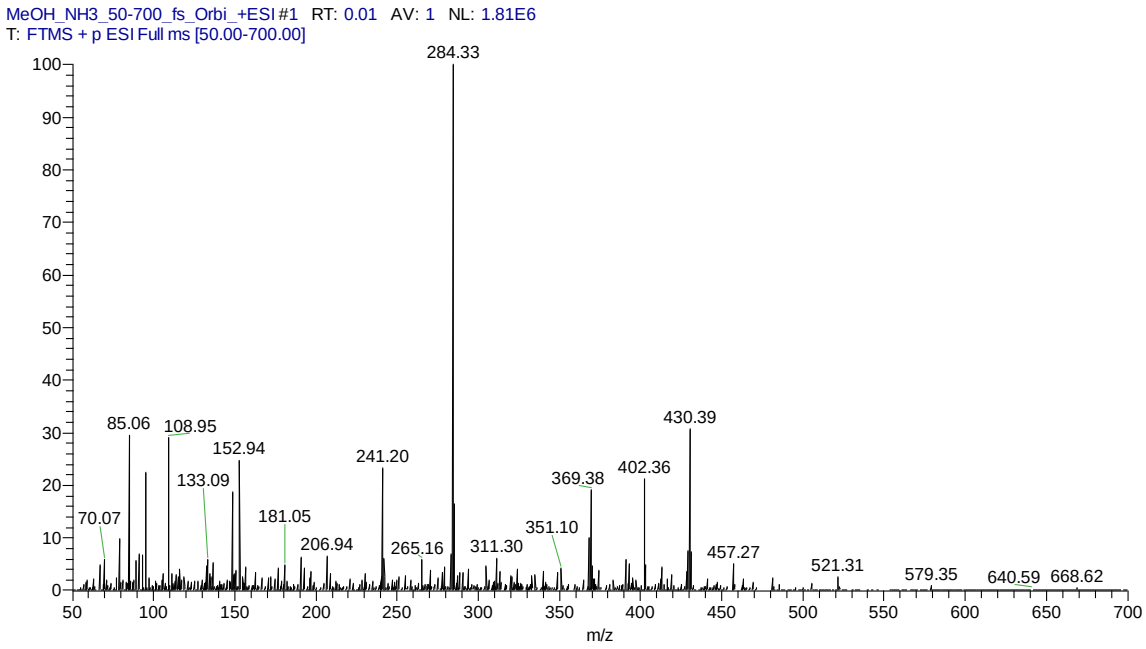

Figure 4. 3. Positive ion mass spectrometry results for background ammonia in methanol. While many peaks are present, their abundance is low in comparison to Ox66™- related peaks.

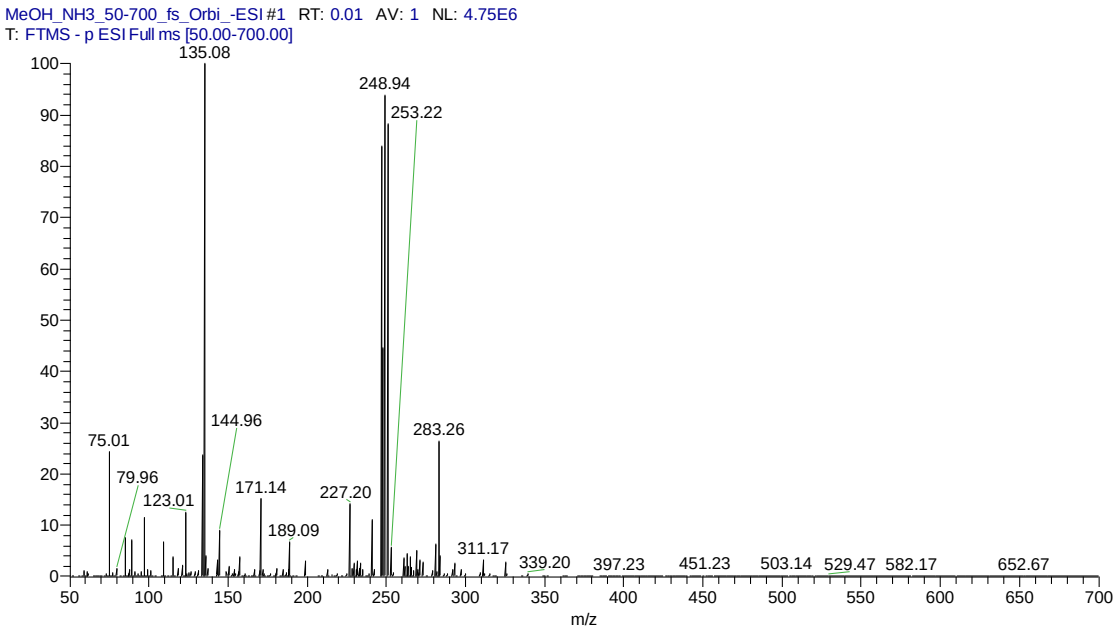

Figure 4. 4 Negative ion mass spectrometry results for background ammonia in methanol. The large number of peaks does not confound Ox66™ results due to lower abundance in comparison to compound signal.

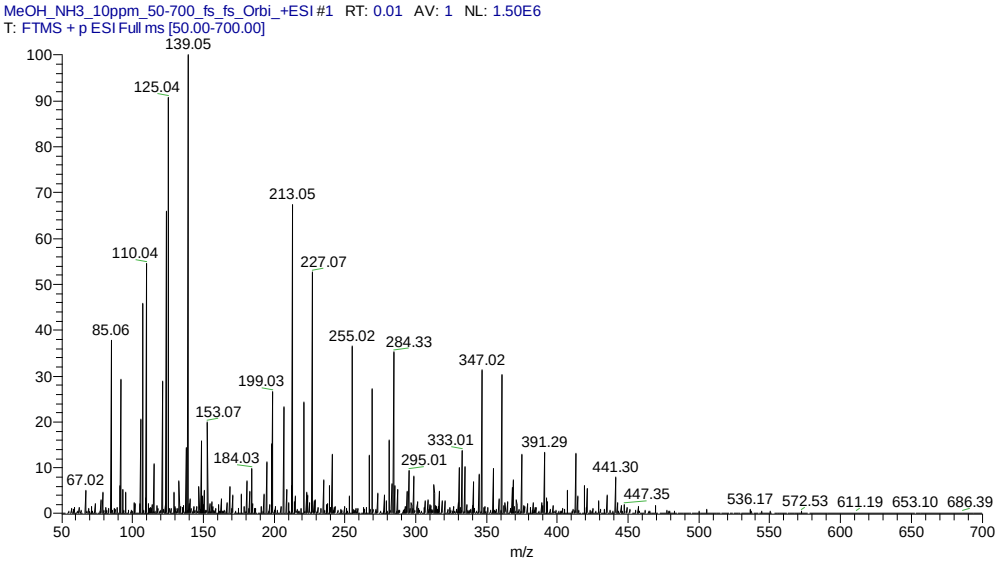

Figure 4. 5. Positive ion mass spectrometry results for Ox66™. The most prominent peaks are at 139.05, 125.04, 110.04, and 85.06.

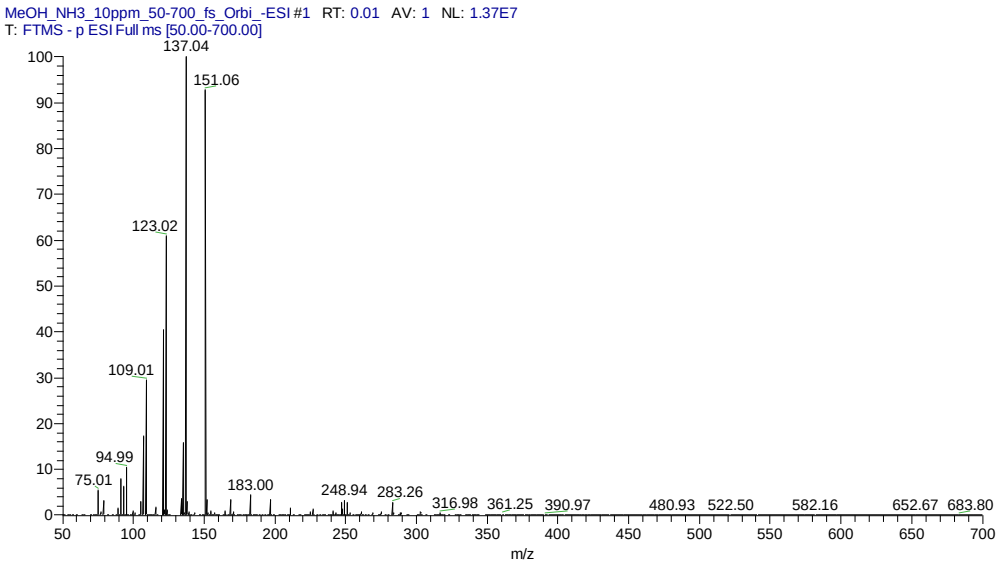

Figure 4. 6. Negative ion mass spectrometry results for Ox66™. The prominent peaks are 151.06, 137.04, 123.02, 109.01, and 94.99. These peaks represent a series of possible ligand substitutions occurring in solution. Removal of two hydrogen atoms and three electrons may explain the difference from the peaks of the positive spectrogram. A small peak at 79 may correspond to another ligand replacement in the series.

The results of the negative ion mass spectrometry analysis shown in figure 4.5 show several peaks with abundances far above the background level. These peaks are at 139.05, 125.04, 110.04, and 85.06. The negative ion spectrogram in figure 4.6 shows high abundance peaks at 151.06, 137.04, 123.02, 109.01, and 94.99. The difference in the m/z ratios between the positive and negative spectrogram peaks is around 2, which could potentially correspond to a difference of the mass of two hydrogen atoms and three electrons. The possible negative ions with exact masses that correspond to the peaks of the negative ion spectrogram are shown in figure 4.7. While this pattern of peaks with varying abundances is usually characteristic of a fragmentation pattern in mass spectrometry experiments, the pattern here seems to arise from a series of ligand substitutions, whereby several forms of aluminum oxide chemistries exist in solution and are able to bind methyl groups donated from methanol. This suggests a dynamic chemical behavior in the dissolved portion of Ox66™ in aqueous solutions.

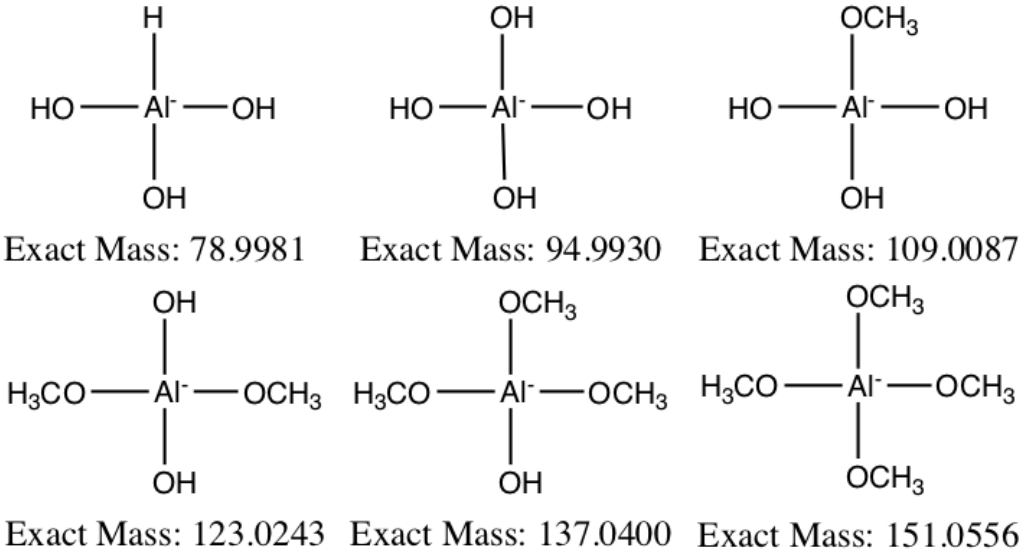

Figure 4. 7. Possible negative ions in solution corresponding to the peaks of the negative ion mass spectrometry results. Methyl groups not normally present in Ox66™ structure are able to bind at different ligands. This suggests that the mechanism of action may be mediated through such ligand exchanges.

Figure 4.8 shows the results of the XRD analysis performed on a sample of Ox66™. The lack of any sharp peaks indicative of crystalline structure indicates that Ox66™ is instead an amorphous compound. Given that a crystalline structure is a prerequisite to the identification of detailed structural information through XRD, amorphousness remains the only conclusion from this technique.

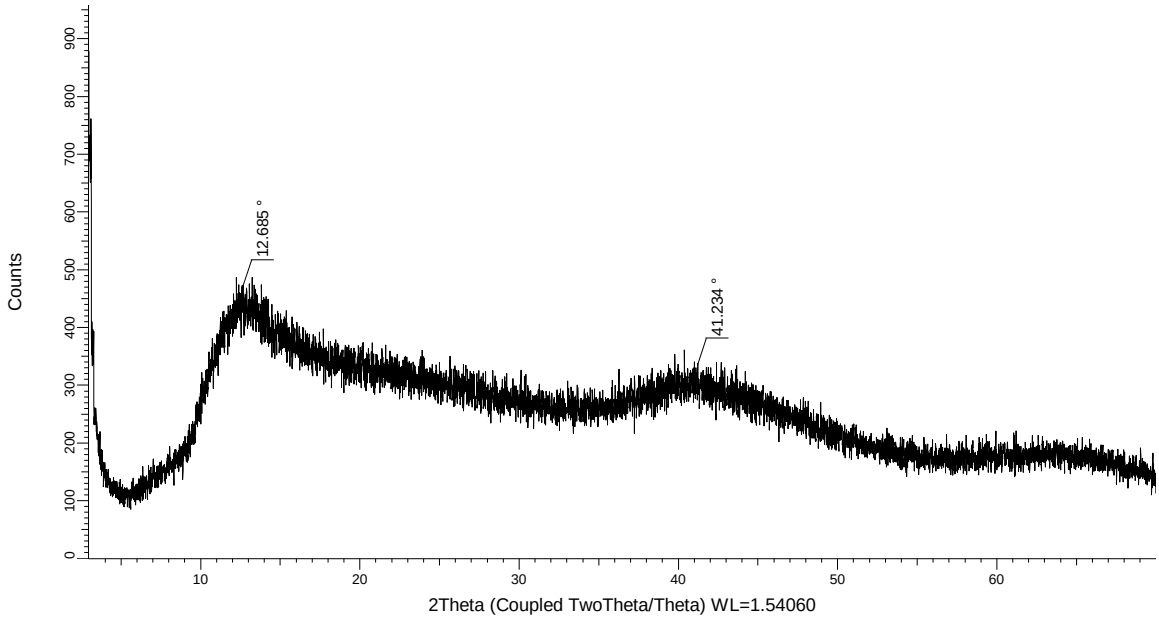

Figure 4. 8. The results of XRD performed on a sample of Ox66™. The lack of sharp peaks suggests an amorphous rather than crystalline structure. No further structural information can be inferred.

Cytotoxicity and Hypoxia

DEP Interference

The results of the analysis of the interference of DEP on the LDH assay are shown in Fig 4.9. DEP appear to lower the absorbance of the LDH assay. However, a Kruskal–Wallis test indicates the difference between the 4 DEP concentrations is not significant (p-value = 0.8748). Given the lack of significance for the interference data, no correction for DEP interference is necessary.

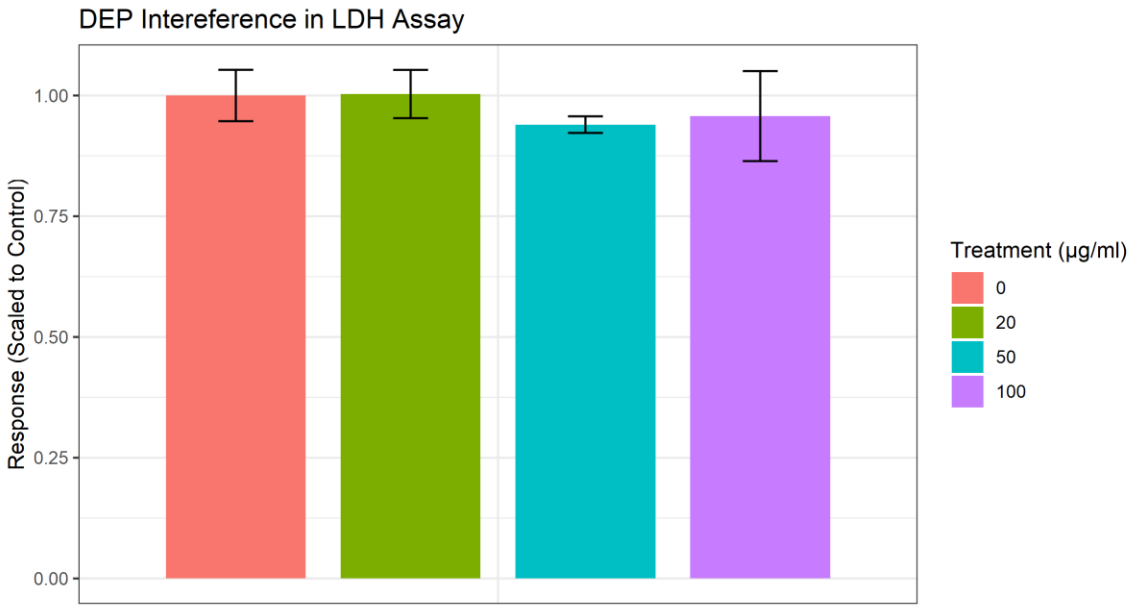

Figure 4. 9. Interference in LDH assay by DEP in media after cell lysis. Error bars indicate standard error (N=3). The two higher concentrations show a small decline in absorbance. However, none of the changes are significant given the results of the one-way Kruskal-Wallis test (p = 0.8748). No correction is required.

Human Type II Alveolar (A549)

Fig 4.10 shows the barplot of scaled LDH and MTT results for the A549 cells across all exposure scenarios. DEP exposure results in a weak response both for LDH and MTT assays. However, Ox66™ and mixture exposures result in a pronounced response in the LDH assay, while MTT is a mix between non-monotonic and a sharp decrease in two scenarios, normoxia at 48 hours with Ox66™ and hypoxia at 48 hours with a mixture exposure.

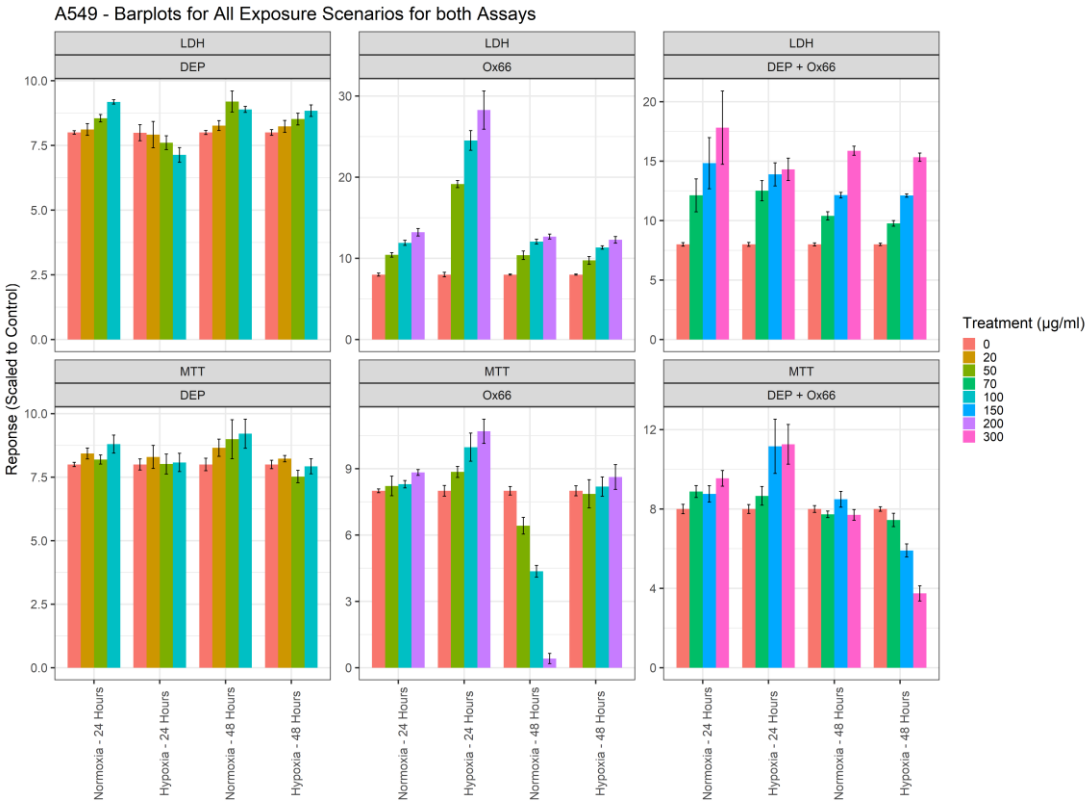

Figure 4. 10. Barplots for LDH and MTT assays for A549 cell line across all exposure scenarios. Response is absorbance at 490 nm scaled to control. Error bars indicate standard error (N=3). DEP responses are weak for both assays and all exposure scenarios. Ox66™ and mixture exposures exhibit a more marked response. Particularly intense are the LDH response for 24-hour exposure to Ox66™ in hypoxia and the 48-hour response to Ox66™ in normoxia. MTT and LDH responses are not always monotonic.

To compare the intensity of the trends and quantify the effects of hypoxia on the cytotoxicity of all exposure scenarios, the confidence intervals and z-tests for the assay trends are shown in Fig 4.11. The fitted lines for which these slopes where calculated can be found in the appendix, Fig A. 4. The slope analysis reveals generally positive trends for LDH, and flat insignificant trends in MTT with 2 exceptions. Three statistically significant differences ($p < 0.05$) between hypoxic and normoxic cytotoxicity trends exist LDH in 24-hour DEP exposures, MTT in 48-hour Ox66™ exposures, and MTT in 48-hour mixture exposures. The decrease in LDH values for the slopes in the linear regression model (trend intensity) for DEP between hypoxia and normoxia is 173%. The

increase in MTT trend intensity for Ox66™ in the 48-hour exposure is 109%. In 48-hour DEP and Ox66™ mixture exposure, the MTT trend decreases by a large 3097%. While those 3 trends vary significantly between hypoxia and normoxia, the variance in MTT is in opposite directions, and none of the trends in either assay correspond to significant trends in the other assay.

Pro-inflammatory cytokine production analysis for 48-hour exposures (Fig 4.12) for this cell line show an increase in IL-8 production in normoxia for both DEP and Ox66™ and their mixture, with Ox66™ and mixture exhibiting a more marked response. Furthermore, a significant reduction in IL-8 secretion in hypoxia compared to normoxia is observed in all exposures, especially for Ox66™ and the mixture. On the other hand, IL-6 production is only slightly elevated from controls in all normoxia exposures, and hypoxia levels are decreased to lower than both normoxia and control, although the difference from normoxia production is only significant in the cases of DEP and Ox66™. For TNF-α, only DEP exposure creates a slight elevation from control, and none of the hypoxia cytokine levels are significantly different from those of normoxia.

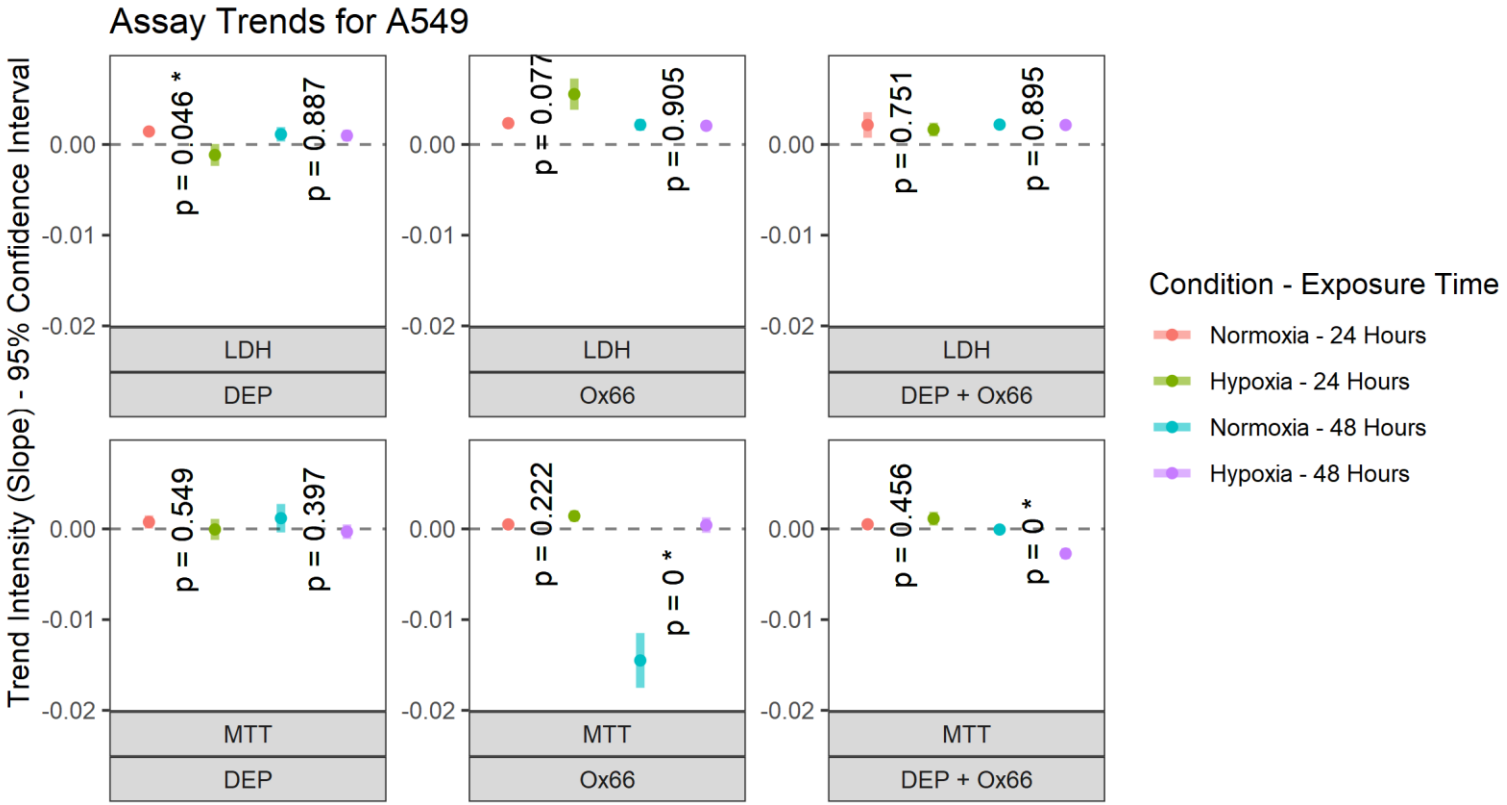

Figure 4. 11. Assay trends based on 95% confidence interval slopes from linear regression for A549 cells. Dots indicate slop values and Slopes near 0 or within a 95% CI containing zero are insignificant trends (N=3). * indicates $p < 0.05$. Three trend differences are significant, two of which are observed in the MTT assay and one observed in the LDH assay. Significant trends in either assay are not associated with a significant trend in the corresponding assay.

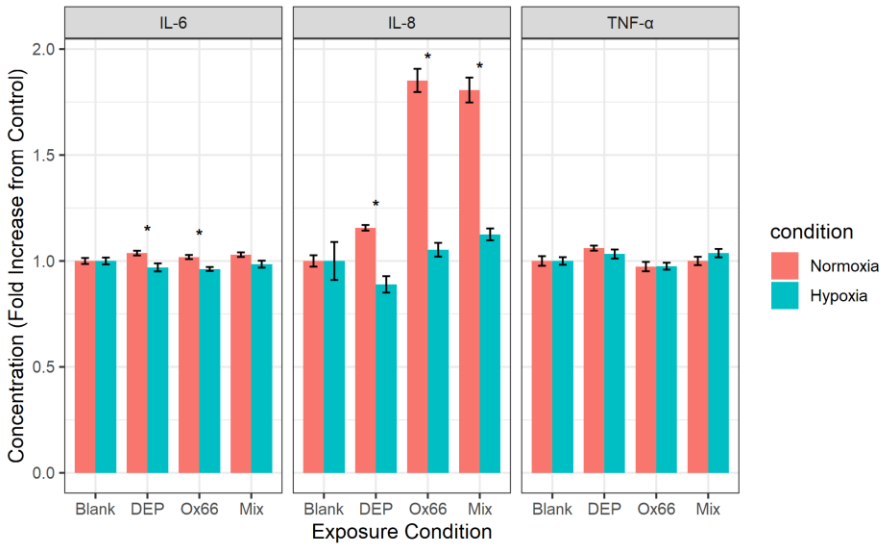

Figure 4. 12. Pro-inflammatory cytokines for A549 cells in 48-hour exposures at the highest dose. Error bars represent standard error (N=3). * indicates $p < 0.05$. IL-6 production is slightly elevated in normoxia for all exposure compounds and is significantly decreased from normoxia in DEP and Ox66™. IL-8 production is increased for all compounds and is significantly decreased from normoxia in all compounds. TNF-α exposure is slightly elevated in DEP normoxia exposure and no statistically significant difference from hypoxia exists in any compound.

Rat Type II Alveolar (RLE6TN)

The results of the barplot for rat lung cells are in Fig 4.13. While the cytotoxic responses of RLE6TN appear to be larger than the human cell line, there is a lack of monotonic responses, especially in 24-hour scenarios for LDH. Furthermore, no markedly differential responses are evident. In both Ox66 ™ and mixture 48-hour exposures a cytotoxic response is confirmed both by an increase in LDH production indicating cellular damage and a decrease in MTT production indicating decreased viability.

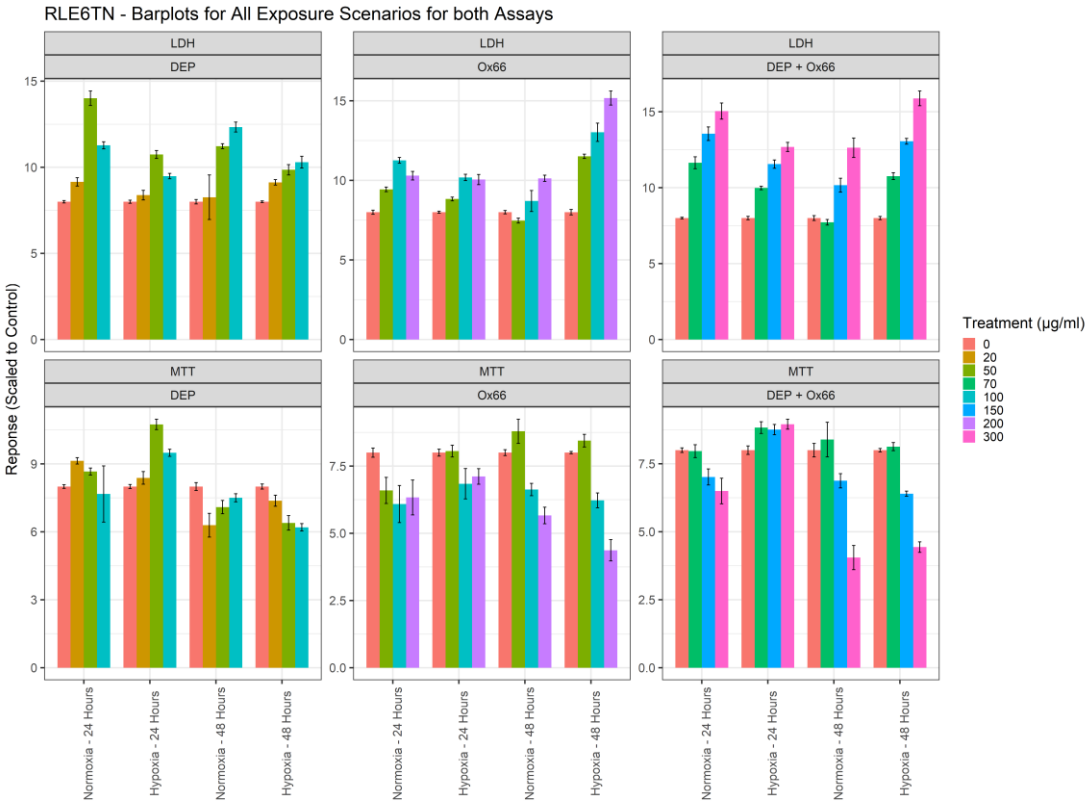

Figure 4. 13. Barplots for all exposures scenarios for rat type II alveolar cells (RLE6TN). Response is absorbance at 490 nm scaled to control. The error bars represent standard error (N=3). Compared to human lung cells, response to DEP and Ox66™ appear non-monotonic, while the mixture responses are clearer. In certain scenarios such as Ox66™ and mixture 48-hour exposures, cellular damage is accompanied by a reduction in cell viability, affirming the cytotoxic dose-related response.

The plotted linear regression lines for this cell line is in the appendix, Fig A.5. The slopes and the corresponding 95% confidence intervals are plotted in Fig 4.14. While some trends can be observed including a decrease in cellular damage accompanied by an increase in viability between hypoxia and normoxia in 24-hour DEP exposures, and an opposite trend in 48-hour Ox66™ exposures, the large uncertainties render these intensity difference statistically insignificant. The only statistically significant trend appears as an increase in viability following 24-hour exposures in the mixture between normoxia and hypoxia ($p = 0.02$). This trend represents a 138% increase in cell viability in hypoxic versus normoxic conditions, indicating an increase in cell viability as a result of hypoxia.

Pro-inflammatory cytokine production (Fig 4.15) is decreased in IL-6 for all three exposures, with hypoxia secretion not being statistically significant in any. For the IL-8 homologue GRO/KC, DEP induced an increase in production in normoxia while Ox66™ and mixture exposure secretion is lower than controls. Hypoxia induced a significant increase compared to normoxia only in the mixture exposure, where hypoxia production is also elevated compared to the control. It is difficult to make inferences about TNF-α secretion in the presence of the compounds in both hypoxia and normoxia due to the large variation in the control measurements resulting in large standard error. However, GRO/KC production following Ox66™ exposure is significantly elevated in hypoxia compared to normoxia.

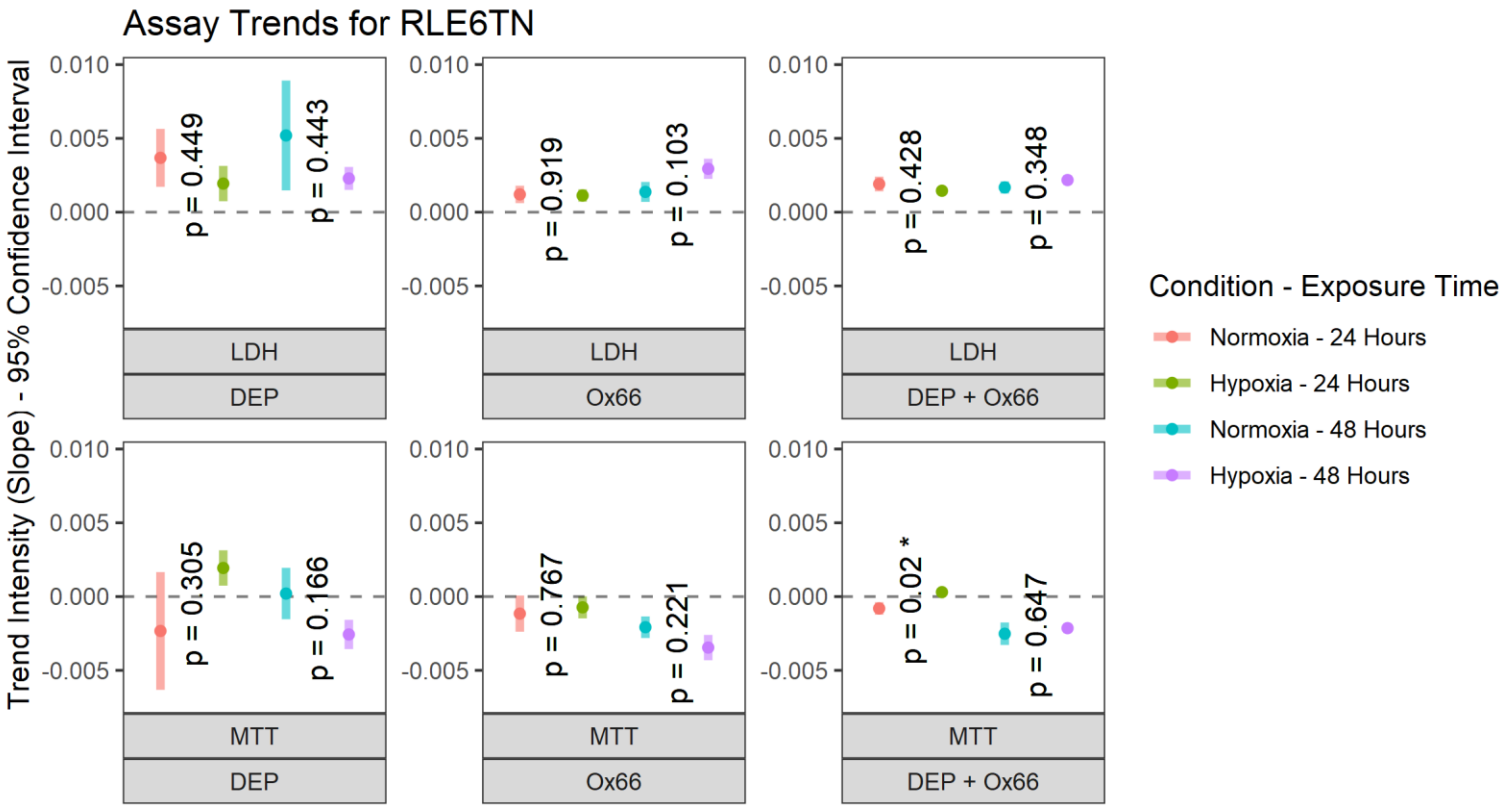

Figure 4. 14. Trend intensity for LDH and MTT assay following exposures in rat type II alveolar cells. Dots indicate slopes and bars indicate 95% CI (N=3). * $p < 0.05$. While most trends do not include 0 in the confidence intervals, less inferences can be made about the difference between the trends. Some trends between normoxic and hypoxic conditions are visible and confirmed by opposite assay trends. However, large variations in the data renders them statistically insignificant. One exception is MTT at 24-hour mixture exposure, where hypoxic conditions result in a statistically significant increase in dose-dependent cell viability suggesting a protective effect.

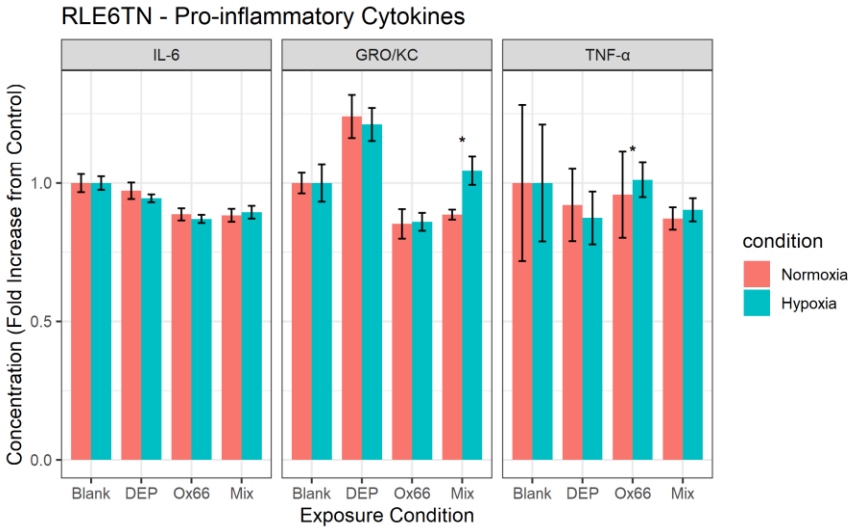

Figure 4. 15. Pro-inflammatory cytokines for RLE6TN cells in 48-hour exposures at the highest dose. Error bars represent standard error (N=3). * indicates $p < 0.05$. IL-6 production is decrease in normoxia for Ox66™ and mixture exposures and no statistically significant effects between hypoxia and normoxia are observed. GRO/KC production in normoxia is elevated for DEP but decreased for Ox66™ and mixture. Statistically significant increase in hypoxia from normoxia production is observed. TNF-α production exhibits large variation, especially for controls, making inferences about normoxia and hypoxia production difficult.

Human Astroglia Cells (SVGp12)

Like the previous cell lines, the response of human astrocytes varies by exposure compounds and scenario. However, some trends appear to be consistent. In Fig 4.16, dose-dependent cellular damage can be seen in all scenarios except for 24-hour exposures to Ox66™, which appear to induce a weak non-monotonic response. Ox66™ LDH results are also unique in the pattern of response for the response in 48-hour exposures, whereby a large increase in cellular damage is followed by a plateau, indicating a possible saturation of the effect at the lower concentration. On the other hand, cellular viability through MTT exhibits mostly non-monotonic responses punctuated by two clear trends in the 24-hour DEP exposures. The increases in MTT levels correlate to increases in LDH levels, indicating both elevation of damage and cellular viability or metabolic activity. Ox66™ exposures appear to reduce MTT in general except in normoxic

conditions at 48-hour exposures. Mixture exposures result in an assortment of unclear non-monotonic responses. The linear regression plots can be seen in the appendix, Fig A.6.

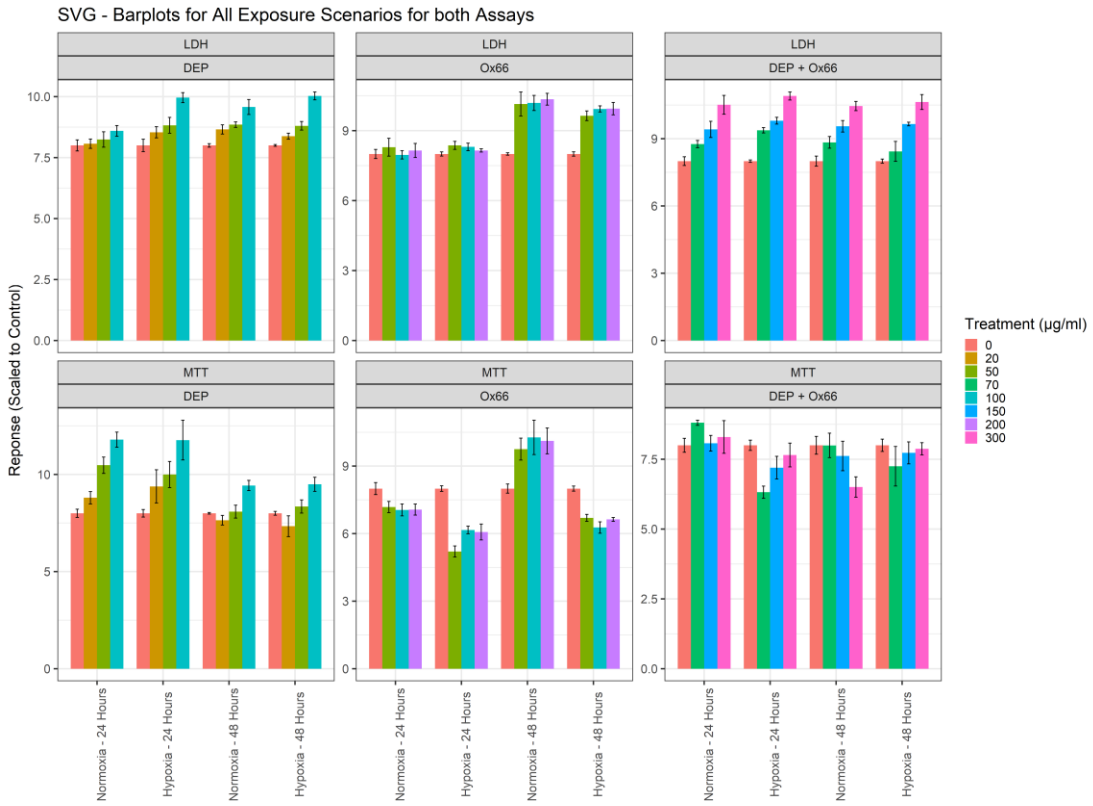

Figure 4. 16. Barplots for LDH and MTT for all exposure scenarios for human astrocytes (SVGp12). Response is absorbance at 490 nm scaled to control. Error bars represent standard error (N=3). LDH exhibits a dose-dependent response except for Ox66™ exposures, where 24-hour exposures exhibit no trend while 48-hour exposures appear to reach a response plateau at the lowest Ox66™ dose. MTT responses are varied, with some increasing in response to increase concentrations while other decrease or exhibit an unclear trend.

The assay trends in Fig 4.17 show statistically significant LDH trends for all exposure scenarios except Ox66™ in 24 hours. MTT trends are almost evenly divided between significant and non-significant trends. When comparing normoxia and hypoxia, a trend of increasing toxicity in hypoxic conditions in 24-hour DEP exposures is present but is not statistically significant. No other trend differences are statistically significant.

Fig 4.18 shows pro-inflammatory cytokine secretions in both normoxia and hypoxia. DEP and mixture exposures appear to dampen IL-6 production in comparison to control, while Ox66™ exacerbates it. In hypoxia IL-6 production is not significantly impacted in comparison to normoxia for DEP and mixture exposures but is significantly reduced in Ox66™ exposure. IL-8 secretions are elevated in Ox66™ and mixture exposures but is similar to the control for DEP exposure. Furthermore, hypoxia appears to have no significant impact on IL-8 production for any of the exposure scenarios although a slight dampening trend is observed. The production of TNFα for all exposures in normoxia is not altered from control levels but is significantly increased in hypoxic conditions in comparison to normoxic conditions for Ox66™ and mixture exposures.

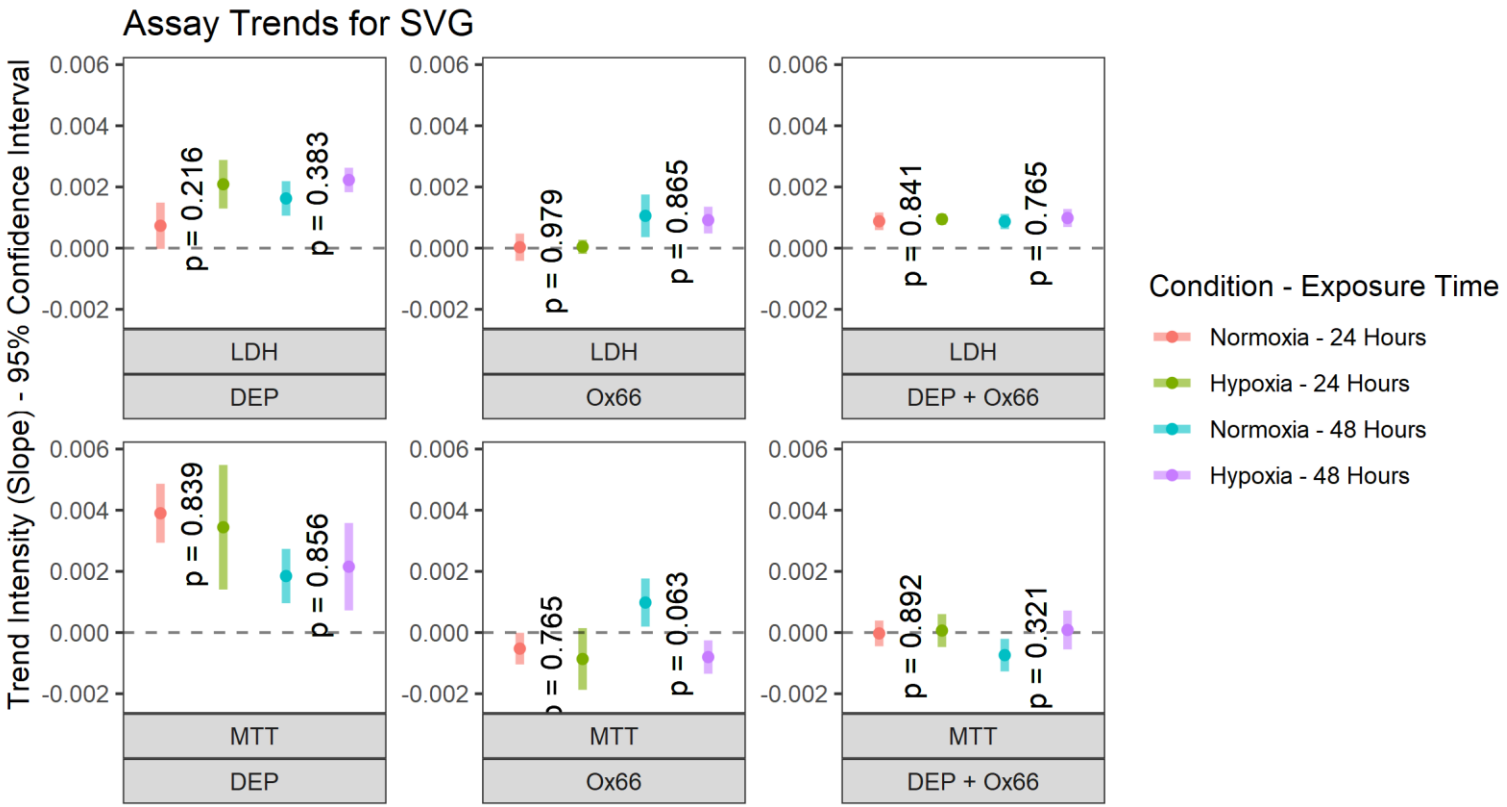

Figure 4. 17. Assay trend intensities for human astrocytes (SVGp12). Dots represent slopes and bars represent 95% CI (N=3). * indicates $p < 0.05$ for difference in assay trends between normoxia and hypoxia. LDH trends are all significant (not overlapping with 0) except for Ox66™ 24-hour exposures. MTT trends are almost evenly split between significant and non-significant. No significant differences between any normoxic or hypoxic responses exist.

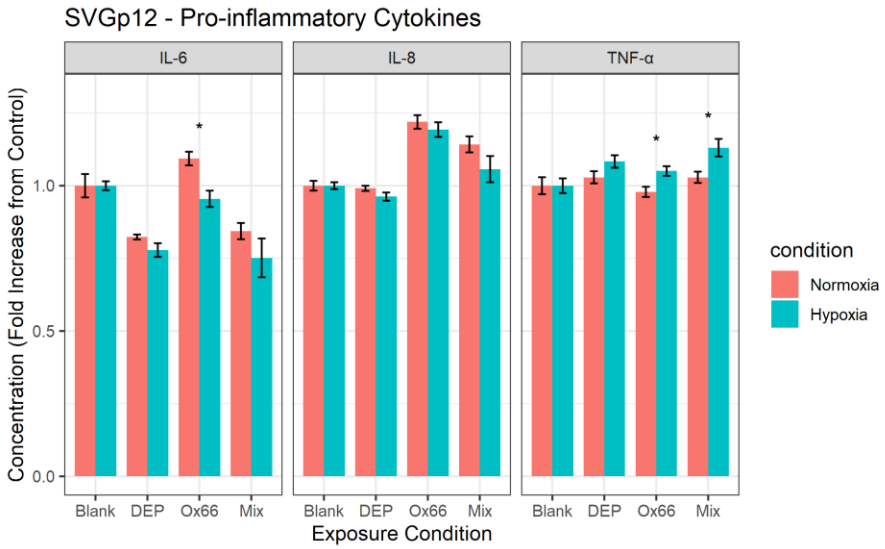

Figure 4. 18. Pro-inflammatory cytokines for SVGp12 cells in 48-hour exposures at the highest dose. Error bars represent standard error (N=3). * indicates $p < 0.05$. IL-6 is decreased from control in DEP and mixture exposures but elevated for Ox66™ exposure. IL-6 production in hypoxia is significantly reduced compared to normoxia. IL-8 exposure is elevated in Ox66™ and mixture exposure compared to control but not in DEP. Hypoxia induced a non-significant decrease in IL-8 production compared to normoxia in all exposure. TNFα secretions in normoxia are similar to control in all exposures but hypoxia production is significantly increased in Ox66™ and mixture exposures compared to normoxia.

Rat Astroglia Cells (DITNC1):

In rat astrocytes, LDH increases in a dose-dependent manner in all scenarios except 48-hour DEP exposure in hypoxia and 24-hour Ox66™ exposure in normoxia (Fig 4.19). MTT on the other hand is non-monotonic with no clear dose-dependent trend across all scenarios. However, in many of the exposures such as exposure to DEP or mixture in normoxia for 48 hours or exposure to Ox66™ in hypoxia for 24 hours, higher doses induce an increase in MTT absorbance, and may therefore be linked to increased cell viability or metabolic activity.

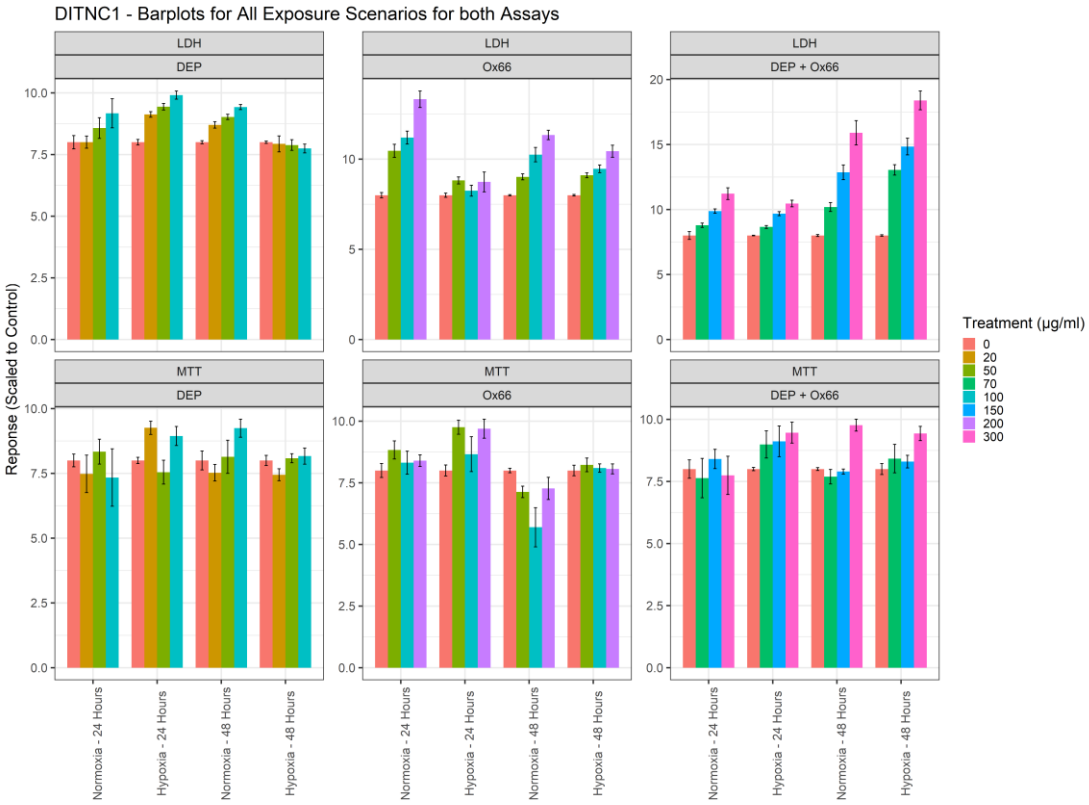

Figure 4. 19. Barplot of LDH and MTT assays for rat astrocytes (DITNC1). Response is absorbance at 490 nm scaled to control. Error bars represent standard error (N=3). LDH exhibits a positive dose-response relationship in all scenarios except for 48-hour hypoxic DEP and 24-hour hypoxic Ox66™ exposures. MTT responses are unclear and non-monotonic, although increases in response can be seen at higher doses in some exposures.

In the assay trend analysis (Fig 4.20), all LDH assay trends are significant except hypoxia exposures in DEP for 48 hours and in Ox66™ for 24 hours. Furthermore, both statistical trends are significantly different from the normoxic trend of their respective exposure. Therefore, in both scenarios, hypoxia had a significant protective effect that eliminated a dose-dependent cellular damage response. However, this reduction in toxicity is not seen significantly in other hypoxia exposures in this cell line and is not accompanied by any significant changes in MTT levels that indicate increased proliferation. The linear regression plots can be found in the appendix, Fig A.7.

Like the previous cell lines, the pro-inflammatory cytokine response (Fig 4.21) is varied depending on the compound and analyte in question. IL-6 production is slightly elevated in DEP normoxic exposure but not in Ox66™ or mixture. Hypoxia appears to significantly reduce the secretion of IL-6 compared to normoxia, with the greatest reduction seen in the DEP exposure. In contrast, all exposures elevate GRO/KC production from that of the control, with hypoxia significantly reducing the observed response. TNFα production follows a similar trend with increases across all normoxia exposures and significant reductions in hypoxia response when compared to those of normoxia.

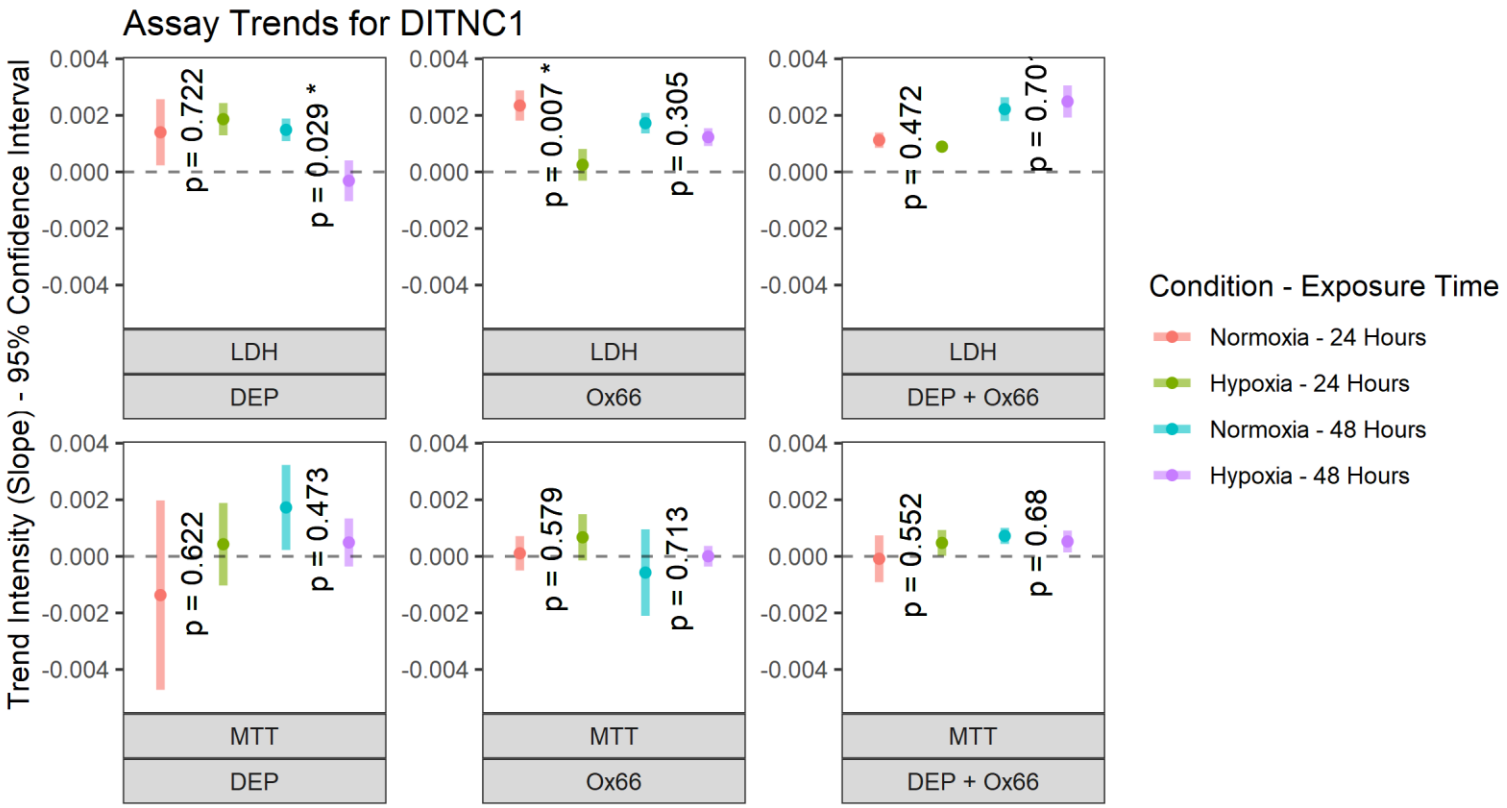

Figure 4. 20. Assay trends for rat astrocytes (DITNC1) from linear regression. Dots represent slopes and bars represent 95% CI (N=3). * represent a significant different between a normoxic and hypoxic assay trend ($p < 0.05$). Two scenarios, DEP in 48 hours and Ox66™ in 24 hours show a significant reduction of an LDH trend to a complete lack of significant response. No significant trend changes between normoxia and hypoxia occur in MTT, and the protective significant LDH shits are not accompanied by MTT upregulation.

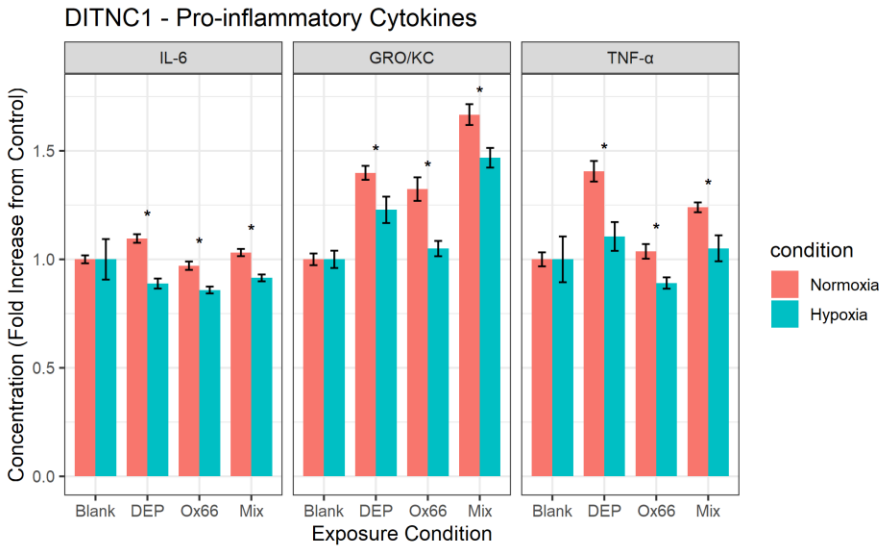

Figure 4. 21. Pro-inflammatory cytokines for DITNC1 cells in 48-hour exposures at the highest dose. Error bars represent standard error (N=3). * indicates $p < 0.05$. IL-6 production is elevated only in DEP normoxia. GTO/KC and TNFα are elevated from controls in all exposure scenarios. Hypoxia significantly reduces the production of all 3 cytokines when compares to normoxia.

The Effect of Ox66™ and DEP mixtures on LDH

The comparisons between the calculated DEP and Ox66™ mixtures responses (the direct addition of their dose-response slopes) and the experimental slopes in hypoxia are divided by cell line. Fig 4.22 shows the LDH experimental and calculated slopes and their 95% confidence intervals for all cell lines in 24-hour exposure scenarios. Here, large confidence intervals due to high standard error obscure the ability to make meaningful inferences. The same issue is present in 48-hour exposures (Fig 4.23), with large confidence intervals making any statistical findings about the relationship between the calculated and experimental trend unattainable.

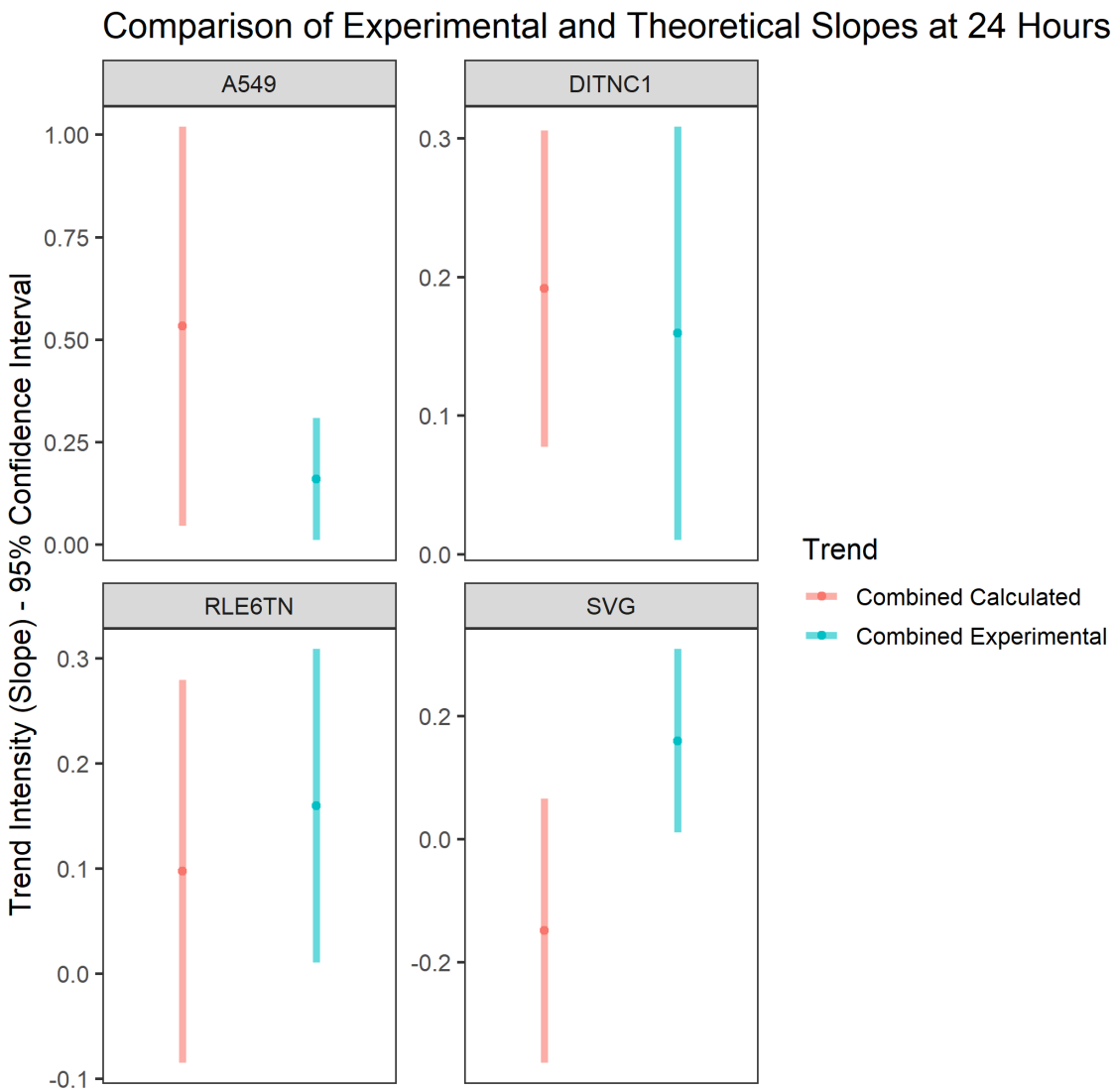

Figure 4. 22. Calculated and Experimental slopes for LDH for all cell lines in hypoxia at 24 hours. Bars represent standard error (N=3). Although some trends may be discerned, large confidence intervals preclude any statistical certainty.

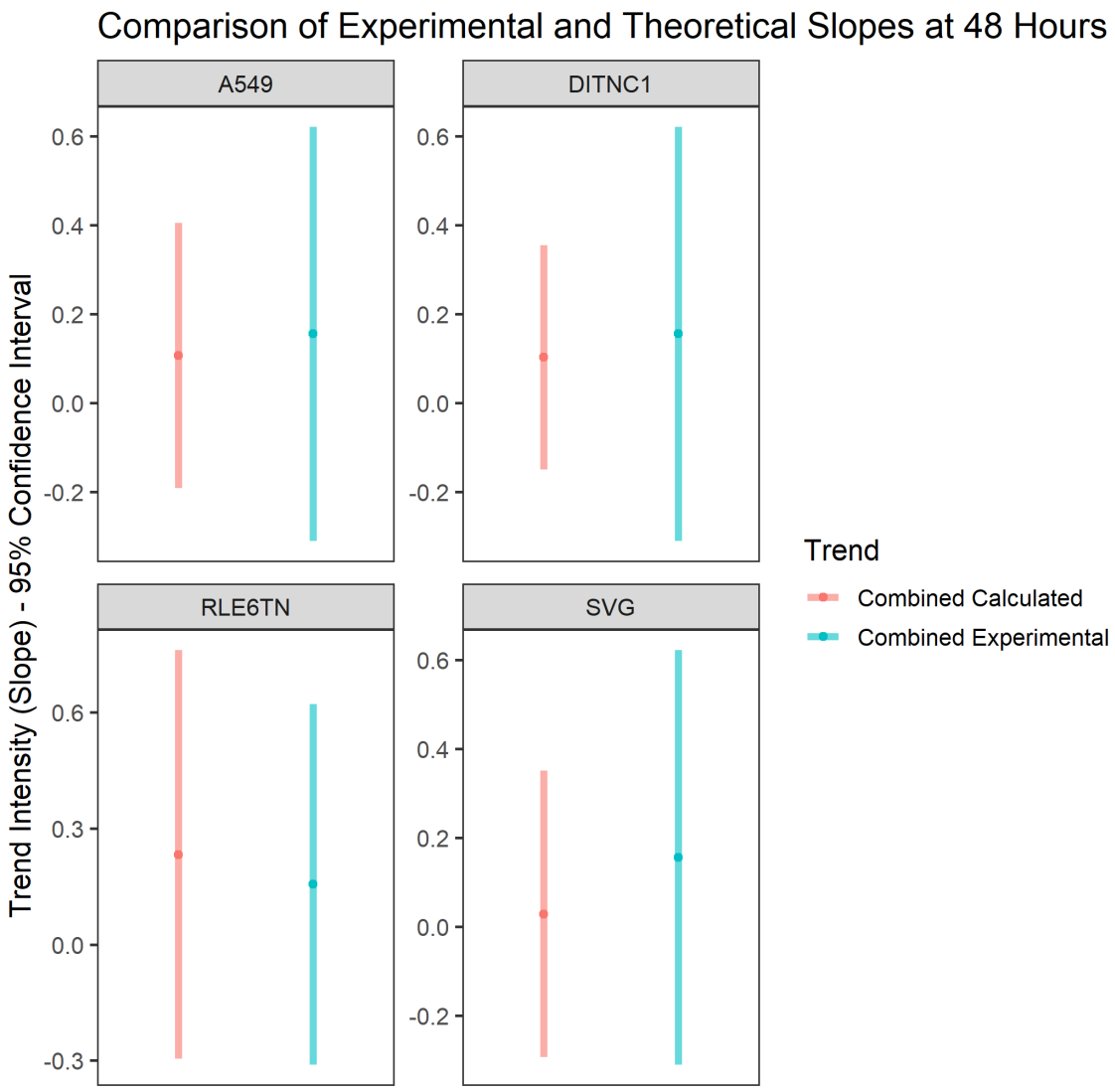

Figure 4. 23. Calculated and Experimental slopes for LDH for all cell lines in hypoxia at 48 hours. Bars represent standard error (N=3). Although some trends may be discerned, large confidence intervals preclude any statistical certainty.

CHAPTER FIVE

Discussion

Ox66™ Chemical Analysis

The elemental analysis of Ox66™ reveals its composition of aluminum and oxygen, with trace presence of chlorine atoms (around 1%). In nature, aluminum and oxygen exist as aluminum hydroxide such as in the naturally occurring gibbsite mineral or aluminum oxide in minerals like corundum (Porto & Krishnan, 1967; Saalfeld & Wedde, 1974). In the case of aluminum oxide, several rations of aluminum to oxygen exist due to the varying aluminum oxygenation states, with two aluminum atoms connecting up to 4 oxygen atoms in the form of Al_2O_4 (Nemukhin & Weinhold, 1992). This gives a starting point for the characterization of the possible structure and chemical behavior of Ox66™. However, of note is that the ration of oxygen atoms in the structure of Ox66™ as evident by EDS analysis is over 63%, which is higher than the observed oxygen ratio of 50% present in the highest aluminum oxidative state in dinucleic aluminum oxide. This suggests enrichment of oxygen in the Ox66™ structure beyond what may typically be observed in naturally occurring compounds of close structure.

The presence of large numbers of -OH ligands suggested by IR hints towards similarity to aluminum hydroxide structures. However, aluminum hydroxide molecules, which typically contain -OH ligands, possess far too many oxygen molecules (300% atomic ratio of oxygen to aluminum) to concur with the EDS analysis. Therefore, Ox66™ structure may be a hybrid of aluminum hydroxide and aluminum oxide structures. A full

elucidation of Ox66™ structure may then be required to understand the exact proportion of aluminum oxide and aluminum hydroxide structures within the compound. This may include more extensive mass spectrometry analysis involving fragmentation data and the use of annealing procedures to acquire a more defined crystalline structure.

The mass spectrometric analysis reveals a dynamic behavior of the dissolved portion of Ox66™ in aqueous solution. As suggested by the positive ion mass spectrogram (Fig 4.6), Ox66™ appears to undergo a series of ligand exchanges, substituting various -OH ligands with methanol (CH_3OH) ligands in solution. Furthermore, some of the ligands may be completely detached from the aluminum center and replaced only with a hydrogen atom. It is unclear whether the exclusive presence of -OH ligands rather than pure -O ligands is a product of these chemical interactions taking place only in the aluminum hydroxide portions of the Ox66™ structure, as it is possible that free -O ligands are quickly protonated by other compounds in solution. However, these ligand exchanges suggest that a chemical exchange mechanism may be partially behind the oxygenating behavior of Ox66™ in biological tissue, including possible protein interactions. Additionally, the exchange of methanol into the ligands suggest that the activity of Ox66™ is initiated or enhanced in organic microenvironments, and that this activity requires the presence of the compound in certain tissue or conditions. One caveat to note is that these behaviors were observed under basic conditions of around 9-10 pH, and that they may not fully represent the chemical behavior of Ox66™ in biological conditions. If a method of increasing Ox66™ solubility in solutions without pH alterations is developed, it would allow confirmation of the ESI-MS findings.

XRD analysis did not prove to be revelatory as to the exact structure of Ox66™, although it indicates the amorphous nature of the raw compound. However, it is common for aluminum-oxygen compounds to exhibit poor crystallinity, as is the case with aluminum oxide (Beevers & Ross, 1937). Such poor crystallinity is attributed to a structural property wherein atoms within the structure occupy crystalline sites only partially. An annealing process is often applied using temperatures exceeding 600 ^{o}C to acquire a better crystalline structure. During this process, aluminum oxide undergoes structural changes, producing polymorphs known as transition aluminas which exhibit decreased disorder and increased crystallinity (Temuujin et al., 2000). Furthermore, the resulting crystalline structures are sensitive to the initial conditions of the aluminum oxide synthesis including the precursors used. Figure 5.1 shows the XRD results for alumina compounds prepared from aluminum hydroxides derived from 3 different aluminum salts. The amorphous structure at lower temperatures is similar for all precursors, but clear differences emerge in the crystalline structure resulting from heating to 1200 ^{o}C.

The transformation of aluminum oxides to more orderly crystalline structure via annealing, and the divergence of such structures depending on synthesis conditions further confirms the chemical flexibility of aluminum-oxygen compounds. The unique behavior of Ox66™ as an oxygen delivery system may then be a result of certain structural qualities resulting from the conditions of the synthesis process. Additionally, it may be possible to induce an enhanced crystal structure and learn more about the properties of Ox66™ by subjecting it to a similar process of annealing, followed by analytical chemical analysis and a re-assessment of biological activity.

In general, and while the exact mechanism and structure of Ox66™ remains unknown, the observed data points to a complex structure that may behave dynamically in solutions, and points towards a better understanding of its possible mechanism of action in biological tissues. The confirmation of this dynamic behavior in biological tissue requires its replication under more biologically relevant pH conditions.

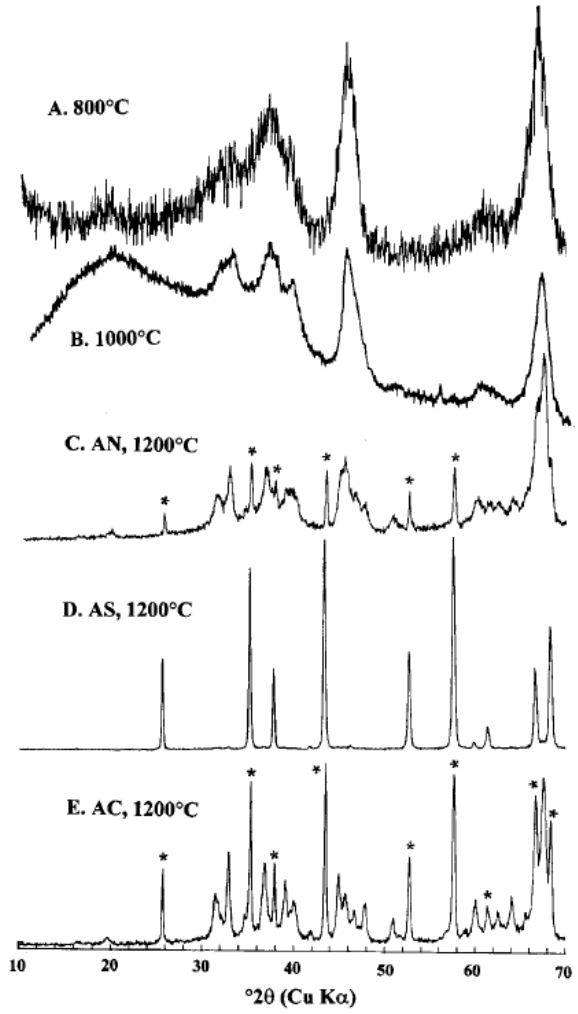

Figure 5. 1. XRD results for aluminas of aluminum hydroxides derived from 3 different aluminum salts and annealed to various temperatures. At 800 ^{0}C and 1000 ^{o}C all three precursors have a similar amorphous structure. At 12000 ^{o}C a clear crystalline structure emerges and is distinct for each precursor. Asterisks denote peaks corresponding to α-alumina (Temuujin et al., 2000).

Cytotoxicity and Hypoxia

While hypoxia has been documented to induce wide-reaching effects on cellular function and metabolism, the effects of hypoxia on the toxicity of DEP, Ox66™, and their mixtures appear to be complex and exhibit a high degree of variance within cell lines, exposure times, and compound of exposure. Physiologically, changes concerning the effect of DEP toxicity on lung cells may be the most physiologically relevant, as lungs form one of the earliest lines of defense against air pollutants following the respiratory epithelium. Furthermore, in real inhalation scenarios, only those particles smaller than 100 nm in dimeter are able to translocate across the lungs and exert extrapulmonary effects (Mühlfeld, 2008). Given that such particles comprise a small fraction of the overall mass of inhaled particulate matter (Annette Peters, Wichmann, Tuch, Heinrich, & Heyder, 1997), the bulk of the physiological interface between hypoxia and toxicity would manifest in the lungs at a given concentration. However, a large limitation remains as to the chronic effects of such an interaction, and the balance of physiological relevance may shift towards neurological tissues in cases of prolonged exposure.

For A549 cells, LDH increase for a 24-hour exposure in normoxia to DEP is around 15%. While this is only a moderate increase in cellular membrane damage, this result is in line with other studies which have shown LDH increases in the range of 5-20% in comparison to control following exposure to similar concentrations of diesel exhaust particle and other related particulate matter for 24 hours (Alessandria, Schilirò, Degan, Traversi, & Gilli, 2014; Danielsen, Loft, Kocbach, Schwarze, & Møller, 2009; M Durga, Nathiya, & Devasena, 2014; Schilirò, Alessandria, Degan, Traversi, & Gilli,

2010). However, the severity of LDH release is highly dependent on the exact composition of the particulate matter being used. For instance, the cytotoxic effect may vary drastically when the particulate matter samples are collected in different seasons (Alessandria et al., 2014) or when different reference materials are used (Danielsen, Loft, & Møller, 2008). It is then important to note that these results may not be consistent for other air pollutants or combustion matter from the engines of different vehicles. For 48 hours normoxia exposures, the toxicity trend appears similar, with no marked increase due to the prolonged exposure. This is also in line with another study which has shown similar toxicity for 24- and 48-hour exposure to particulate matter (Schilirò et al., 2010). Schiliro et al, however, observed a large increase in toxicity for some forms of particulate matter for a 72-hour exposure. Therefore, even a 48-hour exposure may not be sufficient to account for chronic effects. A549 cells Ox66™ and DEP also exhibit an LDH for exposure to Ox66™ and to the mixture. Response to Ox66™ is more elevated in comparison to DEP alone (around 20% change at 100 μg/ml), while response to the mixture is higher than either of the two compounds alone (around 50% change at 100 μg/ml). Just as in with DEP alone, the effects are similar for 24 and 48 hours for Ox66™ and mixture. In general, the LDH response for A549 appears to be mild for DEP and Ox66™ alone and more severe for the mixture, and the response is not remarkably different between 24- and 48- hour exposures.

As for MTT in A549 cells, the DEP exposure elicits a small response of around 15% at the highest dose for both 24- and 48- hour exposures. However, the direction of this response is positive, suggesting increased viability or metabolism with increasing doses of DEP, which is in opposition to the expected response considering the LDH

increase. Furthermore, the linear trend of the MTT response is not significant for either exposure lengths, with the confidence interval encompassing zero. While this lack of MTT response and discrepancy between LDH and MTT does not comport with some studies on the effects of particulate matter toxicity (M Durga et al., 2014; Mohan Durga, Nathiya, Rajasekar, & Devasena, 2014), other studies have found a discrepancy between LDH and MTT results for A549 exposures to aqueous $PM_{2.5}$ extract (Alessandria et al., 2014) and organic extracts from traffic PM (Shang et al., 2013). In both studies, however, the discrepancy is the opposite of the one observed in this study and involves decreases in MTT that are not accompanied by corresponding increases in LDH. The authors of the two studies suggest that such a discrepancy may be explained by a cytotoxicity mechanism which involves an apoptotic pathway that does not result in damage to cell membrane viability, or by the inability of the MTT assay to distinguish between reductions in cell metabolic activity and loss of cell viability. On the other hand, a study on the effects of DEP on serum-deprived A549 cells has found DEP exposure protects cells from decreases in viability by arresting the cell cycle and interfering in apoptotic pathways, while simultaneously inducing an inflammatory response (Bayram et al., 2006). Given these studies, it is possible that the discrepancy between LDH and MTT results observed in this study may be the result of simultaneous protection of cell death via cell cycle arrest of most of the cell population and induction of cellular membrane damage for a smaller portion of the population. The same discrepancy is seen in Ox66™ and mixture exposures, with the one exception being Ox66™ exposure at 48 hours, where a massive reduction in MTT is observed. Therefore, increased cellular membrane damage that does not induce decreased cellular viability may be a common cytotoxic

behavior of A549 cells. It is also possible that Ox66™ alone may produce a unique cytotoxic pathway during longer exposure of A549 cells.

Inflammatory cytokines and chemokines are not released at any notable levels for exposure to DEP in normoxia, although IL-8 is slightly elevated with around a 10% increase. Many studies, on the contrary, have shown much higher increases in IL-6 and IL-8, and TNF-α increases in A549 and other lung epithelial cells following exposure to DEP, including for shorter periods of time (Bayram et al., 1998; Mohan Durga et al., 2014; J Øvrevik, Låg, Holme, Schwarze, & Refsnes, 2009; Tang et al., 2012). However, some disagreement within the literature exists. For instance, one study has shown an inhibition of IL-6 an IL-8 release for short exposures and no different in their release for 48-hour exposures (Juvin et al., 2002), and another study has shown no effect of DEP on the release of IL-8 in A549 cells in the presence of serum in the media (Bayram et al., 2013). These differences in cytokine and chemokine production between different studies may be attributed to the composition of the particulate matter used and the presence and levels of adsorbed compounds. For example, the cytotoxicity and inflammatory potential of particulate matter has been shown to vary greatly between the water-soluble fraction and the organic insoluble fraction, with the insoluble fraction exhibiting a larger cytotoxic effect and the water-soluble fraction increasing the production of inflammatory cytokine mRNA expression (Fujii, Hayashi, Hogg, Vincent, & Van Eeden, 2001; Jalava et al., 2008; Soukup & Becker, 2001). Therefore, the standard used in this experiment may be lacking in any significant water-soluble components, rendering it incapable of eliciting an inflammatory cytokine or chemokine response. On the other hand, Ox66™

and the mixture is associated with a significant increase in IL-8 production, but not IL-6 or TNFα.

To examine the effects of hypoxia on toxicity for A549 cells, the assay trends are the most pertinent indicators, as they allow for the comparison of the entirety of the dose-dependent response between normoxia and hypoxia. For LDH, the only significant decrease is at 24 hours for DEP exposure, where hypoxia ameliorates the small toxic trend observed. However, no meaningful changes between hypoxia and normoxia in LDH production for any of the other scenarios for this cell line exist. Therefore, hypoxia either creates no cellular membrane damage on its own or does not exacerbate the damage already inflicted by DEP, and in fact may slightly ameliorate such damage in the case of 24-hour DEP exposures. For MTT, hypoxia significantly alters the dose-response trend in two scenarios: Ox66™ at 48 hours and mixture at 48 hours. In the case of Ox66™, hypoxia's effect is ameliorative, completely removing the decrease in cell proliferation observed in normoxia. On the other hand, its effect for the mixture exposure is the opposite, with a decrease in MTT levels not observed in normoxic conditions. In both compounds, the MTT trend differences do not correspond to LDH trend differences, mirroring the lack of correspondence between LDH and MTT in normoxic DEP toxicity. Overall, there does not appear to be a consistent effect of hypoxia on toxicity in A549 cells for any of the compounds tested, and when an effect is present, no corroboration between assays exists. The discrepancy between LDH and MTT might be due to the same reasons stated earlier, namely the protective effect of DEP on cell viability and the inability of MTT to discern between cell viability and metabolic activity. In the case of cytokine and chemokine release, hypoxia consistently dampens the inflammatory marker

response induced by the tested compounds, and in fact appears to reduce IL-6 release to a level below the control for the DEP exposure. The reduction in inflammatory marker production is most pronounced and significant for IL-6 in Ox66™ and mixture exposures, where IL-6 production is reduced to levels close to control in hypoxia in contrast to a marked increase in normoxia. While hypoxia by itself has been shown to induce some inflammatory marker production in human cell lines while reducing others (Ghezzi et al., 1991; Karakurum et al., 1994; Naldini, Carraro, Silvestri, & Bocci, 1997), little research has been conducted on the ways in which hypoxia alters inflammatory marker production in response to chemical stresses or particulate matter. One study found no significant differences in LPS-mediated production of IL-8 in A549 cells but also found that dexamethasone exhibits reduced efficacy in the attenuation of IL-8 production in the presence of hypoxia (Y. Huang, Zhao, Lv, Ding, & Liu, 2009). LPS injury, however, is not necessarily representative of particulate matter toxicity. It is possible that the attenuation of inflammatory marker production is due to the downregulation of protein production observed in hypoxia, which would inhibit any protein response to outside cellular stress. It also may be that the induction of inflammatory markers by hypoxia alone may exhaust cellular mechanisms of cytokine and chemokine production, therefore causing a reduction in the ability of such cells to produce sufficient inflammatory markers following long-term hypoxia. Another possible explanation is that the decline in inflammatory cytokine levels is due to decreases in cell viability. However, this would only serve to explain the decline for exposures scenarios with high LDH production or low MTT levels. To summarize, hypoxia's effect on the production of the

inflammatory markers studied appears to be ameliorative, and its magnitude is only relevant for IL-8 production.

In rat RLE6TN cells, the cytotoxic response to DEP in normoxic conditions is different than for the comparable human cells. For instance, DEP exposure at 24 hours produces a non-monotonic response for LDH levels, with the highest response observed at the 50 μg/ml dose rather than the 100 μg/ml. Furthermore, the maximum response at 50 μg/ml is markedly higher than that of A549 cells (84% increase compared to 15%). For DEP toxicity at 48 hours in normoxia, the trend is monotonic again, and the maximum toxicity at the highest dose is lower than for 24 hours but still higher than for A549 cells (66% compared to 15%). The RLE6TN cells then are more sensitive to DEP exposures than their human counterparts, This concurs with a study showing increased sensitivity of RLE6TN cells in comparison to A549 cells to metal toxicity (Riley et al., 2005). However, RLE6TN do exhibit a similarity in that 48-hour exposures do not significantly alter the observed toxicity trend. Additionally, normoxic exposures produce comparable toxic trends in RLE6TN and A549 cells for Ox66™ and mixture exposure. Therefore, the heightened sensitivity of RLE6TN cannot be assumed for all cytotoxic scenarios. For the MTT assay, RLE6TN exhibits a different response in normoxia to that of A549 cells, with rat cells being slightly more sensitive but also exhibiting a more expected pattern of general dose dependent MTT decline in all normoxic scenarios. However, this decline is not monotonic in any but the 24-hour response to mixture exposure. This lack of monotonic response translates to the mostly flat linear trends observed after regression. However, while a decrease of MTT points to better consistency between LDH and MTT for this cell line, the lack of consistency remains when

examining responses at individual levels and the general magnitude of response for specific scenarios. For instance, the large increase in LDH level at the 50 μg/ml dose in the 24-hour normoxia exposure does not correspond to a similar decrease in MTT levels. Furthermore, the MTT trend magnitude is similar for Ox66™ and mixture exposures at 24 hours in normoxia despite the LDH levels for the mixture exposure being markedly higher.

The inflammatory marker release of RLE6TN is similar to that of A549 for IL-6 and TNG-α in all exposures and for DEP IL-8 secretion. However, the effects on GRO/KC are different than those observed for IL-8 in A549 cells for Ox66™ and mixture. While DEP drives a similar increase of GRO/KC in both cell lines, Ox66™ and the mixture results in the opposite, with a decrease in GRO/KC production compared to the control. Given that MTT production is also decreased in both those scenarios, the decrease in observed GRO/KC may be attributed to a decrease in cell viability rather than a decrease of secretion per cell. This has been observed in other cytotoxicity experiments involving RLE6TN cells where a large decrease in inflammatory marker production is almost entirely attributed to plummeting cell viability and metabolic activity (Riley, Boesewetter, Kim, & Sirvent, 2003).

Much like A549 cells, the effect of hypoxia on RLE6TN cells is divergent and not strong. An increase in toxicity is observed for Ox66™ and mixture at 48 hours in hypoxia compared to normoxia. However, the regression lines do not report significantly different slopes, and the increase in LDH production does not correspond to a reduction in MTT between normoxia and hypoxia. The only significant slope differences between normoxia and hypoxia is for the cell lines is for MTT at the 24-hour mixture exposures. Therefore,

the results do not support a strong exacerbation of cytotoxicity by any of the compounds. For inflammatory markers, hypoxia produced a difference in the response compared to normoxia only in GRO/KC for the mixture exposure and TNFα for the Ox66™ exposure. In these scenarios, hypoxia increases cytokine production in comparison to normoxia, an opposite direction to the one observed in A549 cells. RLE6TN cells appear to undergo different metabolic and protein-production changes when exposed to hypoxia from those A549 cells undergo. Only *in vivo* experiments regarding the effects on hypoxia on inflammatory marker production following particulate matter exposure would shed more light on which cell line is more translatable for such studies.

For the human astroglia SVGp12, DEP induce an increase in LDH production of around 16% for the 24-hour normoxia exposure, similar to that of A549 cells. However, unlike the two lung cell lines, the 48-hour toxicity in normoxia for human astrocytes is around 33%, almost double the 24-hour effect, suggesting that SVGp12 may be more sensitive to prolonged exposures than lung cells. Much of the literature surrounding the neurotoxicity of diesel exhaust particles both *in vivo* and *in vitro* has focused on the role of microglia and microglial activation in neurotoxicity of diesel exhaust particle and particulate matter (Allen et al., 2014; Block et al., 2004; L. G. Costa et al., 2017; Levesque et al., 2011). However, studies which examined microglial or astrocyte cell viability have found similar levels of LDH release to those in this study at comparable concentrations (Bai et al., 2019; Block et al., 2004). For Ox66™ exposure, no LDH release is observed for the 24-hour normoxic exposures, but a 40% increase is observed for the 48-hour normoxic exposure, further pointing to an increased susceptibility for this cell line in longer exposures. However, the mixture normoxic exposure shows little

difference between 24- and 48-hour exposures. The lack of corroboration between the two assays is also evident in this cell line. MTT increases for DEP normoxic exposures despite an increase in LDH, a trend also observed in the 48-hour Ox66™ exposure. For mixture exposures, the 24-hour normoxia scenario is associated with a lack of MTT trend despite the LDH increase, while the similar LDH trend for the 48-hour normoxia scenario is accompanied by a decrease in MTT. Like A549 cells, the reasons for this could be multifaceted, including cell cycle arrests which decrease apoptotic activity and changes in cellular metabolic activity that do not necessarily reflect cellular proliferation.

IL-6 is decreased following exposure to DEP and the mixture, while slightly elevated following exposure to Ox66™. IL-8 is only elevated following exposure to Ox66™ and DEP, while TNFα is not affected by exposure to of the compounds compared to the control. In general, all the observed inflammatory marker trends are not very strong. A study of DEP exposure *in vitro* in human astrocytes following exposure to DEP has also found little increase in TNFα following (Campbell, Daher, Solaimani, Mendoza, & Sioutas, 2014). Although the period of exposure (24 hours) and the concentration (20 μg/ml) in that study are of a smaller magnitude, the lack of response in comparison to the microglia highlights a deficiency in inflammatory marker production by astrocyte cells and the importance of microglia in initiating and modulating the inflammatory response following particulate matter exposure.

In a similar vein to the two previous cell lines, hypoxia does not seem to exhibit a consistent impact on cytotoxicity. LDH levels are increased in hypoxic 24-hour exposures compared to normoxia, but not for 48-hour exposures. MTT levels are decreased in Ox66™ exposures both for 24 and 48 hours in hypoxia compared to

normoxia. For mixture exposure, hypoxia decreases MTT production for 24-hour exposures but for 48-hour exposures such a decrease only occurs at the highest dose level. For the linear regression trend lines, none of the differences are statistically significant. In the inflammatory marker territory, hypoxia exhibits a moderate effect on production levels in a few scenarios, although the effect is not significant. IL-6 production is significantly elevated in hypoxia compared to normoxia for Ox66™ while it is slightly but significantly elevated in TNF-α for Ox66™ and mixture exposures. The effect for IL-8 is trending towards reduction but is not statistically significant. The effects of hypoxia for IL-8, although not significant, are following a similar trend to those observed in the A549 cell line. The effects of hypoxia on cellular metabolism and protein production pathways that are present in A549 cells may also be present in SVGp12 cells then but to a much lesser extent.

For the last cell line, DITNC1, the 24-hour normoxia DEP LDH percent change from the control is around 18%, while the 48-hour change is around 33%, rendering its DEP LDH levels close to those of the human astrocytes. Ox66™ and the mixture exposures, on the other hand, are associated with higher LDH levels than those of SVGp12. MTT levels for this cell line are also the least monotonic of all the studied cell lines. However, this cell line shares the lack of correlation between MTT and LDH with the others, with similar LDH levels producing different MTT trends as is the case with normoxic 24- and 48- hour exposures for DEP. Another example is normoxic 48-hour exposure to the mixture, associated with a higher LDH production than the 24-hour normoxic exposure but also a higher MTT production. In contrast to the human astrocytes, inflammatory cytokines are elevated in all normoxic exposures for TNFα and

GRO/KC, except for TNFα at the Ox66™ exposure. The markers are also not significantly changed from the control at all normoxic exposures for the IL-6 marker. In rat brains exposed to particulate matter, the inflammatory marker production is concentrated in the mid brain rather than the cortex or olfactory bulb (Levesque et al., 2011). Given that astrocytes are the most abundant cell type in the brain, the production of inflammatory markers is then not entirely controlled by astrocytes, but rather by the presence and interaction of various neuro cells.

Hypoxia exhibits a divergent effect on cytotoxic assays in this cell line either, with LDH levels decreased for DEP in 48-hour hypoxic exposure compared to normoxic exposure, but not for 24-hour exposures. In mixture exposures, hypoxia also exhibits differential effects on LDH production. Ox66™ exposures appear to be the only ones impacted consistently by hypoxia, which reduces LDH release. The only significant linear slope differences are for DEP at 48 hours and Ox66™ at 24 hours. For inflammatory markers, DITNC1 cells exhibit a very similar but more consistent response to A549, with a significant reduction across all exposure scenarios.

The ability to discern the efficacy of Ox66™ by comparing the LDH trendlines of the mixture exposures with what theoretically would have occurred had the toxic effect been completely additive is unfortunately rendered not possible due to the large uncertainty as indicated by the large confidence interval for each of the slopes. Furthermore, given the low assay trend intensity and the lack of clear toxicity effect present in the MTT assays, their use would not have produced an intelligible result either. Therefore, the question of whether the efficacy of Ox66™ can be demonstrated *in vitro* in

a way that mirrors its observed effects *in vivo* remains open and would require more experiments to achieve higher statistical power.

CHAPTER SIX

Conclusions

The results of this study indicate that Ox66™ is an amorphous compound with structures similar to and derived from aluminum oxide and aluminum hydroxide, with higher oxygen content than that of aluminum oxide but lower than that of aluminum hydroxide, and that it exhibits a dynamic chemical behavior in aqueous solutions through serial ligand substitutions. The complex structure and aqueous behavior suggest that complex chemical processes and possible protein-mediated interactions in biological tissue may be responsible for its mechanism of efficacy.

In examining cytotoxicity of DEP, Ox66™, and their mixtures and the effect of hypoxia in four different cell lines derived from two tissues across two species, the study found that the LDH results for the DEP are in agreement with the established literature on similar compound and exposures conditions. While hypoxia does sometime influence cytotoxicity, no clear trend appears in regards to proliferation and viability. Furthermore, the two assays used, LDH and MTT, are not in agreement to the effect at any exposure, and the cause of this inconsistency is not clear, although several factors may be behind it. When analyzing the difference between calculated additive and experimentally measured LDH responses of mixtures of Ox66™ and DEP in hypoxia, the study found no statistically significant results in either 24 or 48-hour exposures, and therefore the efficacy of Ox66™ *in vivo* could not be evaluated.

In examining the production of the cytokines IL-6, IL-8 and its rat homologue GRO/KC, and TNFα, the study found that the compounds induce significant changes in cytokine expression, although the direction and magnitude is not consistent, with some exposures resulting in a decrease of cytokine production. The effect of hypoxia on the cytokine response was also divergent, with significant decreases of cytokine production observed in A549 and DITNC1 cells and slight significant increases in RLE6TN and SVGp12 cells.

These results suggest that while the risk profiles for particulate matter exposures in patients suffering from concurrent chronic hypoxia may be altered relative to those without persistent hypoxia, the effect varies depending on the cell line, compound, and length of exposure. Further experiments may be carried out on a larger set of cytokines and using primary cells which may alleviate some of the discrepancies present in the colorimetric cytotoxic assays.

APPENDIX

APPENDIX

Additional Figures

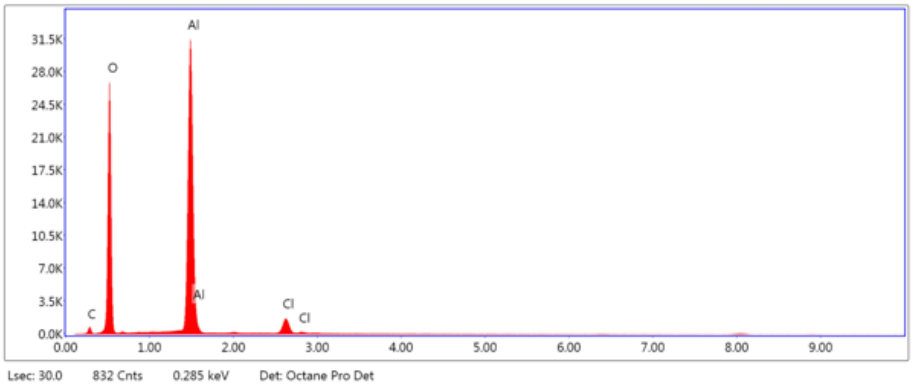

eZAF Smart Quant Results

Element	Weight %	Atomic %	Net Int.	Error %	Kratio	Z	R	A	F
C K	7.79	11.82	218.32	11.18	0.0136	0.0135	1.0823	0.9650	0.1599	1.0000
O K	56.66	64.57	8476.74	7.33	0.2229	0.2223	1.0360	0.9857	0.3788	1.0000
AlK	32.98	22.29	14947.01	4.05	0.2156	0.2156	0.9216	1.0246	0.7075	1.0025
ClK	2.57	1.32	973.10	3.55	0.0190	0.0191	0.8772	1.0477	0.8397	1.0098

Figure A. 1. EDS results for Ox66™ on a different spot from the same grain. The ratio of Oxygen to Aluminum atomic abundance is around 2.95.

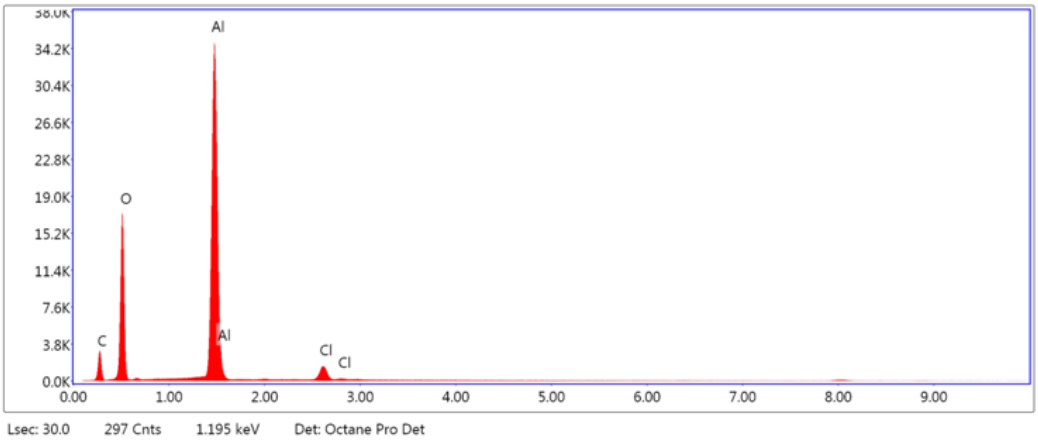

eZAF Smart Quant Results

Element	Weight %	Atomic %	Net Int.	Error %	Kratio	Z	R	A	F
C K	23.62	33.26	867.06	9.87	0.0456	0.0456	1.0694	0.9700	0.1804	1.0000
O K	44.50	47.04	5378.90	8.54	0.1200	0.1201	1.0233	0.9904	0.2638	1.0000
AlK	29.93	18.76	16433.67	3.72	0.2020	0.2020	0.9100	1.0285	0.7398	1.0025
ClK	1.95	0.93	880.15	3.34	0.0147	0.0147	0.8661	1.0511	0.8617	1.0104

Figure A. 2. EDS results for Ox66™ for a spot on a different grain from the same batch. The ratio of oxygen to aluminum atomic abundance is 2.47. The increased presence of carbon abundance is a function of the difference in grain dimensions which creates a larger signal from the background carbon tape the sample is placed on.

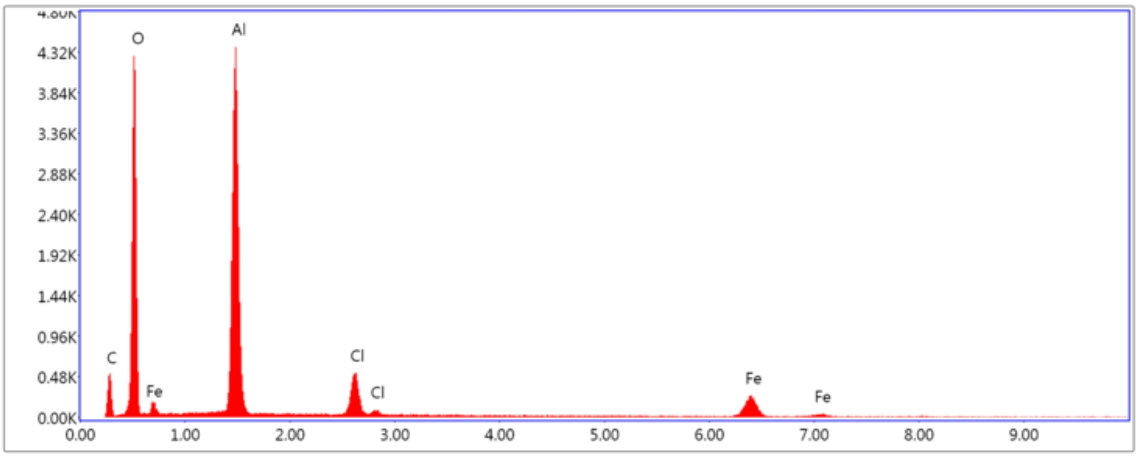

PeBaZAF Smart Quant Results

Element	Weight %	Atomic %	Net Int.	Error %	P/B Ratio	R	F
C K	6.59	10.14	56.76	17.84	0.00 0.00	1	1
O K	60.96	70.40	797.10	16.85	0.00 0.00	1	1
AlK	22.66	15.52	1,030.21	7.12	320.80 320.80	1.01	1
ClK	3.69	1.92	151.45	7.37	71.84 71.84	1.01	1.01
FeK	6.10	2.02	110.72	9.19	136.24 136.24	1.03	1.08

Figure A. 3. EDS results for Ox66™ for a spot on a grain from a different batch. The ratio of oxygen to aluminum atomic abundance is 2.65. The presence of an iron peak is the result of the use of a different placement tape containing iron.

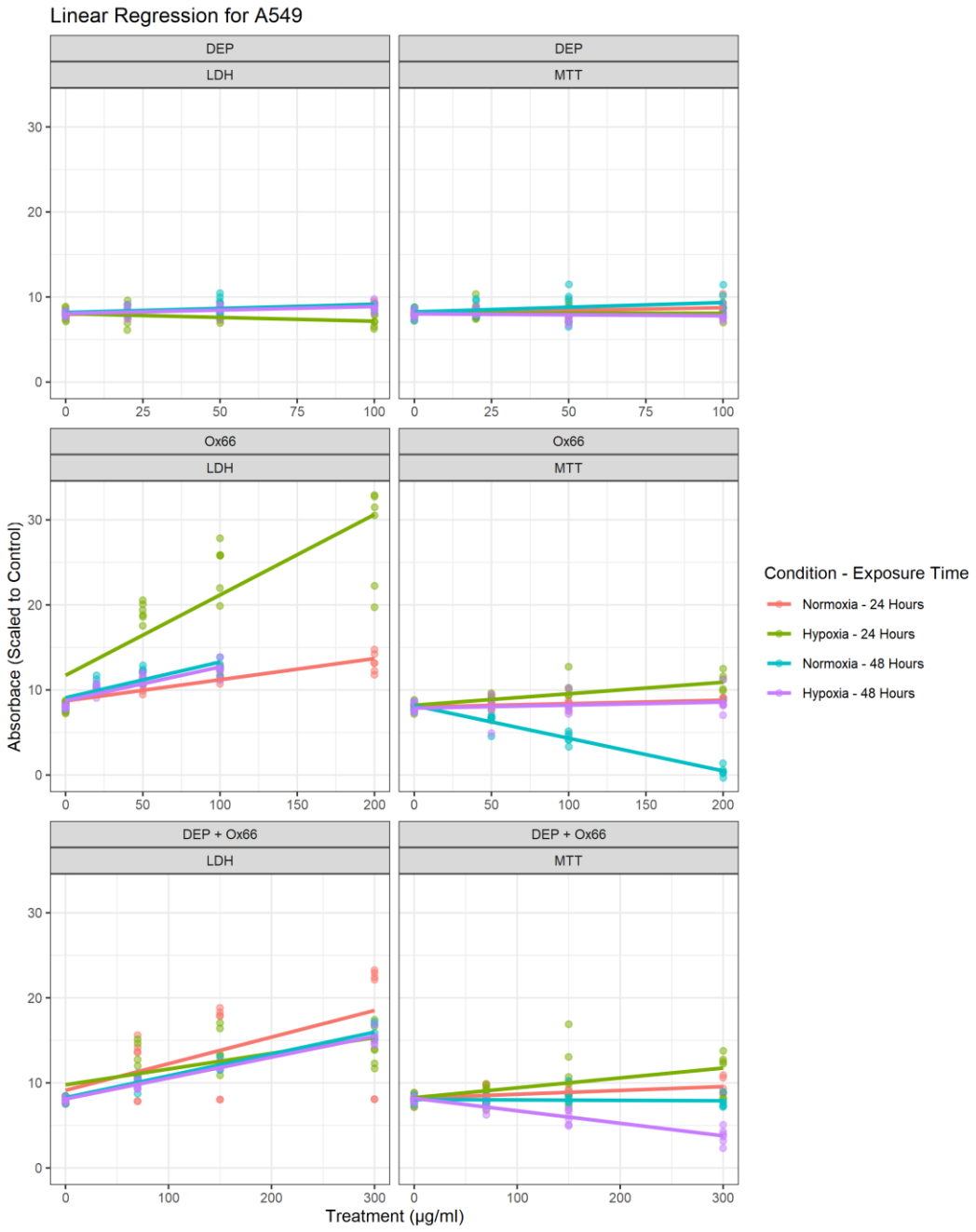

Figure A. 4. Linear regression lines for A549 cells for both LDH and MTT assays. The slopes from these lines where estimated via maximum likelihood estimation (N=3). The slopes of each line and its 95% CI was recorded for use in trend comparison.

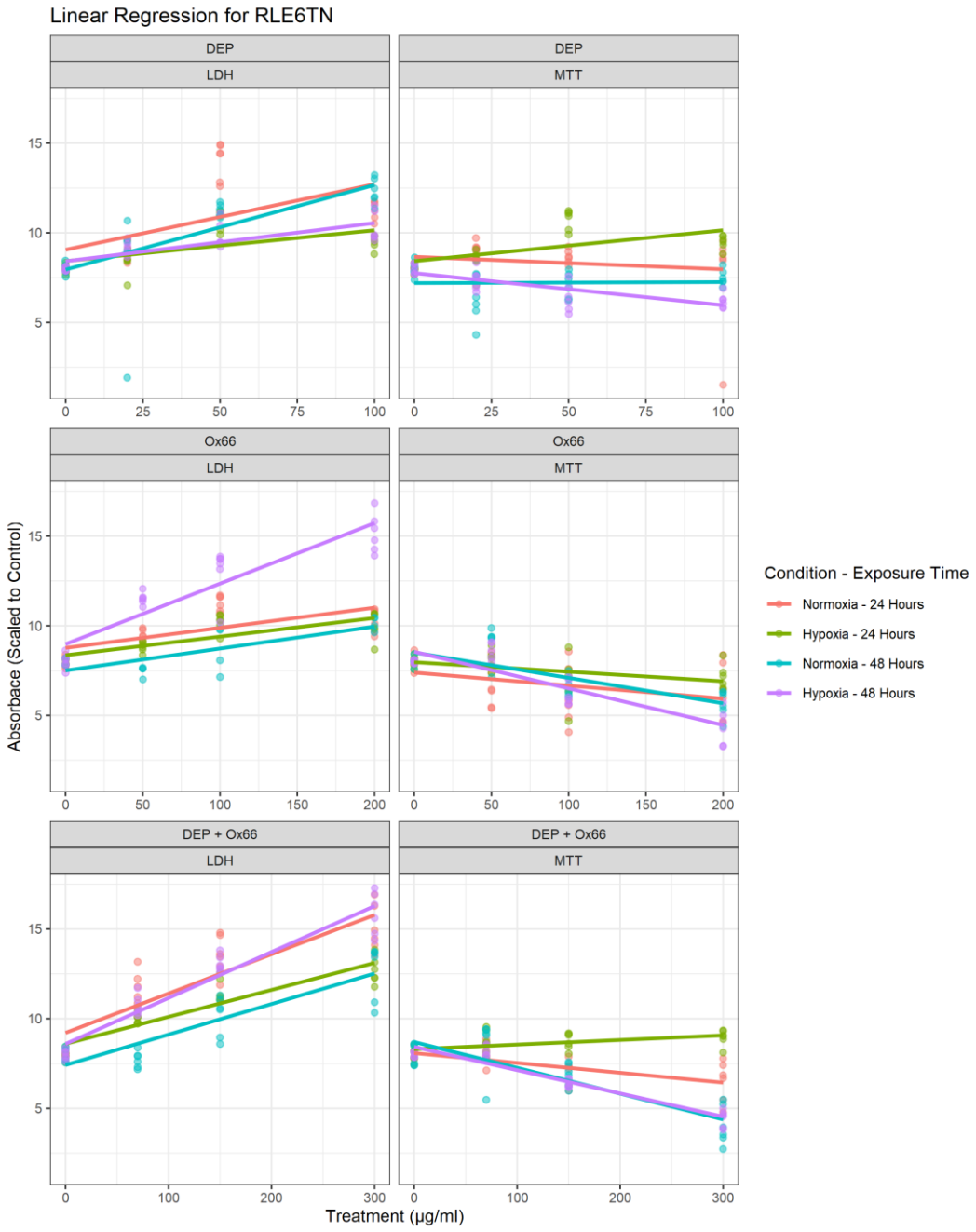

Figure A. 5. Linear regression lines for RLE6TN cells for both LDH and MTT assays. The slopes from these lines where estimated via maximum likelihood estimation (N=3). The slopes of each line and its 95% CI was recorded for use in trend comparison.

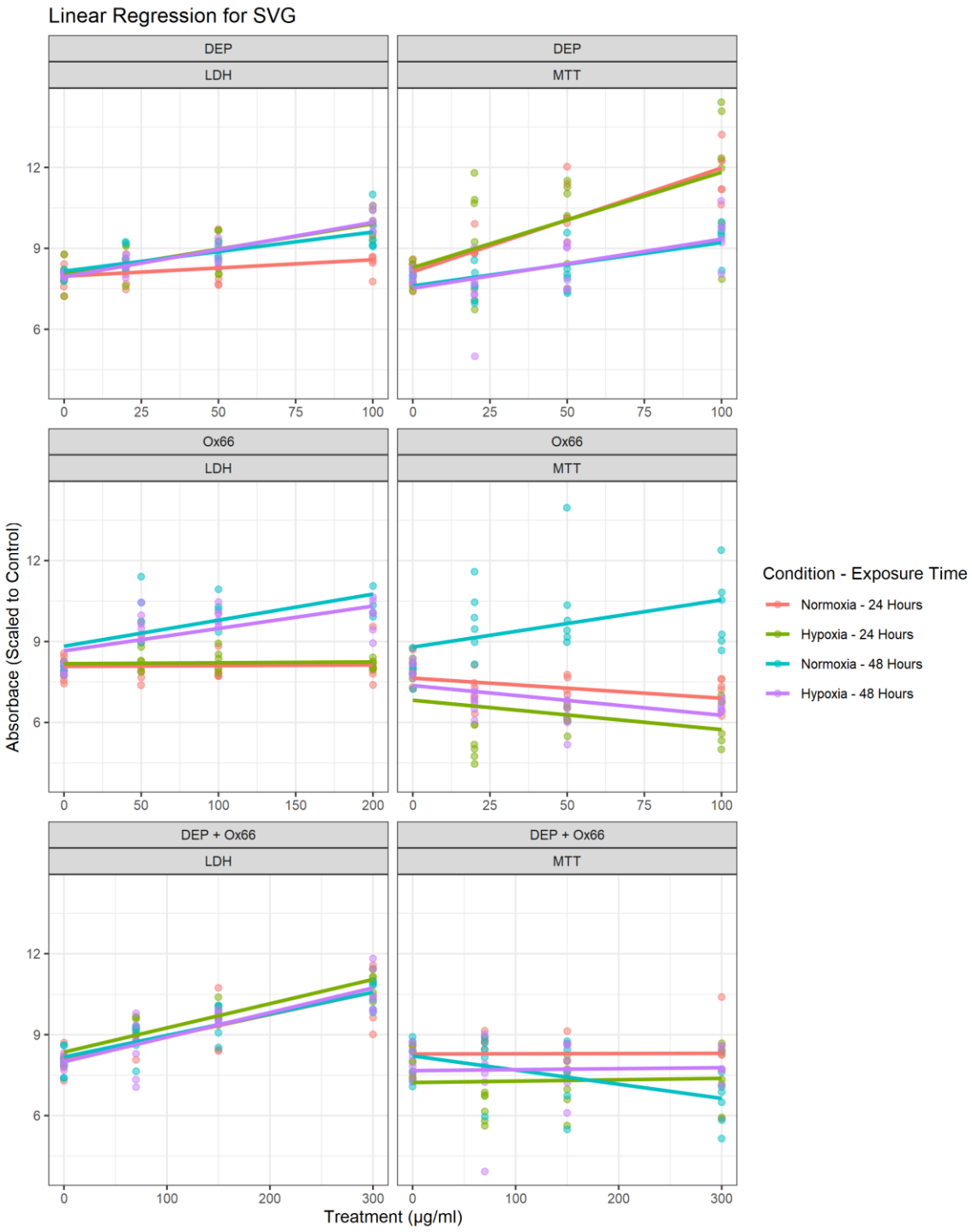

Figure A. 6. Linear regression lines for SVGp12 cells for both LDH and MTT assays. The slopes from these lines where estimated via maximum likelihood estimation (N=3). The slopes of each line and its 95% CI was recorded for use in trend comparison.

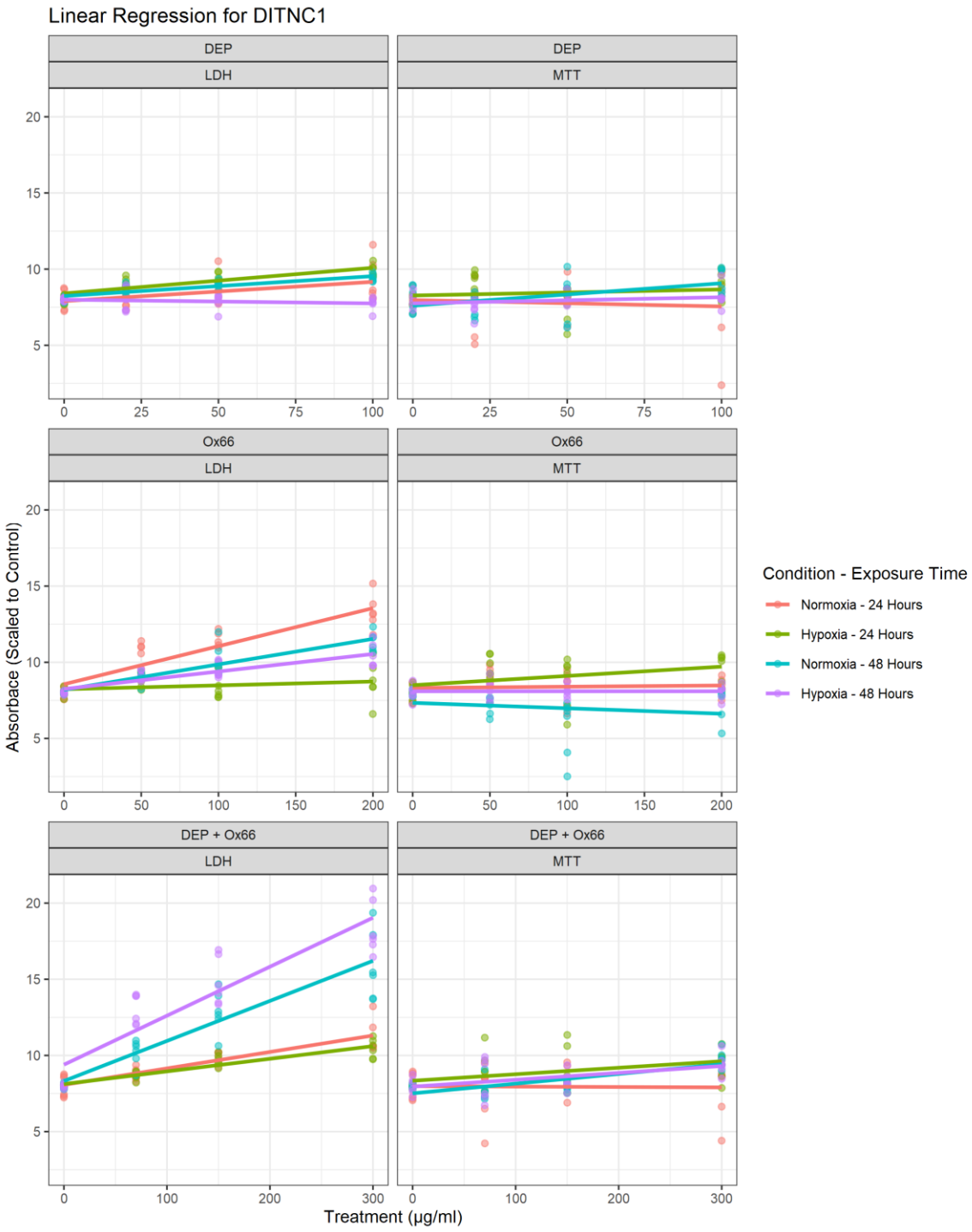

Figure A. 7. Linear regression lines for DITNC1 cells for both LDH and MTT assays. The slopes from these lines where estimated via maximum likelihood estimation (N=3). The slopes of each line and its 95% CI was recorded for use in trend comparison

REFERENCES

Abbey, D. E., Nishino, N., McDonnell, W. F., Burchette, R. J., Knutsen, S. F., Lawrence Beeson, W., & Yang, J. X. (1999). Long-term inhalable particles and other air pollutants related to mortality in nonsmokers. *American journal of respiratory and critical care medicine, 159*(2), 373-382.

Agustí, A. G. N., Noguera, A., Sauleda, J., Sala, E., Pons, J., & Busquets, X. (2003). Systemic effects of chronic obstructive pulmonary disease. *European Respiratory Journal, 21*(2), 347. doi:10.1183/09031936.03.00405703

Alayash, A. I. (2004). Oxygen therapeutics: can we tame haemoglobin? *Nat Rev Drug Discov, 3*(2), 152-159. doi:10.1038/nrd1307

Alessandria, L., Schilirò, T., Degan, R., Traversi, D., & Gilli, G. (2014). Cytotoxic response in human lung epithelial cells and ion characteristics of urban-air particles from Torino, a northern Italian city. *Environmental Science and Pollution Research, 21*(8), 5554-5564.

Allen, J. L., Liu, X., Weston, D., Prince, L., Oberdörster, G., Finkelstein, J. N., . . . Cory-Slechta, D. A. (2014). Developmental exposure to concentrated ambient ultrafine particulate matter air pollution in mice results in persistent and sex-dependent behavioral neurotoxicity and glial activation. *Toxicological Sciences, 140*(1), 160-178.

Amara, N., Bachoual, R., Desmard, M., Golda, S., Guichard, C., Lanone, S., . . . Boczkowski, J. (2007). Diesel exhaust particles induce matrix metalloprotease-1 in human lung epithelial cells via a NADP(H) oxidase/NOX4 redox-dependent mechanism. *American Journal of Physiology-Lung Cellular and Molecular Physiology, 293*(1), L170-L181. doi:10.1152/ajplung.00445.2006

Anderson, J. O., Thundiyil, J. G., & Stolbach, A. (2012). Clearing the air: a review of the effects of particulate matter air pollution on human health. *Journal of Medical Toxicology, 8*(2), 166-175.

Andrade, C. F., Kaneda, H., Der, S., Tsang, M., Lodyga, M., Chimisso Dos Santos, C., . . . Liu, M. (2006). Toll-like receptor and cytokine gene expression in the early phase of human lung transplantation. *The Journal of heart and lung transplantation : the official publication of the International Society for Heart Transplantation, 25*(11), 1317-1323.

Antonelli-Incalzi, R., Corsonello, A., Trojano, L., Pedone, C., Acanfora, D., Spada, A., . . . Rengo, F. (2007). Screening of cognitive impairment in chronic obstructive pulmonary disease. *Dementia and geriatric cognitive disorders, 23*(4), 264-270.

Araujo, J. A., & Nel, A. E. (2009). Particulate matter and atherosclerosis: role of particle size, composition and oxidative stress. *Particle and fibre toxicology, 6*(1), 24.

Arsham, A. M., Howell, J. J., & Simon, M. C. (2003). A novel hypoxia-inducible factor-independent hypoxic response regulating mammalian target of rapamycin and its targets. *Journal of Biological Chemistry, 278*(32), 29655-29660.

Avramovich-Tirosh, Y., Bar-Am, O., Amit, T., Youdim, M., & Weinreb, O. (2010). Up-regulation of hypoxia-inducible factor (HIF)-1α and HIF-target genes in cortical neurons by the novel multifunctional iron chelator anti-Alzheimer drug, M30. *Current Alzheimer Research, 7*(4), 300-306.

Bai, K.-J., Chuang, K.-J., Chen, C.-L., Jhan, M.-K., Hsiao, T.-C., Cheng, T.-J., . . . Chuang, H.-C. (2019). Microglial activation and inflammation caused by traffic-related particulate matter. *Chemico-biological interactions, 311*, 108762.

Balmes, J. R., Fine, J. M., & Sheppard, D. (1987). Symptomatic Bronchoconstriction after Short-Term Inhalation of Sulfur Dioxide1, 2. *Am Rev Respir Dis, 136*, 1117-1121.

Bayram, H., Devalia, J. L., Sapsford, R. J., Ohtoshi, T., Miyabara, Y., Sagai, M., & Davies, R. J. (1998). The effect of diesel exhaust particles on cell function and release of inflammatory mediators from human bronchial epithelial cells in vitro. *American journal of respiratory cell and molecular biology, 18*(3), 441-448.

Bayram, H., Fakili, F., Gögebakan, B., Bayraktar, R., Öztuzcu, S., Dikensoy, Ö., & Chung, K. F. (2013). Effect of serum on diesel exhaust particles (DEP)-induced apoptosis of airway epithelial cells in vitro. *Toxicology letters, 218*(3), 215-223.

Bayram, H., Ito, K., Issa, R., Ito, M., Sukkar, M., & Chung, K. F. (2006). Regulation of human lung epithelial cell numbers by diesel exhaust particles. *European Respiratory Journal, 27*(4), 705-713.

Beevers, C., & Ross, M. A. (1937). The crystal structure of "beta alumina" Na2O· 11Al2O3. *Zeitschrift für Kristallographie-Crystalline Materials, 97*(1-6), 59-66.

Belknap, J. K., Orton, E. C., Ensley, B., Tucker, A., & Stenmark, K. R. (1997). Hypoxia increases bromodeoxyuridine labeling indices in bovine neonatal pulmonary arteries. *American Journal of Respiratory Cell and Molecular Biology, 16*(4), 366-371.

Bennett, M. H., Trytko, B., & Jonker, B. (2012). Hyperbaric oxygen therapy for the adjunctive treatment of traumatic brain injury. *Cochrane Database of Systematic Reviews*(12). doi:10.1002/14651858.CD004609.pub3

Bhavaraju, L., Shannahan, J., William, A., McCormick, R., McGee, J., Kodavanti, U., & Madden, M. (2014). Diesel and biodiesel exhaust particle effects on rat alveolar macrophages with in vitro exposure. *Chemosphere, 104*, 126-133.

Block, M., Wu, X., Pei, Z., Li, G., Wang, T., Qin, L., . . . Veronesi, B. (2004). Nanometer size diesel exhaust particles are selectively toxic to dopaminergic neurons: the role of microglia, phagocytosis, and NADPH oxidase. *The FASEB Journal, 18*(13), 1618-1620.

Bogaert, E., Damme, P. V., Van Den Bosch, L., & Robberecht, W. (2006). Vascular endothelial growth factor in amyotrophic lateral sclerosis and other neurodegenerative diseases. *Muscle & Nerve: Official Journal of the American Association of Electrodiagnostic Medicine, 34*(4), 391-405.

Bogan, R. A., Ohde, S., Arakaki, T., Mori, I., & McLeod, C. W. (2009). Changes in rainwater pH associated with increasing atmospheric carbon dioxide after the industrial revolution. *Water, air, and soil pollution, 196*(1-4), 263-271.

Borrell, P., Burrows, J. P., Platt, U., Richter, A., & Wagner, T. (2003). New directions: New developments in satellite capabilities for probing the chemistry of the troposphere. *Atmospheric Environment, 18*(37), 2567-2570.

Botto, L., Beretta, E., Daffara, R., Miserocchi, G., & Palestini, P. (2006). Biochemical and morphological changes in endothelial cells in response to hypoxic interstitial edema. *Respiratory research, 7*(1), 7.

Brown, J., Cook, K., Ney, F. G., & Hatch, T. (1950). Influence of particle size upon the retention of particulate matter in the human lung. *American Journal of Public Health and the Nations Health, 40*(4), 450-480.

Brown, J. M., & Giaccia, A. J. (1998). The unique physiology of solid tumors: opportunities (and problems) for cancer therapy. *Cancer research, 58*(7), 1408-1416.

Brugarolas, J., Lei, K., Hurley, R. L., Manning, B. D., Reiling, J. H., Hafen, E., . . . Kaelin, W. G. (2004). Regulation of mTOR function in response to hypoxia by REDD1 and the TSC1/TSC2 tumor suppressor complex. *Genes & development, 18*(23), 2893-2904.

Brunekreef, B., & Holgate, S. T. (2002). Air pollution and health. *The lancet, 360*(9341), 1233-1242.

Bünger, J., Krahl, J., Franke, H.-U., Munack, A., & Hallier, E. (1998). Mutagenic and cytotoxic effects of exhaust particulate matter of biodiesel compared to fossil diesel fuel. *Mutation Research/Genetic Toxicology and Environmental Mutagenesis, 415*(1-2), 13-23.

Campbell, A., Daher, N., Solaimani, P., Mendoza, K., & Sioutas, C. (2014). Human brain derived cells respond in a type-specific manner after exposure to urban particulate matter (PM). *Toxicology in vitro, 28*(7), 1290-1295.

Campillo, N., Falcones, B., Montserrat, J. M., Gozal, D., Obeso, A., Gallego-Martin, T., . . . Farré, R. (2017). Frequency and magnitude of intermittent hypoxia modulate endothelial wound healing in a cell culture model of sleep apnea. *Journal of applied physiology (Bethesda, Md. : 1985), 123*(5), 1047-1054. doi:10.1152/japplphysiol.00077.2017

Carpenter, T. C., Schomberg, S., & Stenmark, K. R. (2005). Endothelin-mediated increases in lung VEGF content promote vascular leak in young rats exposed to viral infection and hypoxia. *American Journal of Physiology-Lung Cellular and Molecular Physiology, 289*(6), L1075-L1082.

Cassee, F. R., Héroux, M.-E., Gerlofs-Nijland, M. E., & Kelly, F. J. (2013). Particulate matter beyond mass: recent health evidence on the role of fractions, chemical constituents and sources of emission. *Inhalation toxicology, 25*(14), 802-812.

Chandan, K. S., & Sashwati, R. (2010). Oxygenation State as a Driver of Myofibroblast Differentiation and Wound Contraction: Hypoxia Impairs Wound Closure. *Journal of Investigative Dermatology, 130*(12), 2701. doi:10.1038/jid.2010.316

Chang, T. M. S. (1998). Modified Hemoglobin-based Blood Substitutes: Crosslinked, Recombinant and Encapsulated Hemoglobin. *Vox Sanguinis, 74*(S2), 233-241. doi:10.1111/j.1423-0410.1998.tb05425.x

Chatterjee, R., Welty, E., Walder, R., Pruitt, S., Rogers, P., Arnone, A., & Walder, J. (1986). Isolation and characterization of a new hemoglobin derivative cross-linked between the alpha chains (lysine 99 alpha 1----lysine 99 alpha 2). *Journal of Biological Chemistry, 261*(21), 9929-9937.

Cho, A. K., Di Stefano, E., You, Y., Rodriguez, C. E., Schmitz, D. A., Kumagai, Y., . . . Avol, E. (2004). Determination of four quinones in diesel exhaust particles, SRM 1649a, and atmospheric PM2. 5 special issue of aerosol science and technology on findings from the fine particulate matter supersites program. *Aerosol Science and Technology, 38*(S1), 68-81.

Costa, D. L. (2018). Historical Highlights of Air Pollution Toxicology. *Toxicological Sciences, 164*(1), 5-8.

Costa, L. G., Cole, T. B., Coburn, J., Chang, Y.-C., Dao, K., & Roqué, P. J. (2017). Neurotoxicity of traffic-related air pollution. *Neurotoxicology, 59*, 133-139.

Crobeddu, B., Aragao-Santiago, L., Bui, L.-C., Boland, S., & Squiban, A. B. (2017). Oxidative potential of particulate matter 2.5 as predictive indicator of cellular stress. *Environmental Pollution, 230*, 125-133.

D'Agostino Dias, M., Fontes, B., Poggetti, R., & Birolini, D. (2008). Hyperbaric oxygen therapy: types of injury and number of sessions--a review of 1506 cases.

Dalton, T. P., Kerzee, J. K., Wang, B., Miller, M., Dieter, M. Z., Lorenz, J. N., . . . Puga, A. (2001). Dioxin exposure is an environmental risk factor for ischemic heart disease. *Cardiovascular toxicology, 1*(4), 285-298.

Damek-Poprawa, M., & Sawicka-Kapusta, K. (2003). Damage to the liver, kidney, and testis with reference to burden of heavy metals in yellow-necked mice from areas around steelworks and zinc smelters in Poland. *Toxicology, 186*(1-2), 1-10.

Danielsen, P. H., Loft, S., Kocbach, A., Schwarze, P. E., & Møller, P. (2009). Oxidative damage to DNA and repair induced by Norwegian wood smoke particles in human A549 and THP-1 cell lines. *Mutation Research/Genetic Toxicology and Environmental Mutagenesis, 674*(1-2), 116-122.

Danielsen, P. H., Loft, S., & Møller, P. (2008). DNA damage and cytotoxicity in type II lung epithelial (A549) cell cultures after exposure to diesel exhaust and urban street particles. *Particle and Fibre Toxicology, 5*(1), 6.

Daugherty, W. P., Levasseur, J. E., Sun, D., Rockswold, G. L., & Bullock, M. R. (2004). Effects of hyperbaric oxygen therapy on cerebral oxygenation and mitochondrial function following moderate lateral fluid-percussion injury in rats. *Journal of neurosurgery, 101*(3), 499-504.

De la Torre, J. (2000). Critically attained threshold of cerebral hypoperfusion: the CATCH hypothesis of Alzheimer's pathogenesis. *Neurobiology of aging, 21*(2), 331-342.

De Perrot, M., Sekine, Y., Fischer, S., Waddell, T. K., McRae, K., Liu, M., . . . Keshavjee, S. (2002). Interleukin-8 release during early reperfusion predicts graft function in human lung transplantation. *American journal of respiratory and critical care medicine, 165*(2), 211. doi:10.1164/ajrccm.165.2.2011151

Devos, D., Moreau, C., Lassalle, P., Perez, T., De Seze, J., Brunaud-Danel, V., . . . Just, N. (2004). Low levels of the vascular endothelial growth factor in CSF from early ALS patients. *Neurology, 62*(11), 2127-2129.

Don Porto Carero, A., Hoet, P., Verschaeve, L., Schoeters, G., & Nemery, B. (2001). Genotoxic effects of carbon black particles, diesel exhaust particles, and urban air particulates and their extracts on a human alveolar epithelial cell line (A549) and a human monocytic cell line (THP-1). *Environmental and molecular mutagenesis, 37*(2), 155-163.

Donaldson, K., Stone, V., Borm, P. J., Jimenez, L. A., Gilmour, P. S., Schins, R. P., . . . Brown, D. M. (2003). Oxidative stress and calcium signaling in the adverse effects of environmental particles (PM10). *Free Radical Biology and Medicine, 34*(11), 1369-1382.

Donaldson, K., Tran, L., Jimenez, L. A., Duffin, R., Newby, D. E., Mills, N., . . . Stone, V. (2005). Combustion-derived nanoparticles: a review of their toxicology following inhalation exposure. *Particle and fibre toxicology, 2*(1), 10.

Donohoe, P. H., & Boutilier, R. G. (1998). The protective effects of metabolic rate depression in hypoxic cold submerged frogs. *Respiration physiology, 111*(3), 325-336.

Drevytska, T., Gavenauskas, B., Drozdovska, S., Nosar, V., Dosenko, V., & Mankovska, I. (2012). HIF-3α mRNA expression changes in different tissues and their role in adaptation to intermittent hypoxia and physical exercise. *Pathophysiology, 19*(3), 205-214.

Durga, M., Nathiya, S., & Devasena, T. (2014). In vitro evaluation of cytotoxicity, oxidative stress, DNA damage and inflammation induced by diesel exhaust particles in human a549 lung cells and murine raw 264.7 macrophages. *Int J Pharm Pharm Sci, 6*, 105-110.

Durga, M., Nathiya, S., Rajasekar, A., & Devasena, T. (2014). Effects of ultrafine petrol exhaust particles on cytotoxicity, oxidative stress generation, DNA damage and inflammation in human A549 lung cells and murine RAW 264.7 macrophages. *Environmental Toxicology and Pharmacology, 38*(2), 518-530.

Dybdahl, M., Risom, L., Bornholdt, J., Autrup, H., Loft, S., & Wallin, H. (2004). Inflammatory and genotoxic effects of diesel particles in vitro and in vivo. *Mutation Research/Genetic Toxicology and Environmental Mutagenesis, 562*(1-2), 119-131.

Esworthy, R. (2013). *Air quality: EPA's 2013 changes to the particulate matter (PM) standard*.

Ewan, K., & Pamphlett, R. (1996). Increased inorganic mercury in spinal motor neurons following chelating agents. *Neurotoxicology, 17*(2), 343-349.

Fardel, O. (2013). Cytokines as molecular targets for aryl hydrocarbon receptor ligands: implications for toxicity and xenobiotic detoxification. *Expert opinion on drug metabolism & toxicology, 9*(2), 141-152.

Fariss, M. W., Gilmour, M. I., Reilly, C. A., Liedtke, W., & Ghio, A. J. (2013). Emerging mechanistic targets in lung injury induced by combustion-generated particles. *Toxicological Sciences, 132*(2), 253-267.

Floyd, R. A. (1990). The role of 8-hydroxyguanine in carcinogenesis. *Carcinogenesis, 11*(9), 1447-1450.

Fujii, T., Hayashi, S., Hogg, J. C., Vincent, R., & Van Eeden, S. F. (2001). Particulate matter induces cytokine expression in human bronchial epithelial cells. *American journal of respiratory cell and molecular biology, 25*(3), 265-271.

Furuyama, A., Kanno, S., Kobayashi, T., & Hirano, S. (2009). Extrapulmonary translocation of intratracheally instilled fine and ultrafine particles via direct and alveolar macrophage-associated routes. *Archives of toxicology, 83*(5), 429-437.

Gardner, L. B., Li, Q., Park, M. S., Flanagan, W. M., Semenza, G. L., & Dang, C. V. (2001). Hypoxia inhibits G1/S transition through regulation of p27 expression. *Journal of Biological Chemistry, 276*(11), 7919-7926.

Gebert, L. F., & MacRae, I. J. (2019). Regulation of microRNA function in animals. *Nature reviews Molecular cell biology, 20*(1), 21-37.

Ghezzi, P., Dinarello, C. A., Bianchi, M., Rosandich, M. E., Repine, J. E., & White, C. W. (1991). Hypoxia increases production of interleukin-1 and tumor necrosis factor by human mononuclear cells. *Cytokine, 3*(3), 189-194.

Ghio, A. J., & Huang, Y.-C. T. (2004). Exposure to concentrated ambient particles (CAPs): a review. *Inhalation toxicology, 16*(1), 53-59.

Gill, A., & Bell, C. N. (2004). Hyperbaric oxygen: its uses, mechanisms of action and outcomes. *Qjm, 97*(7), 385-395.

Gille, J., Drummond, J., Edwards, D., Deeter, M., Worden, H., Masters, D., . . . Pfister, G. (2010, 25-30 July 2010). *The impact of MOPITT data on tropospheric chemistry.* Paper presented at the 2010 IEEE International Geoscience and Remote Sensing Symposium.

Goh, F., Gross, J. D., Simpson, N. E., & Sambanis, A. (2010). Limited beneficial effects of perfluorocarbon emulsions on encapsulated cells in culture: Experimental and modeling studies. *Journal of Biotechnology, 150*(2), 232-239. doi:10.1016/j.jbiotec.2010.08.013

Goldstein, J. I., Newbury, D. E., Michael, J. R., Ritchie, N. W., Scott, J. H. J., & Joy, D. C. (2017). *Scanning electron microscopy and X-ray microanalysis*: Springer.

Graeber, T. G., Osmanian, C., Jacks, T., Housman, D. E., Koch, C. J., Lowe, S. W., & Giaccia, A. J. (1996). Hypoxia-mediated selection of cells with diminished apoptotic potential in solid tumours. *nature, 379*(6560), 88-91.

Graeber, T. G., Peterson, J. F., Tsai, M., Monica, K., Fornace, A., & Giaccia, A. J. (1994). Hypoxia induces accumulation of p53 protein, but activation of a G1-phase checkpoint by low-oxygen conditions is independent of p53 status. *Molecular and cellular biology, 14*(9), 6264-6277.

Green, S. L., & Giaccia, A. J. (1998). Tumor hypoxia and the cell cycle: implications for malignant progression and response to therapy. *The cancer journal from Scientific American, 4*(4), 218-221.

Gu, Y.-Z., Moran, S. M., Hogenesch, J. B., Wartman, L., & Bradfield, C. A. (1998). Molecular characterization and chromosomal localization of a third α-class hypoxia inducible factor subunit, HIF3α. *Gene Expression The Journal of Liver Research, 7*(3), 205-213.

Gustafson, D., Rothenberg, E., Blennow, K., Steen, B., & Skoog, I. (2003). An 18-year follow-up of overweight and risk of Alzheimer disease. *Arch Intern Med, 163*(13), 1524-1528. doi:10.1001/archinte.163.13.1524

Gwak, G.-Y., Yoon, J.-H., Kim, K. M., Lee, H.-S., Chung, J. W., & Gores, G. J. (2005). Hypoxia stimulates proliferation of human hepatoma cells through the induction of hexokinase II expression. *Journal of hepatology, 42*(3), 358-364.

Halliwell, B. (1999). Oxygen and nitrogen are pro-carcinogens. Damage to DNA by reactive oxygen, chlorine and nitrogen species: measurement, mechanism and the effects of nutrition. *Mutation Research/Genetic Toxicology and Environmental Mutagenesis, 443*(1-2), 37-52.

Hasheminassab, S., Daher, N., Schauer, J. J., & Sioutas, C. (2013). Source apportionment and organic compound characterization of ambient ultrafine particulate matter (PM) in the Los Angeles Basin. *Atmospheric Environment, 79*, 529-539.

Hashimoto, S., Gon, Y., Takeshita, I., Matsumoto, K., Jibiki, I., TAKIZAWA, H., . . . HORIE, T. (2000). Diesel exhaust particles activate p38 MAP kinase to produce interleukin 8 and RANTES by human bronchial epithelial cells and N-acetylcysteine attenuates p38 MAP kinase activation. *American journal of respiratory and critical care medicine, 161*(1), 280-285.

Hazenkamp-von Arx, M. E., Schindler, C., Ragettli, M. S., Künzli, N., Braun-Fahrländer, C., & Liu, L.-J. S. (2011). Impacts of highway traffic exhaust in alpine valleys on the respiratory health in adults: a cross-sectional study. *Environmental Health, 10*(1), 13.

He, Z., Chen, Y., Chen, P., Wu, G., & Cai, S. (2010). Local inflammation occurs before systemic inflammation in patients with COPD. *Respirology, 15*(3), 478-484.

Heerlein, K., Schulze, A., Hotz, L., Bartsch, P., & Mairbaurl, H. (2005). Hypoxia decreases cellular ATP demand and inhibits mitochondrial respiration of a549 cells. *American Journal of Respiratory Cell and Molecular Biology, 32*(1), 44-51.

Hendrik Bergert, M. D., Klaus-Peter, K., Ronny, M., Melanie, J., Joke, O., Stephan, K., . . . Michele, S. (2005). Effect of Oxygenated Perfluorocarbons on Isolated Rat Pancreatic Islets in Culture. *Cell Transplantation, 14*(7). doi:10.3727/000000005783982873

Hinz, B., Celetta, G., Tomasek, J. J., Gabbiani, G., & Chaponnier, C. (2001). Alpha-smooth muscle actin expression upregulates fibroblast contractile activity. *Molecular Biology of the Cell, 12*(9), 2730-2741.

Hirano, S., Furuyama, A., Koike, E., & Kobayashi, T. (2003). Oxidative-stress potency of organic extracts of diesel exhaust and urban fine particles in rat heart microvessel endothelial cells. *Toxicology, 187*(2-3), 161-170.

Ho, C. S., Lam, C., Chan, M., Cheung, R., Law, L., Lit, L., . . . Tai, H. (2003). Electrospray ionisation mass spectrometry: principles and clinical applications. *The Clinical Biochemist Reviews, 24*(1), 3.

Hochachka, P., Buck, L., Doll, C., & Land, S. (1996). Unifying theory of hypoxia tolerance: molecular/metabolic defense and rescue mechanisms for surviving oxygen lack. *Proceedings of the National Academy of Sciences, 93*(18), 9493-9498.

Hoffman, S. J., Looker, D. L., Roehrich, J. M., Cozart, P. E., Durfee, S. L., Tedesco, J. L., & Stetler, G. L. (1990). Expression of fully functional tetrameric human hemoglobin in Escherichia coli. *Proceedings of the National Academy of Sciences, 87*(21), 8521-8525.

Hu, C.-J., Iyer, S., Sataur, A., Covello, K. L., Chodosh, L. A., & Simon, M. C. (2006). Differential regulation of the transcriptional activities of hypoxia-inducible factor 1 alpha (HIF-1alpha) and HIF-2alpha in stem cells. *Molecular and cellular biology, 26*(9), 3514-3526. doi:10.1128/MCB.26.9.3514-3526.2006

Huang, R.-Q., Cheng, H.-L., Zhao, X.-D., Dai, W., Zhuang, Z., Wu, Y., . . . Shi, J.-X. (2010). Preliminary study on the effect of trauma-induced secondary cellular hypoxia in brain injury. *Neuroscience Letters, 473*(1), 22-27. doi:10.1016/j.neulet.2010.02.011

Huang, Y., Zhao, J.-J., Lv, Y.-Y., Ding, P.-S., & Liu, R.-Y. (2009). Hypoxia down-regulates glucocorticoid receptor alpha and attenuates the anti-inflammatory actions of dexamethasone in human alveolar epithelial A549 cells. *Life sciences, 85*(3-4), 107-112.

Hubbi, M. E., & Semenza, G. L. (2015). Regulation of cell proliferation by hypoxia-inducible factors. *American Journal of Physiology-Cell Physiology, 309*(12), C775-C782.

Hung, W. W., Wisnivesky, J. P., Siu, A. L., & Ross, J. S. (2009). Cognitive decline among patients with chronic obstructive pulmonary disease. *American journal of respiratory and critical care medicine, 180*(2), 134-137.

Incalzi, R. A., Gemma, A., Marra, C., Muzzolon, R., Capparella, O., & Carbonin, P. (1993). Chronic obstructive pulmonary disease. An original model of cognitive decline. *Am Rev Respir Dis, 148*(2), 418-424. doi:10.1164/ajrccm/148.2.418

Incalzi, R. A., Marra, C., Giordano, A., Calcagni, M. L., Cappa, A., Basso, S., . . . Fuso, L. (2003). Cognitive impairment in chronic obstructive pulmonary disease. *Journal of neurology, 250*(3), 325-332.

Inoki, K., Li, Y., Zhu, T., Wu, J., & Guan, K.-L. (2002). TSC2 is phosphorylated and inhibited by Akt and suppresses mTOR signalling. *Nature cell biology, 4*(9), 648-657.

Ivan, M., Kondo, K., Yang, H., Kim, W., Valiando, J., Ohh, M., . . . Kaelin Jr, W. G. (2001). HIFα targeted for VHL-mediated destruction by proline hydroxylation: implications for O2 sensing. *Science, 292*(5516), 464-468.

Jacobsen, N. R., Pojana, G., White, P., Møller, P., Cohn, C. A., Smith Korsholm, K., . . . Wallin, H. (2008). Genotoxicity, cytotoxicity, and reactive oxygen species induced by single-walled carbon nanotubes and C60 fullerenes in the FE1-Muta™ Mouse lung epithelial cells. *Environmental and molecular mutagenesis, 49*(6), 476-487.

Jalava, P. I., Salonen, R. O., Pennanen, A. S., Happo, M. S., Penttinen, P., Hälinen, A. I., . . . Hirvonen, M.-R. (2008). Effects of solubility of urban air fine and coarse particles on cytotoxic and inflammatory responses in RAW 264.7 macrophage cell line. *Toxicology and applied pharmacology, 229*(2), 146-160.

Jeremitsky, E., Omert, L., Dunham, C. M., Protetch, J., & Rodriguez, A. (2003). Harbingers of poor outcome the day after severe brain injury: hypothermia, hypoxia, and hypoperfusion. *Journal of Trauma and Acute Care Surgery, 54*(2), 312-319.

Ji, J. S., Zhu, A., Lv, Y., & Shi, X. (2019). Residential greenness and air pollution mortality using the Chinese Longitudinal Healthy Longevity Survey: a longitudinal analysis. *The lancet, 394*, S16.

Jin, K. L., Mao, X. O., & Greenberg, D. A. (2000). Vascular endothelial growth factor: direct neuroprotective effect in in vitro ischemia. *Proceedings of the National Academy of Sciences, 97*(18), 10242-10247.

Juvin, P., Fournier, T., Boland, S., Soler, P., Marano, F., Desmonts, J.-M., & Aubier, M. (2002). Diesel particles are taken up by alveolar type II tumor cells and alter cytokines secretion. *Archives of Environmental Health: An International Journal, 57*(1), 53-60.

Kaelin, W. G., & Ratcliffe, P. J. (2008). Oxygen Sensing by Metazoans: The Central Role of the HIF Hydroxylase Pathway. *Molecular Cell, 30*(4), 393-402. doi:https://doi.org/10.1016/j.molcel.2008.04.009

Kagawa, J. (1985). Evaluation of biological significance of nitrogen oxides exposure. *The Tokai journal of experimental and clinical medicine, 10*(4), 348-353.

Kalmijn, S., Foley, D., White, L., Burchfiel, C., Curb, J., Petrovitch, H., . . . Launer, L. (2000). Metabolic cardiovascular syndrome and risk of dementia in Japanese-American elderly men: the Honolulu-Asia Aging Study. *Arteriosclerosis, thrombosis, and vascular biology, 20*(10), 2255-2260.

Karakurum, M., Shreeniwas, R., Chen, J., Pinsky, D., Yan, S., Anderson, M., . . . Kuwabara, K. (1994). Hypoxic induction of interleukin-8 gene expression in human endothelial cells. *The Journal of Clinical Investigation, 93*(4), 1564-1570.

Kay, K. (1957). Air Pollution. *Analytical Chemistry, 29*(4), 589-604. doi:10.1021/ac60124a015

Keipert, P. E., Faithfull, N. S., Bradley, J. D., Hazard, D. Y., Hogan, J., Levisetti, M. S., & Peters, R. M. (1994). Oxygen delivery augmentation by low-dose perfluorochemical emulsion during profound normovolemic hemodilution. In *Oxygen Transport to Tissue XV* (pp. 197-204): Springer.

Kim, K.-H., Kabir, E., & Kabir, S. (2015). A review on the human health impact of airborne particulate matter. *Environment international, 74*, 136-143.

Korzeniewski, C., & Callewaert, D. M. (1983). An enzyme-release assay for natural cytotoxicity. *Journal of immunological methods, 64*(3), 313-320.

Koshiji, M., Kageyama, Y., Pete, E. A., Horikawa, I., Barrett, J. C., & Huang, L. E. (2004). HIF-1α induces cell cycle arrest by functionally counteracting Myc. *The EMBO journal, 23*(9), 1949-1956.

Koumenis, C., Naczki, C., Koritzinsky, M., Rastani, S., Diehl, A., Sonenberg, N., . . . Wouters, B. G. (2002). Regulation of protein synthesis by hypoxia via activation of the endoplasmic reticulum kinase PERK and phosphorylation of the translation initiation factor eIF2α. *Molecular and cellular biology, 22*(21), 7405-7416.

Kreyling, W. G., Semmler-Behnke, M., & Möller, W. (2006). Ultrafine particle–lung interactions: does size matter? *Journal of Aerosol Medicine, 19*(1), 74-83.

Kulshreshtha, R., Ferracin, M., Negrini, M., Calin, G. A., Davuluri, R. V., & Ivan, M. (2007). Regulation of microRNA Expression: the Hypoxic Component. *Cell Cycle, 6*(12), 1425-1430. doi:10.4161/cc.6.12.4410

Kulshreshtha, R., Ferracin, M., Wojcik, S. E., Garzon, R., Alder, H., Agosto-Perez, F. J., . . . Negrini, M. (2007). A microRNA signature of hypoxia. *Molecular and cellular biology, 27*(5), 1859-1867.

Kuo, C.-Y., Wong, R.-H., Lin, J.-Y., Lai, J.-C., & Lee, H. (2006). Accumulation of chromium and nickel metals in lung tumors from lung cancer patients in Taiwan. *Journal of Toxicology and Environmental Health, Part A, 69*(14), 1337-1344.

Kwast, K. E., & Hand, S. C. (1996). Acute depression of mitochondrial protein synthesis during anoxia contributions of oxygen sensing, matrix acidification, and redox state. *Journal of Biological Chemistry, 271*(13), 7313-7319.

Lamarque, J. F., Edwards, D. P., Emmons, L. K., Gille, J. C., Wilhelmi, O., Gerbig, C., . . . Drummond, J. R. (2003). Identification of CO plumes from MOPITT data: Application to the August 2000 Idaho-Montana forest fires. *Geophysical Research Letters, 30*(13). doi:10.1029/2003GL017503

Lawal, A., Davids, L. M., & Marnewick, J. L. (2016). Diesel exhaust particles and endothelial cells dysfunction: An update. *Toxicology in vitro, 32*, 92-104.

Le Bail, A., Cranswick, L. M., Madsen, I., Fitch, A., Allmann, R., Giacovazzo, C., . . . Norby, P. (2008). *Powder diffraction: theory and practice*: Royal society of chemistry.

Levesque, S., Taetzsch, T., Lull, M. E., Kodavanti, U., Stadler, K., Wagner, A., . . . Surace, M. J. (2011). Diesel exhaust activates and primes microglia: air pollution, neuroinflammation, and regulation of dopaminergic neurotoxicity. *Environmental health perspectives, 119*(8), 1149-1155.

Li, N., Wang, M., Oberley, T. D., Sempf, J. M., & Nel, A. E. (2002). Comparison of the pro-oxidative and proinflammatory effects of organic diesel exhaust particle chemicals in bronchial epithelial cells and macrophages. *The Journal of Immunology, 169*(8), 4531-4541.

Li, X., Jin, L., & Kan, H. (2019). Air pollution: a global problem needs local fixes. In: Nature Publishing Group.

Liu, L., Cash, T. P., Jones, R. G., Keith, B., Thompson, C. B., & Simon, M. C. (2006). Hypoxia-Induced Energy Stress Regulates mRNA Translation and Cell Growth. *Molecular Cell, 21*(4), 521-531. doi:https://doi.org/10.1016/j.molcel.2006.01.010

Logan, W. P. (1953). Mortality in the London fog incident, 1952. *Lancet*, 336-338.

Looker, D., Abbott-Brown, D., Cozart, P., Durfee, S., Hoffman, S., Mathews, A. J., . . . Stetler, G. L. (1992). A human recombinant haemoglobin designed for use as a blood substitute. *Nature, 356*(6366), 258-260. doi:10.1038/356258a0

Lowe, G. D. (2006). Local inflammation, endothelial dysfunction and fibrinolysis in coronary heart disease. *Clinical Science, 110*(3), 327-328.

Lowe, K. C. (1994). Perfluorochemicals in Vascular Medicine. *Vascular Medicine Review, vmr-5*(1), 15-32. doi:10.1177/1358863X9400500103

Lowe, K. C. (1997). Perfluorochemical respiratory gas carriers: applications in medicine and biotechnology. *Science progress, 80*, 169.

Lowe, K. C. (1999). Perfluorinated blood substitutes and artificial oxygen carriers. *Blood Reviews, 13*(3), 171-184. doi:https://doi.org/10.1054/blre.1999.0113

Makino, Y., Uenishi, R., Okamoto, K., Isoe, T., Hosono, O., Tanaka, H., . . . Morimoto, C. (2007). Transcriptional Up-regulation of Inhibitory PAS Domain Protein Gene Expression by Hypoxia-inducible Factor 1 (HIF-1) A NEGATIVE FEEDBACK REGULATORY CIRCUIT IN HIF-1-MEDIATED SIGNALING IN HYPOXIC CELLS. *Journal of Biological Chemistry, 282*(19), 14073-14082.

Mandal, P. K. (2005). Dioxin: a review of its environmental effects and its aryl hydrocarbon receptor biology. *Journal of Comparative Physiology B, 175*(4), 221-230.

Manojkumar, N., Srimuruganandam, B., & Nagendra, S. S. (2018). Quantification of Size Segregated Particulate Matter Deposition in Human Airways. *Journal of Advanced Research in Alternative Energy, Environment and Ecology, 5*(4), 15-22.

Marsin, A.-S., Bouzin, C., Bertrand, L., & Hue, L. (2002). The stimulation of glycolysis by hypoxia in activated monocytes is mediated by AMP-activated protein kinase and inducible 6-phosphofructo-2-kinase. *Journal of Biological Chemistry, 277*(34), 30778-30783.

Mathur, R., Cox, I. J., Oatridge, A., Shephard, D. T., Shaw, R. J., & Taylor-Robinson, S. D. (1999). Cerebral bioenergetics in stable chronic obstructive pulmonary disease. *Am J Respir Crit Care Med, 160*(6), 1994-1999. doi:10.1164/ajrccm.160.6.9810069

Maxwell, P., Pugh, C., & Ratcliffe, P. (1993). Inducible operation of the erythropoietin 3'enhancer in multiple cell lines: evidence for a widespread oxygen-sensing mechanism. *Proceedings of the National Academy of Sciences, 90*(6), 2423-2427.

Maxwell, P. H., Wiesener, M. S., Chang, G.-W., Clifford, S. C., Vaux, E. C., Cockman, M. E., . . . Ratcliffe, P. J. (1999). The tumour suppressor protein VHL targets hypoxia-inducible factors for oxygen-dependent proteolysis. *Nature, 399*(6733), 271.

McGeer, P. L., & McGeer, E. G. (2002). Innate immunity, local inflammation, and degenerative disease. *Science of Aging Knowledge Environment, 2002*(29), 3.

Meng, F., Kassa, T., Jana, S., Wood, F., Zhang, X., Jia, Y., . . . Alayash, A. I. (2018). Comprehensive Biochemical and Biophysical Characterization of Hemoglobin-Based Oxygen Carrier Therapeutics: All HBOCs Are Not Created Equally. *Bioconjugate Chemistry, 29*(5), 1560-1575. doi:10.1021/acs.bioconjchem.8b00093

Meyrick, B., & Reid, L. (1980). Endothelial and subintimal changes in rat hilar pulmonary artery during recovery from hypoxia. A quantitative ultrastructural study. *Laboratory investigation; a journal of technical methods and pathology, 42*(6), 603-615.

Mills, B. J. (2012). Wound healing: the evidence for hyperbaric oxygen therapy. *British Journal of Nursing, 21*(20), S28-S34. doi:10.12968/bjon.2012.21.Sup20.S28

Mitsushima, D., Yamamoto, S., Fukushima, A., Funabashi, T., Kobayashi, T., & Fujimaki, H. (2008). Changes in neurotransmitter levels and proinflammatory cytokine mRNA expressions in the mice olfactory bulb following nanoparticle exposure. *Toxicology and Applied Pharmacology, 226*(2), 192-198.

MohanKumar, S. M., Campbell, A., Block, M., & Veronesi, B. (2008). Particulate matter, oxidative stress and neurotoxicity. *Neurotoxicology, 29*(3), 479-488.

Møller, P., Christophersen, D. V., Jacobsen, N. R., Skovmand, A., Gouveia, A. C. D., Andersen, M. H. G., . . . Roursgaard, M. (2016). Atherosclerosis and vasomotor dysfunction in arteries of animals after exposure to combustion-derived particulate matter or nanomaterials. *Critical reviews in toxicology, 46*(5), 437-476.

Møller, P., Danielsen, P. H., Karottki, D. G., Jantzen, K., Roursgaard, M., Klingberg, H., . . . Cao, Y. (2014). Oxidative stress and inflammation generated DNA damage by exposure to air pollution particles. *Mutation research/Reviews in mutation research, 762*, 133-166.

Moreau, C., Devos, D., Brunaud-Danel, V., Defebvre, L., Perez, T., Destee, A., . . . Just, N. (2006). Paradoxical response of VEGF expression to hypoxia in CSF of patients with ALS. *Journal of Neurology, Neurosurgery & Psychiatry, 77*(2), 255-257.

Morgan, D. M. (1998). Tetrazolium (MTT) assay for cellular viability and activity. In *Polyamine protocols* (pp. 179-184): Springer.

Mosca, R. S., Rohs, T. J., Waterford, R. R., Childs, K. F., Brunsting, L. A., & Bolling, S. F. (1996). Perfluorocarbon supplementation and postischemic cardiac function. *Surgery, 120*(2), 197-204.

Mühlfeld, C. (2008). Translocation and cellular entering mechanisms of nanoparticles in the respiratory tract. *Swiss medical weekly, 138*(2728).

Murray, J. A., Ledlow, A., Launspach, J., Evans, D., Loveday, M., & Conklin, J. L. (1995). The effects of recombinant human hemoglobin on esophageal motor function in humans. *Gastroenterology, 109*(4), 1241-1248. doi:https://doi.org/10.1016/0016-5085(95)90584-7

Muz, B., de la Puente, P., Azab, F., & Azab, A. K. (2015). The role of hypoxia in cancer progression, angiogenesis, metastasis, and resistance to therapy. *Hypoxia, 3*, 83.

Myers, R. A. M. (2000). Hyperbaric Oxygen Therapy for Trauma: Crush Injury, Compartment Syndrome, and Other Acute Traumatic Peripheral Ischemias. *International Anesthesiology Clinics, 38*(1), 139-151.

Naldini, A., Carraro, F., Silvestri, S., & Bocci, V. (1997). Hypoxia affects cytokine production and proliferative responses by human peripheral mononuclear cells. *Journal of cellular physiology, 173*(3), 335-342.

Namiki, A., Brogi, E., Kearney, M., Kim, E. A., Wu, T., Couffinhal, T., . . . Isner, J. M. (1995). Hypoxia induces vascular endothelial growth factor in cultured human endothelial cells. *Journal of Biological Chemistry, 270*(52), 31189-31195.

Nawrot, T., Plusquin, M., Hogervorst, J., Roels, H. A., Celis, H., Thijs, L., . . . Staessen, J. A. (2006). Environmental exposure to cadmium and risk of cancer: a prospective population-based study. *The lancet oncology, 7*(2), 119-126.

Nemukhin, A., & Weinhold, F. (1992). Structures of the aluminum oxides studied by ab initio methods with natural bond orbital analysis. *The Journal of chemical physics, 97*(5), 3420-3430.

Øvrevik, J., Låg, M., Holme, J., Schwarze, P., & Refsnes, M. (2009). Cytokine and chemokine expression patterns in lung epithelial cells exposed to components characteristic of particulate air pollution. *Toxicology, 259*(1-2), 46-53.

Øvrevik, J., Refsnes, M., Låg, M., Holme, J. A., & Schwarze, P. E. (2015). Activation of proinflammatory responses in cells of the airway mucosa by particulate matter: oxidant-and non-oxidant-mediated triggering mechanisms. *Biomolecules, 5*(3), 1399-1440.

Palumbo, F. S., Di Stefano, M., Palumbo Piccionello, A., Fiorica, C., Pitarresi, G., Pibiri, I., . . . Giammona, G. (2014). Perfluorocarbon functionalized hyaluronic acid derivatives as oxygenating systems for cell culture. *RSC Advances, 4*(44), 22894-22901. doi:10.1039/c4ra01502a

Parhamifar, L., Andersen, H., & Moghimi, S. M. (2013). Lactate dehydrogenase assay for assessment of polycation cytotoxicity. In *Nanotechnology for Nucleic Acid Delivery* (pp. 13-22): Springer.

Perraut, R., Richard, V., Varela, M.-L., Trape, J.-F., Guillotte, M., Tall, A., . . . Mercereau-Puijalon, O. (2014). Comparative analysis of IgG responses to Plasmodium falciparum MSP1p19 and PF13-DBL1α1 using ELISA and a magnetic bead-based duplex assay (MAGPIX®-Luminex) in a Senegalese meso-endemic community. *Malaria journal, 13*(1), 410.

Peters, A., Veronesi, B., Calderon-Garciduenas, L., Gehr, P., Chen, L. C., Geiser, M., . . . Schulz, H. (2006). Translocation and potential neurological effects of fine and ultrafine particles a critical update. *Part Fibre Toxicol, 3*, 13. doi:10.1186/1743-8977-3-13

Peters, A., Wichmann, H. E., Tuch, T., Heinrich, J., & Heyder, J. (1997). Respiratory effects are associated with the number of ultrafine particles. *American journal of respiratory and critical care medicine, 155*(4), 1376-1383.

Pope, C. A., Thun, M. J., Namboodiri, M. M., Dockery, D. W., Evans, J. S., Speizer, F. E., & Heath, C. W. (1995). Particulate air pollution as a predictor of mortality in a prospective study of US adults. *American journal of respiratory and critical care medicine, 151*(3), 669-674.

Pope III, C. A., Burnett, R. T., Thun, M. J., Calle, E. E., Krewski, D., Ito, K., & Thurston, G. D. (2002). Lung cancer, cardiopulmonary mortality, and long-term exposure to fine particulate air pollution. *Jama, 287*(9), 1132-1141.

Porto, S., & Krishnan, R. (1967). Raman effect of corundum. *The Journal of chemical physics, 47*(3), 1009-1012.

Pourazar, J., Blomberg, A., Kelly, F. J., Davies, D. E., Wilson, S. J., Holgate, S. T., & Sandström, T. (2008). Diesel exhaust increases EGFR and phosphorylated C-terminal Tyr 1173 in the bronchial epithelium. *Particle and fibre toxicology, 5*(1), 8.

Probst, G., Riedinger, H.-J., Martin, P., Engelcke, M., & Probst, H. (1999). Fast control of DNA replication in response to hypoxia and to inhibited protein synthesis in CCRF-CEM and HeLa cells. *Biological chemistry, 380*(12), 1371-1382.

Probst, H., Hamprecht, K., & Gekeler, V. (1983). Replicon initiation frequency and intracellular levels of ATP, ADP, AMP and of diadenosine 5′, 5‴-P1, P4-tetraphosphate in Ehrlich ascites cells cultured aerobically and anaerobically. *Biochemical and biophysical research communications, 110*(2), 688-693.

Raaschou-Nielsen, O., Andersen, Z. J., Jensen, S. S., Ketzel, M., Sørensen, M., Hansen, J., . . . Overvad, K. (2012). Traffic air pollution and mortality from cardiovascular disease and all causes: a Danish cohort study. *Environmental Health, 11*(1), 60.

Ratnaike, R. N. (2003). Acute and chronic arsenic toxicity. *Postgraduate medical journal, 79*(933), 391-396.

Reeve, H. L., Archer, S. L., & Weir, E. K. (1997). Ion channels in the pulmonary vasculature. *Pulmonary pharmacology & therapeutics, 10*(5-6), 243-252.

Rich, P. (2003). The molecular machinery of Keilin's respiratory chain. In: Portland Press Ltd.

Riediker, M., Cascio, W. E., Griggs, T. R., Herbst, M. C., Bromberg, P. A., Neas, L., . . . Devlin, R. B. (2004). Particulate Matter Exposure in Cars Is Associated with Cardiovascular Effects in Healthy Young Men. *American journal of respiratory and critical care medicine, 169*(8), 934-940. doi:10.1164/rccm.200310-1463OC

Riley, M. R., Boesewetter, D. E., Kim, A. M., & Sirvent, F. P. (2003). Effects of metals Cu, Fe, Ni, V, and Zn on rat lung epithelial cells. *Toxicology, 190*(3), 171-184.

Riley, M. R., Boesewetter, D. E., Turner, R. A., Kim, A. M., Collier, J. M., & Hamilton, A. (2005). Comparison of the sensitivity of three lung derived cell lines to metals from combustion derived particulate matter. *Toxicology in vitro, 19*(3), 411-419.

Robin, E. D., Murphy, B. J., & Theodore, J. (1984). Coordinate regulation of glycolysis by hypoxia in mammalian cells. *Journal of Cellular Physiology, 118*(3), 287-290. doi:10.1002/jcp.1041180311

Rodriguez, A., Vigorito, E., Clare, S., Warren, M. V., Couttet, P., Soond, D. R., . . . Miska, E. A. (2007). Requirement of bic/microRNA-155 for normal immune function. *Science, 316*(5824), 608-611.

Rolfe, D., & Brown, G. C. (1997). Cellular energy utilization and molecular origin of standard metabolic rate in mammals. *Physiological reviews, 77*(3), 731-758.

Rosi, N. L., Eckert, J., Eddaoudi, M., Vodak, D. T., Kim, J., Keeffe, M., & Yaghi, O. M. (2003). Hydrogen Storage in Microporous Metal-Organic Frameworks. *Science, 300*(5622), 1127. doi:10.1126/science.1083440

Saalfeld, H., & Wedde, M. (1974). Refinement of the crystal structure of gibbsite, A1 (OH) 3. *Zeitschrift für Kristallographie-Crystalline Materials, 139*(1-6), 129-135.

Samoli, E., Stergiopoulou, A., Santana, P., Rodopoulou, S., Mitsakou, C., Dimitroulopoulou, C., . . . Marí-Dell'Olmo, M. (2019). Spatial variability in air pollution exposure in relation to socioeconomic indicators in nine European metropolitan areas: A study on environmental inequality. *Environmental Pollution, 249*, 345-353.

Schilirò, T., Alessandria, L., Degan, R., Traversi, D., & Gilli, G. (2010). Chemical characterisation and cytotoxic effects in A549 cells of urban-air PM10 collected in Torino, Italy. *Environmental Toxicology and Pharmacology, 29*(2), 150-157.

Schmelzle, T., & Hall, M. N. (2000). TOR, a central controller of cell growth. *Cell, 103*(2), 253-262.

Schofield, C. J., & Ratcliffe, P. J. (2004). Oxygen sensing by HIF hydroxylases. *Nature reviews Molecular cell biology, 5*(5), 343.

Schreml, S., Szeimies, R. M., Prantl, L., Karrer, S., Landthaler, M., & Babilas, P. (2010). Oxygen in acute and chronic wound healing. *British Journal of Dermatology, 163*(2), 257-268. doi:10.1111/j.1365-2133.2010.09804.x

Schuetzle, D., Lee, F. S.-C., Prater, T. J., & Tejada, S. B. (1981). The identification of polynuclear aromatic hydrocarbon (PAH) derivatives in mutagenic fractions of diesel particulate extracts. *International Journal of Environmental Analytical Chemistry, 9*(2), 93-144.

Schumacker, P. T., Chandel, N., & Agusti, A. (1993). Oxygen conformance of cellular respiration in hepatocytes. *American Journal of Physiology-Lung Cellular and Molecular Physiology, 265*(4), L395-L402.

Seagroves, T. N., Ryan, H. E., Lu, H., Wouters, B. G., Knapp, M., Thibault, P., . . . Johnson, R. S. (2001). Transcription factor HIF-1 is a necessary mediator of the pasteur effect in mammalian cells. *Molecular and cellular biology, 21*(10), 3436-3444.

Selkoe, D. J. (2001). Alzheimer's disease results from the cerebral accumulation and cytotoxicity of amyloid\beta-protein. *Journal of Alzheimer's Disease, 3*(1), 75-82.

Semenza, G. L. (2003). Targeting HIF-1 for cancer therapy. *Nature reviews cancer, 3*(10), 721-732.

Semenza, G. L. (2007). Life with Oxygen. *Science, 318*(5847), 62-64. doi:10.1126/science.1147949

Semenza, G. L., Roth, P. H., Fang, H.-M., & Wang, G. L. (1994). Transcriptional regulation of genes encoding glycolytic enzymes by hypoxia-inducible factor 1. *Journal of Biological Chemistry, 269*(38), 23757-23763.

Semenza, G. L., & Wang, G. L. (1992). A nuclear factor induced by hypoxia via de novo protein synthesis binds to the human erythropoietin gene enhancer at a site required for transcriptional activation. *Molecular and cellular biology, 12*(12), 5447-5454.

Shang, Y., Fan, L., Feng, J., Lv, S., Wu, M., Li, B., & Zang, Y.-S. (2013). Genotoxic and inflammatory effects of organic extracts from traffic-related particulate matter in human lung epithelial A549 cells: the role of quinones. *Toxicology in vitro, 27*(2), 922-931.

Shoshani, T., Faerman, A., Mett, I., Zelin, E., Tenne, T., Gorodin, S., . . . Feinstein, E. (2002). Identification of a Novel Hypoxia-Inducible Factor 1-Responsive Gene, RTP801, Involved in Apoptosis. *Molecular and cellular biology, 22*(7), 2283. doi:10.1128/MCB.22.7.2283-2293.2002

Silverman, T. A., & Weiskopf, R. B. (2009). Hemoglobin-based oxygen carriers: current status and future directions. *Anesthesiology, 111*(5), 946-963. doi:10.1097/ALN.0b013e3181ba3c2c

Sloan, E. P., Koenigsberg, M., Gens, D., Cipolle, M., Runge, J., Mallory, M. N., & Rodman, G., Jr. (1999). Diaspirin cross-linked hemoglobin (DCLHb) in the treatment of severe traumatic hemorrhagic shock: a randomized controlled efficacy trial. *Jama, 282*(19), 1857-1864. doi:10.1001/jama.282.19.1857

Smith, B. C. (2011). *Fundamentals of Fourier transform infrared spectroscopy*: CRC press.

Soucek, T., Cumming, R., Dargusch, R., Maher, P., & Schubert, D. (2003). The regulation of glucose metabolism by HIF-1 mediates a neuroprotective response to amyloid beta peptide. *Neuron, 39*(1), 43-56.

Soukup, J. M., & Becker, S. (2001). Human alveolar macrophage responses to air pollution particulates are associated with insoluble components of coarse material, including particulate endotoxin. *Toxicology and applied pharmacology, 171*(1), 20-26.

Spahn, D. R. (1999). Blood substitutes. Artificial oxygen carriers: perfluorocarbon emulsions. *Critical care (London, England), 3*(5), R93-R97. doi:10.1186/cc364

Spahn, Donat R. M. D., van Brempt, R. M. D., Theilmeier, G. M. D., Reibold, J.-P. M. D., Welte, M. M. D., Heinzerling, H. M. D., . . . Messmer, K. M. D. (1999). Perflubron Emulsion Delays Blood Transfusions in Orthopedic Surgery *Anesthesiology: The Journal of the American Society of Anesthesiologists, 91*(5), 1195-1195.

Stadtman, E., & Berlett, B. (1991). Fenton chemistry. Amino acid oxidation. *Journal of Biological Chemistry, 266*(26), 17201-17211.

Stenmark, K., & Mecham, R. (1997). Cellular and molecular mechanisms of pulmonary vascular remodeling. *Annual review of physiology, 59*(1), 89-144.

Stenmark Kurt, R., Fagan Karen, A., & Frid Maria, G. (2006). Hypoxia-Induced Pulmonary Vascular Remodeling. *Circulation Research, 99*(7), 675-691. doi:10.1161/01.RES.0000243584.45145.3f

Su, D. S., Serafino, A., Müller, J.-O., Jentoft, R. E., Schlögl, R., & Fiorito, S. (2008). Cytotoxicity and inflammatory potential of soot particles of low-emission diesel engines. *Environmental Science & Technology, 42*(5), 1761-1765.

Suzuki, A. K., Taneda, S., Fujitani, Y., & Li, C. (2008). Diesel exhaust particles contained high concentration nanoparticles affects on cardiovascular system. *Toxicology Letters*(180), S226.

Swenson, E. R. (2006). Hypoxic Lung Whiteout: Further Clearing but More Questions from on High. *Annals of Internal Medicine, 145*(7), 550-552. doi:10.7326/0003-4819-145-7-200610030-00015

Tager, I. B., Balmes, J., Lurmann, F., Ngo, L., Alcorn, S., & Künzli, N. (2005). Chronic exposure to ambient ozone and lung function in young adults. *Epidemiology*, 751-759.

Tang, M., Li, Q., Xiao, L., Li, Y., Jensen, J. L., Liou, T. G., & Zhou, A. (2012). Toxicity effects of short term diesel exhaust particles exposure to human small airway epithelial cells (SAECs) and human lung carcinoma epithelial cells (A549). *Toxicology Letters, 215*(3), 181-192.

Taylor, C. T. (2008). Mitochondria and cellular oxygen sensing in the HIF pathway. *Biochemical journal, 409*(1), 19-26.

Taylor, D. E., Kantrow, S. P., & Piantadosi, C. A. (1998). Mitochondrial respiration after sepsis and prolonged hypoxia. *American Journal of Physiology-Lung Cellular and Molecular Physiology, 275*(1), L139-L144.

Tekpli, X., A Holme, J., Sergent, O., & Lagadic-Gossmann, D. (2011). Importance of plasma membrane dynamics in chemical-induced carcinogenesis. *Recent patents on anti-cancer drug discovery, 6*(3), 347-353.

Tekpli, X., Holme, J. A., Sergent, O., & Lagadic-Gossmann, D. (2013). Role for membrane remodeling in cell death: implication for health and disease. *Toxicology, 304*, 141-157.

Temuujin, J., Jadambaa, T., Mackenzie, K., Angerer, P., Porte, F., & Riley, F. (2000). Thermal formation of corundum from aluminium hydroxides prepared from various aluminium salts. *Bulletin of Materials Science, 23*(4), 301-304.

Tian, H., McKnight, S. L., & Russell, D. W. (1997). Endothelial PAS domain protein 1 (EPAS1), a transcription factor selectively expressed in endothelial cells. *Genes & development, 11*(1), 72-82.

Tinton, S., Tran-Nguyen, Q. N., & Buc-Calderon, P. (1997). Role of Protein-Phosphorylation Events in the Anoxia Signal-Transduction Pathway Leading to the Inhibition of Total Protein Synthesis in Isolated Hepatocytes. *European journal of biochemistry, 249*(1), 121-126.

Tobwala, S., Zhang, X., Zheng, Y., Wang, H.-J., Banks, W. A., & Ercal, N. (2013). Disruption of the integrity and function of brain microvascular endothelial cells in culture by exposure to diesel engine exhaust particles. *Toxicology Letters, 220*(1), 1-7.

Totlandsdal, A. I., Cassee, F. R., Schwarze, P., Refsnes, M., & Låg, M. (2010). Diesel exhaust particles induce CYP1A1 and pro-inflammatory responses via differential pathways in human bronchial epithelial cells. *Particle and fibre toxicology, 7*(1), 41.

Tseng, C.-Y., Wang, J.-S., & Chao, M.-W. (2017). Causation by diesel exhaust particles of endothelial dysfunctions in cytotoxicity, pro-inflammation, permeability, and apoptosis induced by ROS generation. *Cardiovascular toxicology, 17*(4), 384-392.

Tuder, R. M., Yun, J. H., Bhunia, A., & Fijalkowska, I. (2007). Hypoxia and chronic lung disease. *Journal of Molecular Medicine, 85*(12), 1317-1324. doi:10.1007/s00109-007-0280-4

Vandegriff, K. D., McCarthy, M., Rohlfs, R. J., & Winslow, R. M. (1997). Colloid osmotic properties of modified hemoglobins: chemically cross-linked versus polyethylene glycol surface-conjugated. *Biophysical Chemistry, 69*(1), 23-30. doi:https://doi.org/10.1016/S0301-4622(97)00079-3

Vaupel, P. (2004). Tumor microenvironmental physiology and its implications for radiation oncology. *Semin Radiat Oncol, 14*(3), 198-206. doi:10.1016/j.semradonc.2004.04.008

Vermylen, J., Nemmar, A., Nemery, B., & Hoylaerts, M. F. (2005). Ambient air pollution and acute myocardial infarction. *Journal of Thrombosis and Haemostasis, 3*(9), 1955-1961.

Voelkel, N. F., & Tuder, R. M. (2000). Hypoxia-induced pulmonary vascular remodeling: a model for what human disease? *The Journal of Clinical Investigation, 106*(6), 733-738. doi:10.1172/JCI11144

Volm, M., & Koomägi, R. (2000). Hypoxia-inducible factor (HIF-1) and its relationship to apoptosis and proliferation in lung cancer. *Anticancer research, 20*(3A), 1527-1533.

Walkowiak, J., Wiener, J.-A., Fastabend, A., Heinzow, B., Krämer, U., Schmidt, E., . . . Winneke, G. (2001). Environmental exposure to polychlorinated biphenyls and quality of the home environment: effects on psychodevelopment in early childhood. *The lancet, 358*(9293), 1602-1607.

Wang, G. L., Jiang, B.-H., Rue, E. A., & Semenza, G. L. (1995). Hypoxia-inducible factor 1 is a basic-helix-loop-helix-PAS heterodimer regulated by cellular O2 tension. *Proceedings of the National Academy of Sciences, 92*(12), 5510-5514.

Wang, G. L., & Semenza, G. L. (1993). General involvement of hypoxia-inducible factor 1 in transcriptional response to hypoxia. *Proceedings of the National Academy of Sciences, 90*(9), 4304. doi:10.1073/pnas.90.9.4304

Wang, S., Zhang, J., Zeng, X., Zeng, Y., Wang, S., & Chen, S. (2009). Association of traffic-related air pollution with children's neurobehavioral functions in Quanzhou, China. *Environmental Health Perspectives, 117*(10), 1612-1618.

Wang, Y., Wang, L., Yu, W., Gao, D., You, G., Li, P., . . . Zhou, H. (2017). A PEGylated bovine hemoglobin as a potent hemoglobin-based oxygen carrier. *Biotechnol Prog, 33*(1), 252-260. doi:10.1002/btpr.2380

Watterson, T. L., Sorensen, J., Martin, R., & Coulombe Jr, R. A. (2007). Effects of PM2. 5 collected from Cache Valley Utah on genes associated with the inflammatory response in human lung cells. *Journal of Toxicology and Environmental Health, Part A, 70*(20), 1731-1744.

Weiss, D., Shotyk, W., Appleby, P. G., Kramers, J. D., & Cheburkin, A. K. (1999). Atmospheric Pb deposition since the industrial revolution recorded by five Swiss peat profiles: enrichment factors, fluxes, isotopic composition, and sources. *Environmental Science & Technology, 33*(9), 1340-1352.

Wichmann, H. E. (2007). Diesel Exhaust Particles. *Inhalation Toxicology, 19*, 241-244. doi:10.1080/08958370701498075

Wilhelm, M., & Ritz, B. (2003). Residential proximity to traffic and adverse birth outcomes in Los Angeles county, California, 1994-1996. *Environmental Health Perspectives, 111*(2), 207-216.

Winslow, R. M. (2000). Blood substitutes. *Advanced Drug Delivery Reviews, 40*(3), 131-142. doi:https://doi.org/10.1016/S0169-409X(99)00045-9

Wright, J. L., Levy, R. D., & Churg, A. (2005). Pulmonary hypertension in chronic obstructive pulmonary disease: current theories of pathogenesis and their implications for treatment. *Thorax, 60*(7), 605. doi:10.1136/thx.2005.042994

Wykoff, C. C., Pugh, C. W., Maxwell, P. H., Harris, A. L., & Ratcliffe, P. J. (2000). Identification of novel hypoxia dependent and independent target genes of the von Hippel-Lindau (VHL) tumour suppressor by mRNA differential expression profiling. *Oncogene, 19*(54), 6297-6305.

Xu, X., Ha, S. U., & Basnet, R. (2016). A review of epidemiological research on adverse neurological effects of exposure to ambient air pollution. *Frontiers in public health, 4*, 157.

Xue, M., Li, X., Li, Z., & Chen, W. (2014). Urothelial carcinoma associated 1 is a hypoxia-inducible factor-1α-targeted long noncoding RNA that enhances hypoxic bladder cancer cell proliferation, migration, and invasion. *Tumor Biology, 35*(7), 6901-6912.

Yaghi, O. M., O'Keeffe, M., Ockwig, N. W., Chae, H. K., Eddaoudi, M., & Kim, J. (2003). Reticular synthesis and the design of new materials. *Nature, 423*(6941), 705.

Yang, Y., Zhang, J., Liu, H., Wang, J., Xin, J., & Deng, M. (2013). Changes in Levels of Hypoxia-Induced Mediators in Rat Hippocampus During Chronic Cerebral Hypoperfusion. *Neurochemical Research, 38*(11), 2433-2439. doi:10.1007/s11064-013-1158-1

Yao, K., Gietema, J., Shida, S., Selvakumaran, M., Fonrose, X., Haas, N., . . . O'Dwyer, P. (2005). In vitro hypoxia-conditioned colon cancer cell lines derived from HCT116 and HT29 exhibit altered apoptosis susceptibility and a more angiogenic profile in vivo. *British journal of cancer, 93*(12), 1356-1363.

Ye, J. (2008). Emerging role of adipose tissue hypoxia in obesity and insulin resistance. *International Journal of Obesity, 33*(1), 54. doi:10.1038/ijo.2008.229

Yorifuji, T., Kashima, S., Tsuda, T., Ishikawa-Takata, K., Ohta, T., Tsuruta, K.-i., & Doi, H. (2013). Long-term exposure to traffic-related air pollution and the risk of death from hemorrhagic stroke and lung cancer in Shizuoka, Japan. *Science of the total environment, 443*, 397-402.

Zhang, F., Aquino, G. V., Dabi, A., Nugent, W. H., Song, B. K., & Bruce, E. D. (2019). Oral ingestion of a novel oxygenating compound, Ox66™, is non-toxic and has the potential to increase oxygenation. *Food and chemical toxicology, 125*, 217-224.

Zuck, T. F., Riess, J. G., & Biro, G. (1994). Current status of injectable oxygen carriers. *Critical reviews in clinical laboratory sciences, 31*(4), 295-324.